

Applications Notebook

Issue 1, June 2009

**Thermo Scientific
Hypercarb Columns**



A unique solution for difficult separations

Table of Contents

Introduction

Thermo Scientific Hypercarb Columns Introduction	4
--	---

Application Notes

Biochemical

Porous Graphitic Carbon for the Sample Preparation of Hydrophilic Biomolecules.....	6
Porous Graphitic Carbon for the LC/MS Analysis of Hydrophilic Biomolecules.....	7
Analysis of Glycopeptides Using Porous Graphite Chromatography and LTQ Orbitrap XL ETD Hybrid MS.....	10
The Use of Porous Graphitic Carbon LC-MS for the Analysis of Underivatized Carbohydrates from Wheat Stems.....	17

Food Safety

Quantitation of Acrylamide in Food Samples on the TSQ Quantum Discovery by LC/APCI-MS/MS	20
--	----

Environmental

Fast LC Separation of Triazine Herbicides at Elevated Temperature	23
Analysis of Polar Metabolites of Atrazine in Ground Waters Using Hypercarb as SPE Sorbent Coupled On-Line with Hypercarb LC Column.....	27
Fast and Versatile Analysis of Desphenyl-Chloridazone and Methyl-Desphenyl-Chloridazone in Surface, Ground and Drinking Water Using LC-MS/MS and EQuan.....	30

Clinical

Determination of Leucine and its Isomers by LC-MS/MS Using a Porous Graphitic Carbon Column	33
Determination of Occupational Exposure to Toluene, Xylene and Styrene Through Metabolite Monitoring Using Isocratic HPLC	35

Food and Beverage

Porous Graphitic Carbon for Inorganic Ion Analysis in Drinking Water.....	37
---	----

Legal Notices

©2009 Thermo Fisher Scientific Inc. All rights reserved. All trademarks not specifically referenced are the property of Thermo Fisher Scientific Inc. and its subsidiaries. This information is presented as an example of the capabilities of Thermo Fisher Scientific Inc. products. It is not intended to encourage use of these products in any manners that might infringe the intellectual property rights of others. Not all products are available in all countries. Please consult your local sales representative for details.

Applications Review

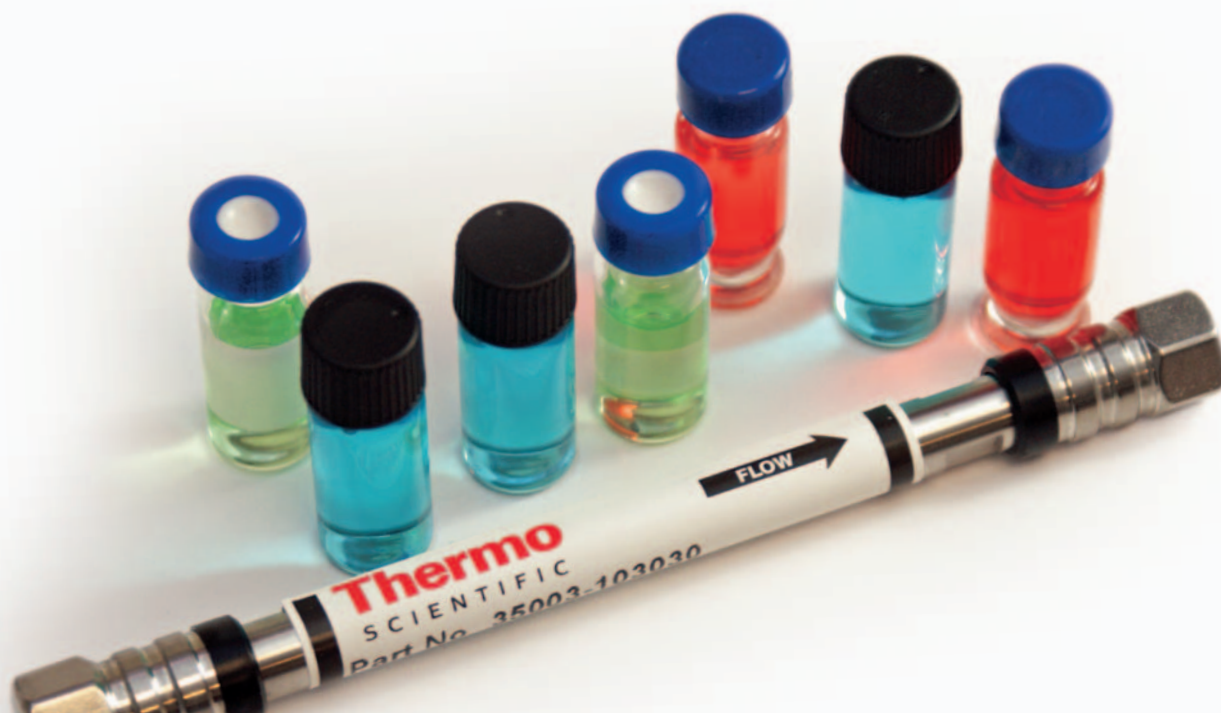
Applications Reference Guide (<i>Application by Solute Type</i>).....	40
References.....	42

Application Chromatograms

Biochemical	44
<i>Allantoin</i>	44
<i>Ceramides</i>	44
<i>Cyclic Monophosphates</i>	44
<i>L-Carnitine</i>	44
<i>Purines and Pyrimidines (UHT-LC)</i>	44
<i>RNB-Glycopeptides</i>	44
Food Safety	45
<i>Aflatoxins</i>	45
<i>Methylamines in Fish</i>	45
Environmental.....	45
<i>Nonylphenol Isomers</i>	45
<i>Quaternary Ammonium Salts</i>	45
<i>Water Pollutants</i>	45
Clinical	45-46
<i>Arginine and Methylated Arginines</i>	45
<i>Creatine in Serum</i>	46
Pharmaceutical	46
<i>Acyclovir</i>	46
<i>Fosfomycin</i>	46
<i>Glucosamine Sulfate</i>	46
<i>Tuberculostatics</i>	46
<i>Uracil and Metabolite</i>	46

Ordering Information

Hypercarb Columns, Hypercarb Drop-in Guard Cartridges, Hypercarb KAPPA Capillary Columns, Hypercarb Nanobore Columns, Hypercarb Specialized Column Hardware for High Throughput, Hypercarb Preparative Columns, Hypercarb High Temperature Columns	47
--	----



Thermo Scientific Hypercarb Columns

Introduction

Porous graphitic carbon (PGC, Hypercarb) has unique properties as a stationary phase in high performance liquid chromatography (HPLC). Its chemical surface properties distinguish PGC from more conventional LC packings such as bonded-silica gels and polymers. PGC behaves as a strongly retentive alkyl-bonded silica gel for non-polar analytes, however its retention and selectivity behaviour towards polar and structurally related compounds is very different. PGC provides unique retention and separation of very polar compounds. Its surface is stereo-selective with the capability to separate geometric isomers, diastereomers and other closely related compounds. Hypercarb is stable throughout the entire pH range 0-14, and is not affected by aggressive mobile phases. Its compatibility with all solvent systems enables separation of a wide range of polarities within a single chromatographic run. The selectivity of the Hypercarb packing is different from the selectivity of silica and polymeric phases. Its retention mechanism is different from conventional C18 columns.

Reference 1 gives an in-depth review of its HPLC behaviour and application areas.

Physical and Chemical Properties of PGC

PGC particles are spherical and fully porous with a porosity of approximately 75%. The surface of PGC is crystalline and highly reproducible and does not contain micropores. At the molecular level, PGC is made up of sheets of hexagonally arranged carbon atoms linked by the same conjugated 1.5-order bonds which are present in any large polynuclear aromatic hydrocarbon.² In principle, there are no functional groups on the surface since the aromatic carbon atoms have fully satisfied valencies within the graphitic sheets. Table 1 lists the more important physical properties of PGC. The requirements placed on its physical properties are similar to other HPLC supports where factors such as narrow particle size distribution are essential to the ultimate performance of the phase, if good bed uniformity and low operating pressures are to be achieved. PGC also has a tight pore size distribution with a mean value around 250 Å, allowing for good mass transfer of a wide range of analyte shapes and sizes. Surface homogeneity and absence of highly adsorptive sites are essential for good peak symmetry. PGC meets all the conventional operating criteria of a chromatographic support.

Property		To meet requirement of
Particle shape	Spherical, fully porous	No micropores
Specific surface area	120 m ² /g	Retention linearity and loading capacity
Median pore diameter	250 Å	Mass transfer for wide range of analyte's shapes and sizes
Pore volume	0.7 m ³ /g	
Mean particle diameters	3, 5 µm	Analytical HPLC columns
	7 µm	Preparative HPLC columns
	30 µm	SPE applications
Porosity	75%	Mass transfer within particles
% C	100%	Chemical stability
Mechanical strength	> 400 bar	Operational particle stability; pressure gradients in packing process

Table 1: Physical properties of PGC



Retention Mechanisms on PGC

On a molecular scale, the surface of the graphite is flat and highly crystalline unlike that of alkyl-bonded silicas, which possess a brush type surface with the bonded phase and residual silanols. Consequently, the PGC mechanism of interaction is very different. The retention by graphite from aqueous/organic eluents is determined by the balance of two factors: (1) hydrophobicity, which is primarily a solution effect that tends to drive analytes out of solution and (2) the interaction of polarisable or polarised groups in the analyte with the graphite (these are additional to the normal dispersive interactions). The strength of interaction depends on both the molecular area of an analyte in contact with the graphite surface and upon the nature and type of functional groups at the point of interaction with the flat graphite surface. The more planar the analyte, the closer its alignment is to the graphite surface, and so the greater the number of points of interaction possible – hence, maximum retention. Retention is reduced for highly structured, 3-dimensional and rigid molecules that can contact the surface with only a small part of their surface, compared with planar molecules with the same molecular mass. This is illustrated in Figure 1.

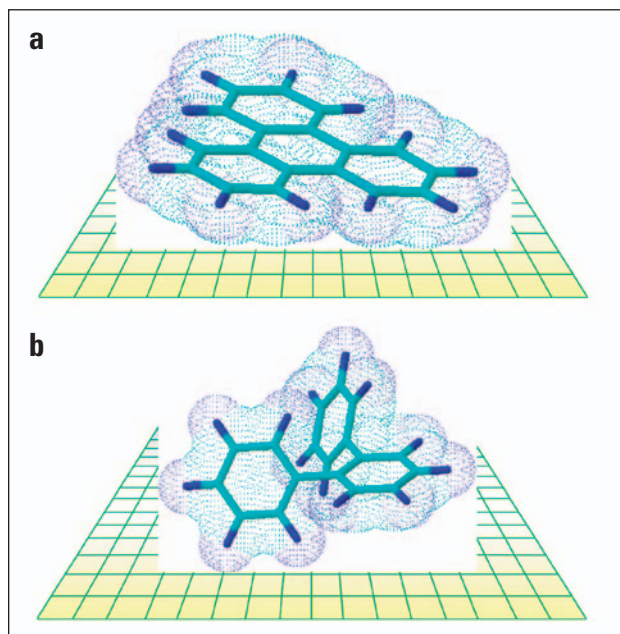


Figure 1: Effect of the solute shape on the strength of the interaction with the graphite surface: (a) Good alignment of planar molecule to the flat graphite surface; (b) Poor alignment of non-planar molecule to the flat graphite surface.

Retention of Polar Compounds on PGC

In a traditional reversed phase (RP) system, analyte retention increases as its hydrophobicity increases. This is due to the increased dispersive interactions that take place between the stationary phase and the analyte. Conversely, as the polarity of the analyte increases, analyte-solvent interactions begin to dominate and retention is reduced. This simple observation holds true for all reversed-phase systems with the exception of PGC. For Hypercarb columns, it has been observed that in some cases retention increases as the polarity of the analyte increases. This effect has been called “the polar retention effect on graphite” or PREG. The effect of PREG makes Hypercarb columns particularly useful for the separation of highly polar compounds, such as carbohydrates, and compounds with several hydroxyl, carboxyl and amino groups, which are difficult to retain on conventional alkyl-silica phases.

PREG defines the ability of molecules having lone-pair or aromatic-ring electrons to apparently interact through an electron transfer mechanism to the electronic cloud of the graphite. PREG is particularly pronounced when the polar groups are attached to a benzene ring and other larger aromatic systems. Knox *et al.*² have attributed this to some type of orbital overlap between the conductivity electrons in graphite and lone pair and/or π electrons in analytes. The polarizable properties of the graphite hold the key to understanding the mechanism by which polar molecules are retained at the surface (Figure 2).

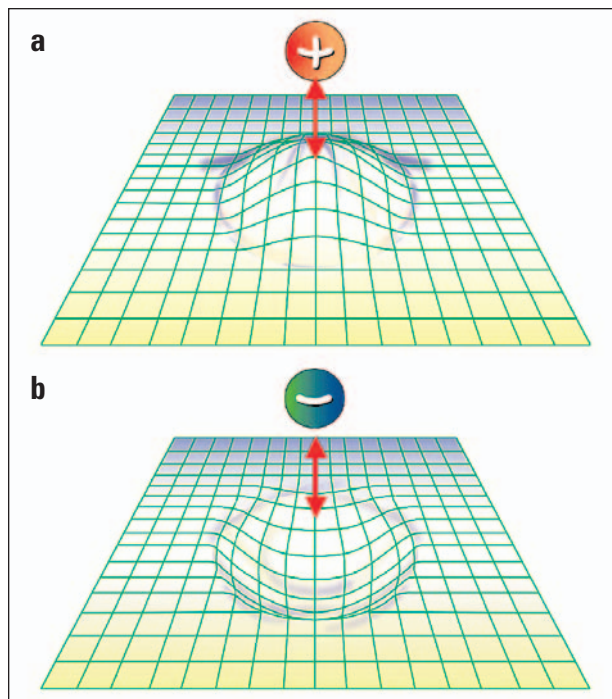


Figure 2: Schematic representation of polar analyte retention in which (a) positive charge and (b) negative charges approach the graphite surface, resulting in a charge-induced dipole at the graphite surface.

References

1. L. Pereira, *J. Liq. Chrom. & Rel Technol.*, 2008, 31, 1687–1731
2. J. Knox, P. Ross, *Advances in Chromatography*, 1997, 37, 73–119

Porous Graphitic Carbon for the Sample Preparation of Hydrophilic Biomolecules

Luisa Pereira, Thermo Fisher Scientific, Runcorn, UK

Introduction

Micro-scale solid phase extraction (SPE) can be used as a sample purification process to remove contaminants; this technique has the advantage of effectively handling limited sample volumes (low microlitre) to maximise sensitivity. When the analytes are very hydrophilic it is necessary to select a sorbent that provides good retention and minimises sample loss through breakthrough in the aqueous matrix. Desalting of hydrophilic peptides can be accomplished by using microscale tips packed with porous graphitic carbon. This enables the off-line preparation and clean-up of biological samples for further analysis and identification by mass spectrometry (MS). In this approach it is important that the sorbent in the tip is capable of retaining the hydrophilic analytes with no breakthrough in the aqueous matrix, and that good recovery of the retained analytes from the tip is achieved.

Goal

To demonstrate the capability of porous graphitic carbon (PGC) in micro-scale SPE of hydrophilic peptides.

Experimental

Peptides

Arg-Gly-Glu-Ser (RGES) and Asp-Ser-Asp-Pro-Arg (DSDPR).

Tips

Thermo Scientific HyperSep Hypercarb Tips 10-200 μL volume (part number 60109-212).

Micro-scale SPE Protocol:

Solvents: A – H_2O + 0.1% formic acid; B – $\text{H}_2\text{O}/\text{ACN}$ (30:70) + 0.1% formic acid.

Tip conditioning: Aspirate and expel 5 times 20 μL of solvent B. Aspirate and expel 5 times 20 μL of solvent A.

Sample loading (binding): Aspirate and expel 20 times 20 μL of sample.

Sample washing: Aspirate and expel 5 times 20 μL of solvent A, discarding the expelled solvent each time.

Sample elution: Aspirate and expel 20 times 20 μL of solvent B, collecting the expelled solution in a clean micro-centrifuge tube. Transfer solution to micro-vial for injection.

A flow-through fraction from a proteolytic digest was simulated by diluting a solution containing RGES and DSDPR in Tris buffer (100 mM, pH 8.0) to concentrations of 0.1 and 0.5 ng/ μL respectively.

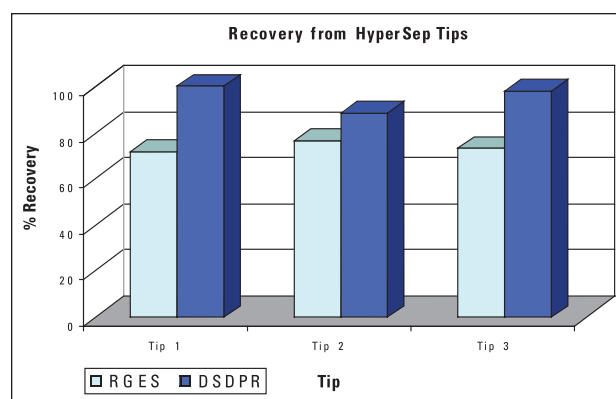


Figure 1. Recovery from HyperSep Hypercarb Tips for 2 peptides, RGES and DSDPR.

Results and Discussion

Following the procedure detailed in the experimental section, the recoveries were measured by comparison of the ESI-MS signal for the tip eluate with the ESI-MS signal for the solution of the same concentration. Recoveries are between 72 and 101%, as shown in Figure 1.

Conclusion

Micro-scale SPE with porous graphitic carbon packed tips gives good recovery of small hydrophilic peptides from buffer matrices.

Porous Graphitic Carbon for the LC/MS Analysis of Hydrophilic Biomolecules

Luisa Pereira, Thermo Fisher Scientific, Runcorn, UK

Introduction

The sensitivity of the analysis of small hydrophilic peptides by mass spectrometric detection is often compromised by the presence of salts and non-volatile buffers. These peptides are not retained and, therefore, are often found in the flow-through fraction from a C18 LC column, the type of stationary phase most commonly used for the separation of proteolytic digests of proteins. The analysis of the flow-through fraction requires either a stationary phase that can retain the peptides away from the solvent front, where the biological salts and buffers elute, or a sample clean-up step to remove the salts.¹ Porous Graphitic Carbon (PGC) is a material that provides strong retention of very polar compounds; the retention mechanism involves a charge-induced interaction of the polar analyte with the polarizable surface of the graphite.² PGC is ideal to retain and resolve very polar, hydrophilic molecules, which are normally not retained under reversed-phase LC using typical MS compatible mobile phases.

The work presented in this application note demonstrates the advantages of using PGC in the LC/MS analysis of a phosphopeptide and di-, tri- and penta-peptides containing polar and basic terminal amino acid residues. Analytical parameters investigated are chromatographic retention and resolution, and spectral cleanliness.

Goal

To demonstrate the advantages of using porous graphitic carbon (PGC) in the LC/MS analysis of polar molecules of biological interest such as small hydrophilic peptides and phosphopeptides.

Experimental

Columns

Thermo Scientific Hypercarb 5 μm , 50 x 2.1 mm; (part number 35005-052130)
Thermo Scientific Hypersil GOLD 5 μm , 100 x 2.1 mm. (part number 25005-102130)

Instrumentation

Thermo Scientific Surveyor and Thermo Scientific LCQ Deca XP.

Peptides

Arg-Gly-Glu-Ser (RGES), Asp-Ser-Asp-Pro-Arg (DSDPR), Gly-Tyr (GY), Phe-Gln-pSer-Glu-Glu-Gln-Gln-Gln-Thr-Glu-Asp-Glu-Leu-Gln-Asp-Lys.

LC/MS Conditions

Mobile phase: A – H₂O + 0.1% formic acid; B – ACN + 0.1% formic acid

Gradient: 5 to 100% B in 10 min

Flow rate: 0.2 mL/min

Temperature: 30 °C

Detection: +ESI

Results and Discussion

Phosphopeptide retention on PGC

When analyzed under identical conditions the capacity factor for the monophosphopeptide on a porous graphitic carbon column is 3 times greater than when analyzed using an alkyl-silica stationary phase (Figure 1). On the PGC column

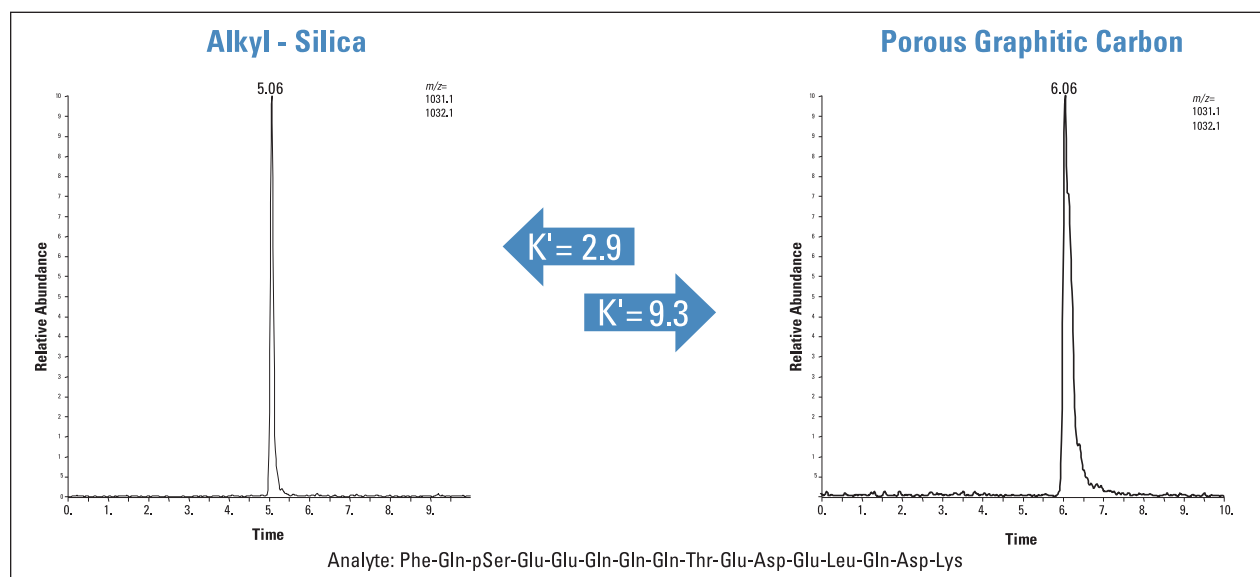


Figure 1: Comparison of the capacity factor of a monophosphorylated peptide on an alkyl-silica phase and PGC.

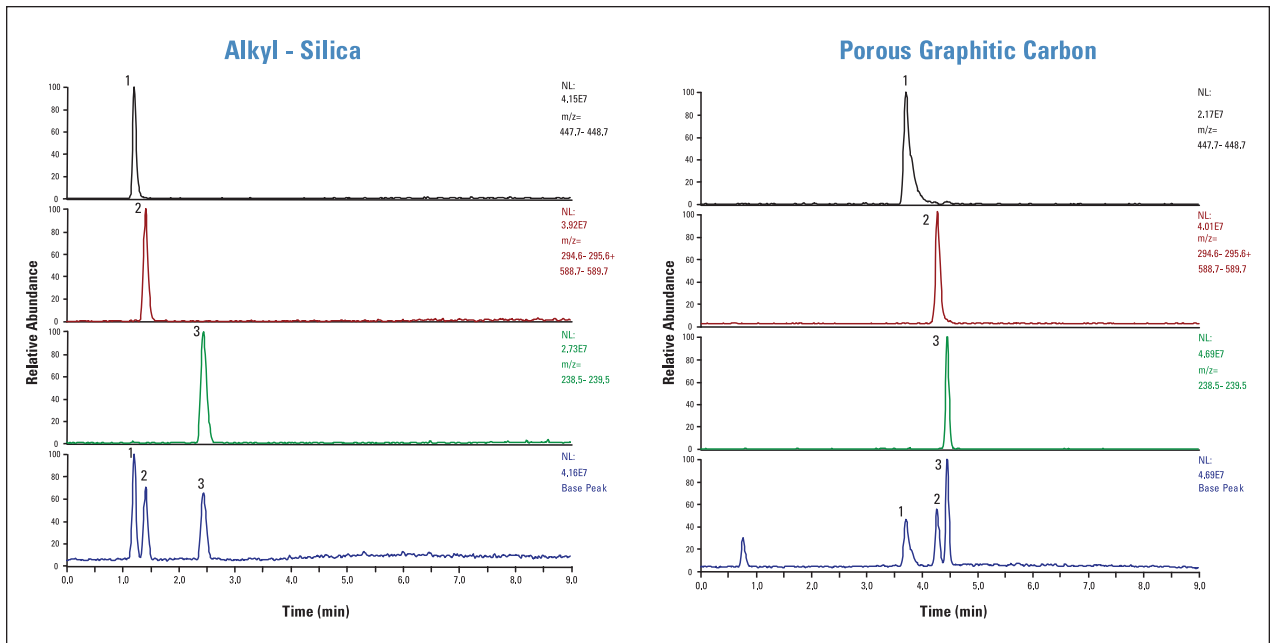


Figure 2: Comparison of the retention of 3 hydrophilic peptides on alkyl-silica and porous graphitic carbon. PGC provides higher retention and different selectivity. Analytes: 1. Arg-Gly-Glu-Ser (RGES); 2. Asp-Ser-Asp-Pro-Arg (DSDPR); 3. Gly-Tyr (GY)

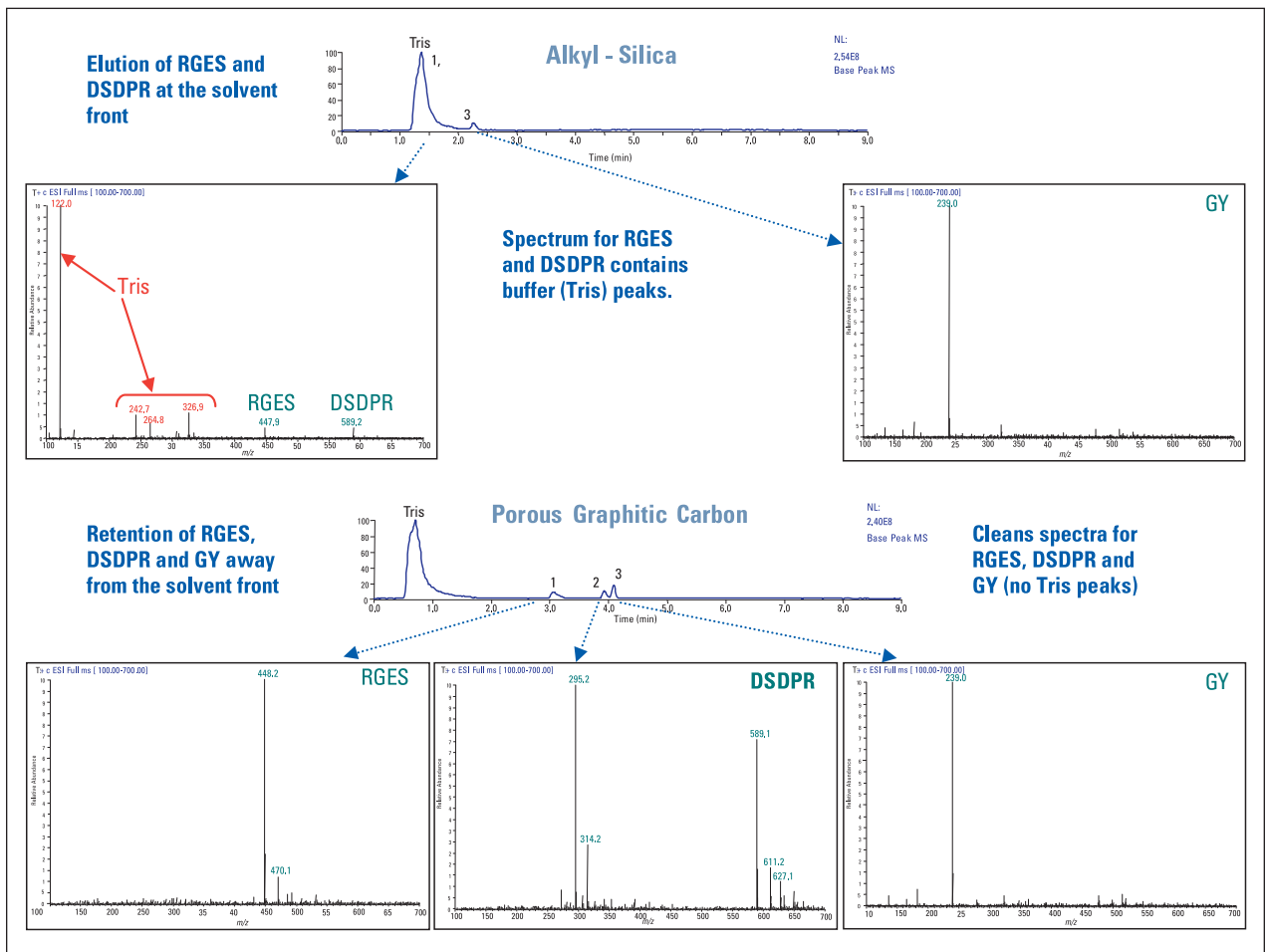


Figure 3: Comparison of the spectra obtained for 3 hydrophilic peptides in Tris buffer on alkyl-silica and porous graphitic carbon stationary phases

the retention mechanism is a combination of hydrophobic or dispersive interaction with the hydrophobic amino acid chain, and a polar interaction between the phosphate group and the polarizable surface of the graphite.

Di- to penta- hydrophilic Peptides

In Figure 2 the retention of a di-, a tetra- and a penta-peptide is compared on the alkyl-silica phase and on PGC. On the alkyl-silica phase, typically used in the separation of proteolytic digests, RGES elutes at the solvent front, closely followed by DSDPR. The basic (Arg) and alcohol (Ser) terminal residues make these short peptides hydrophilic and difficult to retain under conventional reversed-phase LC/MS conditions. On the PGC column these short peptides are well retained away from the solvent front.

A flow-through fraction from a proteolytic digest was simulated by diluting a solution containing three hydrophilic peptides in Tris buffer (100 mM, pH 8.0) to concentrations in the range of 15 to 30 pmol/ μ L. This fraction was injected and separated on an alkyl-silica phase and on PGC (Figure 3). On the alkyl-silica phase the two more polar peptides (RGES and DSDPR) elute at the solvent front, co-eluting with the chromatographic peak for Tris. The spectrum for these peptides is dominated by the Tris peaks at m/z 122, 243, 265 and 327, showing very weak signals for the $[M+H]^+$ at m/z 448 and 589. On the other hand, the PGC stationary

phase effectively separates these peptides away from the Tris chromatographic peak, producing clean and intense spectra, that allow for good identification.

The chromatographic retention and resolution of the hydrophilic peptides on the PGC column enables quantitative data to be obtained. On Figure 4 the linearity of the response is demonstrated for concentrations in the range of 5 pg/ μ L to 1 ng/ μ L of each peptide.

Conclusion

- Porous graphitic carbon columns show increased capacity factors over alkyl-silica columns for phosphorylated peptides.
- In contrast to alkyl-silica stationary phases, porous graphitic carbon retains small hydrophilic peptides away from the solvent front under typical reversed-phase LC/MS conditions; as a result the spectra are free from biological buffer and salts allowing for good peptide identification even at low levels.
- Quantitative analysis of small hydrophilic peptides on porous graphitic carbon columns can be achieved with excellent linearity.

References

1. E. T. Chin, D. I. Papac, *Anal. Biochem.*, 273 (1999) 179-185.
2. P. Ross, *LCGC Europe*, May 2000

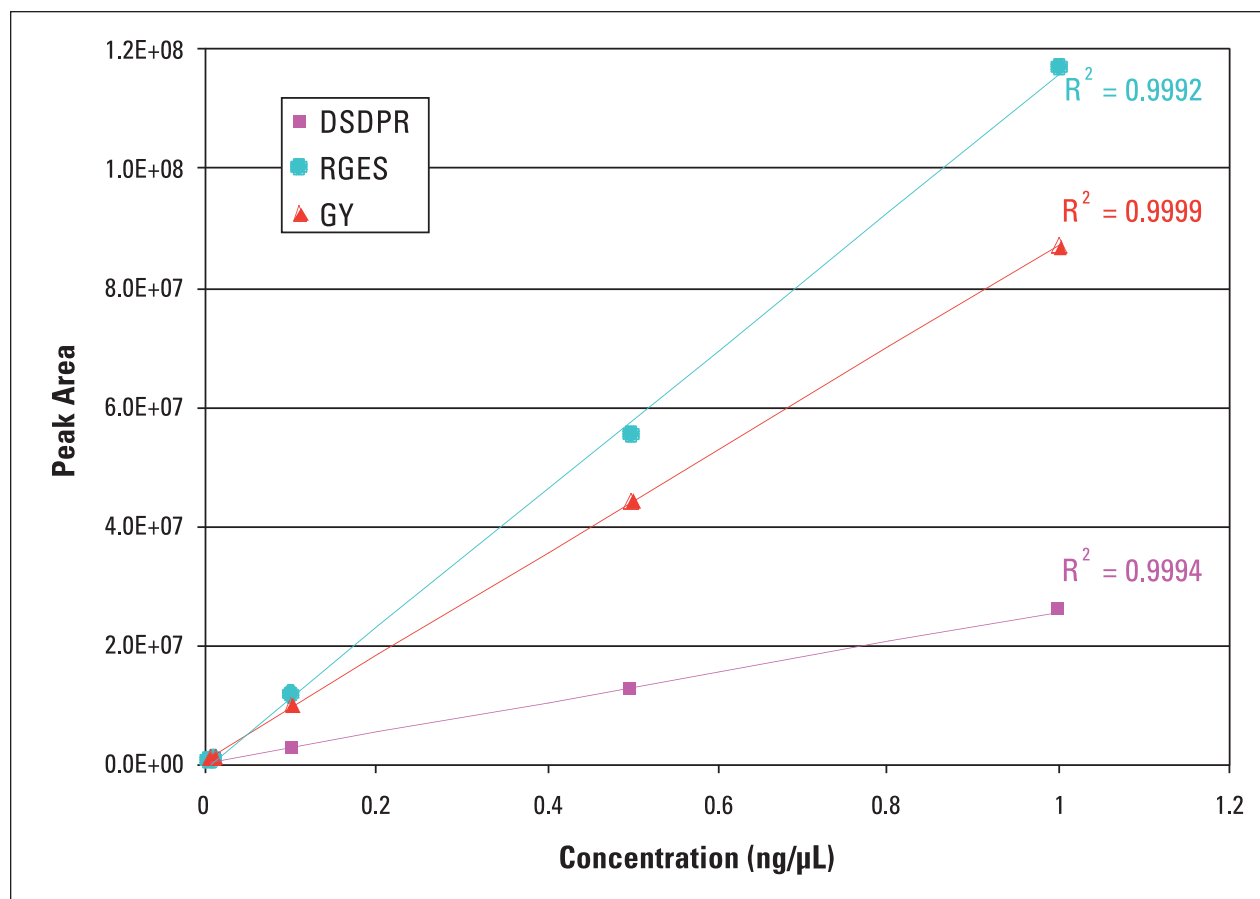


Figure 4: Linearity data for concentrations of 5 pg/ μ L to 1 ng/ μ L of each peptide injected on the Hypercarb column

Analysis of Glycopeptides Using Porous Graphite Chromatography and LTQ Orbitrap XL ETD Hybrid MS

Terry Zhang, Rosa Viner, Zhiqi Hao, Vlad Zabrouskov, Thermo Fisher Scientific, San Jose, CA, USA

Introduction

Glycosylation of Asn, Ser or Thr is arguably the most common known post-translational modification (PTM), resulting in a multitude of highly heterogeneous protein isoforms.^{1,2} While the physicochemical differences among the glycosylated protein molecules are often minute, their characterization remains a great analytical challenge. To date, although there are reports of glycoproteome analyses based on electrophoresis techniques, an LC-MS/MS based approach offers advantages in speed, sensitivity, and automation³. It remains the most powerful and versatile technique for elucidation of glycopeptide structure. However, in addition to the difficulties in capturing minor glycopeptides efficiently from samples containing large amounts of non-glycosylated peptides produced by proteolytic digestion of complex protein mixtures, commonly used collision-induced dissociation (CID) has limitations for determining the modification site due to the labile nature of the glycan attachment to the peptide ion.³ CID MS/MS predominantly generates fragment ions from cleavages of glycosidic bonds without breaking amide bonds.^{1,2} In contrast to CID, electron transfer dissociation (ETD) preserves labile PTMs while cleaving peptide bonds, making the identification of modification sites possible.^{4,5} Since glycosylated proteins and the resulting peptides are generally very heterogeneous, their mass spectra are highly complex, consequently high-quality liquid chromatography, high mass resolution, and accurate mass measurements of ETD precursors and fragments are essential for glycopeptide analysis. The high-resolution, high-mass-accuracy measurements of the Thermo Scientific LTQ Orbitrap XL ETD hybrid mass spectrometer coupled with additional capabilities such as parallel acquisition, in-source CID, and alternating CID/ETD dissociation can enable a thorough characterization of glycopeptides in a single analysis.

In this study, several glycoproteins: bovine α 1-acid glycoprotein, fetuin and human α 1-acid glycoprotein, were analyzed using nano LC-MS/MS. The performance of C₈, C₁₈, and porous graphite columns were systematically evaluated and optimized for glycopeptide separation prior to mass spectrometry analysis by an LTQ Orbitrap XL ETD™.

Goal

To demonstrate the advantages of porous graphite chromatography and electron transfer dissociation for analysis of N-glycopeptides on an LTQ Orbitrap XL ETD hybrid mass spectrometer.

Experimental Conditions

Sample Preparation

Glycoproteins purchased from Sigma were denatured in 0.1% SDS 50 mM Tris HCl buffer (pH 8.5), reduced with 5 mM DTT for 1 hr at 60 °C and alkylated with 25 mM iodoacetamide for 2 hr in the dark at room temperature. Then reduced and alkylated proteins were precipitated with acetone, digested, and analyzed by nano-LC-MS². The experiments were conducted on LTQ XL ETD and LTQ Orbitrap XL ETD mass spectrometers using the following conditions:

LC Separation

HPLC System:	Thermo Scientific Surveyor MS Pump with a flow splitter
Columns:	C8 column (75 μ m x 5 cm); C18 column (150 μ m x 10 cm) Thermo Scientific Hypercarb porous graphite column, 75 μ m x 5 cm (part number 35005-050065)
Mobile Phases:	A: 0.1% Formic acid; B: 0.1% Formic acid in acetonitrile
Gradient:	For Hypercarb™ column 5–50% B in 30 minutes For RP columns 5–35% B in 30 minutes

MS Analysis

Mass Spectrometer:	LTQ XL™ linear ion trap mass spectrometer with ETD and nano-ESI source
Spray Voltage:	2 kV
Capillary Temp:	160 °C
Capillary Voltage:	35 V
Tube Lens:	125 V
MS ⁿ Target:	1e4
Mass Range:	50–2000 m/z or 100–4000 m/z
Anion Reagent:	Fluoranthene
Anion Reagent Isolation:	On
Anion Target:	2e5
Max Anion Injection Time:	50 ms
ETD Reaction Time:	75–150 ms
Mass Spectrometer:	LTQ Orbitrap XL ETD hybrid MS
Mass Range:	400–2000 m/z , resolution 60,000–100,000 @ m/z 400
FT MS AGC Target:	5e5
FT MS/MS AGC Target:	1e5, 3 amu isolation width
MS/MS Resolution:	7,500 FWHM at m/z 400, 3 microscans
Monoisotopic Precursor Selection:	On
Exclusion Mass Tolerance:	10 ppm
Max Ion Time FT MS:	500 ms
Max Ion Time FT MS/MS:	500 ms
Full MS Range:	400–2000 m/z
MS/MS Mass Range:	100–2000 m/z
Survey Scan:	Source CID at 65 V for m/z 204

Data Processing

Thermo Scientific Xtract software was used for deconvolution of multiply charged precursors and MS/MS spectra. The GlycoMod tool from the Swiss-Prot website was used to assign possible oligosaccharide structures and compositions.

Results and Discussion

LTQ Orbitrap XL ETD Instrument

The LTQ Orbitrap XL ETD mass spectrometer is a high-resolution, accurate-mass hybrid mass spectrometer equipped with an ETD source.⁶ Figure 1 is the schematic of the LTQ Orbitrap XL ETD MS. The ETD anion reagent ions travel from the ETD source through the HCD collision cell and C-trap into the linear ion trap. There they are isolated and reacted with the precursor peptides ions in the ion trap. The resulting fragments can be measured in either the ion trap or Orbitrap™ mass analyzers. There are three additional fragmentation modes available on this instrument: higher-energy collisional dissociation (HCD), CID, and pulsed-Q dissociation (PQD).

Since CID and ETD can provide complementary glycopeptide structural information, coupling high-resolution, high-mass-accuracy full MS with alternating CID and ETD MS/MS makes comprehensive glycopeptide analysis achievable (Figure 2).^{4,5}

Choosing a Stationary Phase for Glycopeptide Analysis

We evaluated the performance of three stationary phases for LC analysis of glycosylated peptides. Figure 3 shows analysis of bovine α 1-acid glycoprotein on C_{18} and porous graphite columns. One pmol of protein digest was injected into C_{18} column versus 500 fmol on porous graphite column. The profiles are the extracted ion chromatograms of m/z 1706.3, 1138.5 and 867.3 belonging to 2+, 3+ and 4+ molecular ions of the bi-antennary glycopeptide ${}_{91}CVY\text{NCSFIK}_{99}$. The intensities of the 2+ and 3+ glycopeptide precursor ions from analysis with the porous graphite column were similar to the intensities from analysis with the C_{18} column despite 50% lower load on-column. This was likely due to the

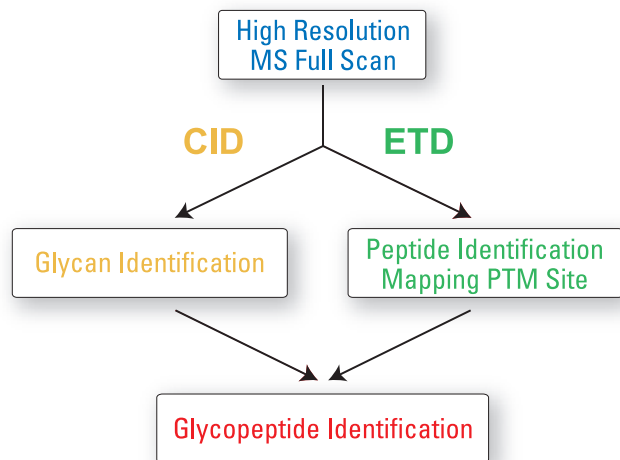


Figure 2: Glycopeptide analysis flow chart using an LTQ Orbitrap XL ETD hybrid mass spectrometer

higher affinity of porous graphite for hydrophilic peptides. In addition, chromatography using a porous graphite stationary phase promoted formation of abundant higher-charge-state metal-adducted precursor ions, which improved detection limits for all observed charge states of glycopeptides.

Figure 4 shows a high-resolution deconvoluted spectrum of these glycopeptides. At least one potassium adduct was observed for each glycoform. As demonstrated in Figure 3, formation of a metal adduct is likely responsible for producing higher-charge-state ions: $(M+K+3H)^{4+}$ precursor at m/z 867.3 was the dominant peak for glycopeptide 5 (Figure 4) while $(M+3H)^{3+}$ precursor at m/z 1138.6 was the dominant signal for glycopeptide 2 (Figure 4). Formation of higher-charge precursors can be explained by partial neutralization of sialic acid negative charges by metal cations.^{7,8}

Bovine and human α 1-acid glycoproteins contains five N-glycosylation sites with hybrid-type glycan structures.^{9,10} Four out of five glycopeptides were detected and identified using a porous graphite column compared to two out of five peptides on C_{18} and three out of five peptides on C_8 columns

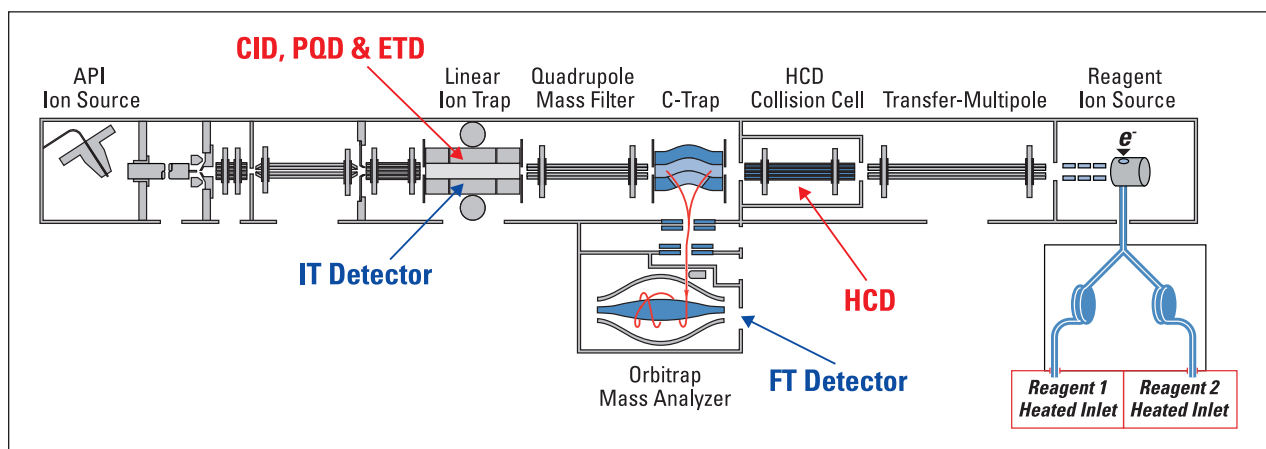


Figure 1: Schematic diagram of an LTQ Orbitrap XL ETD hybrid mass spectrometer

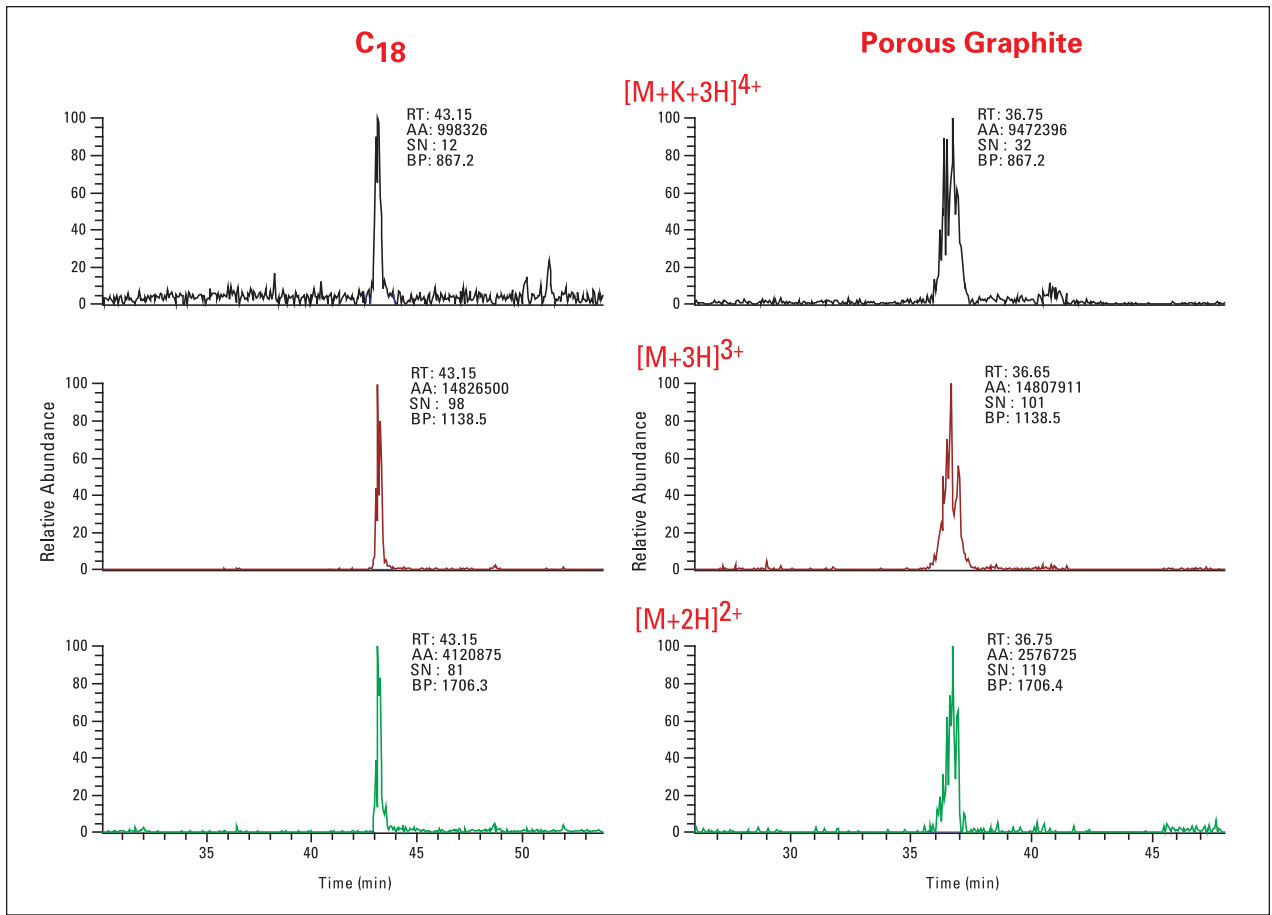


Figure 3: Comparison of different charge state extracted ion chromatograms of bovine α 1-acid glycoprotein bi-antennary peptide $_{91}$ CVYNCSEFIK $_{99}$ using C18 and porous graphite columns

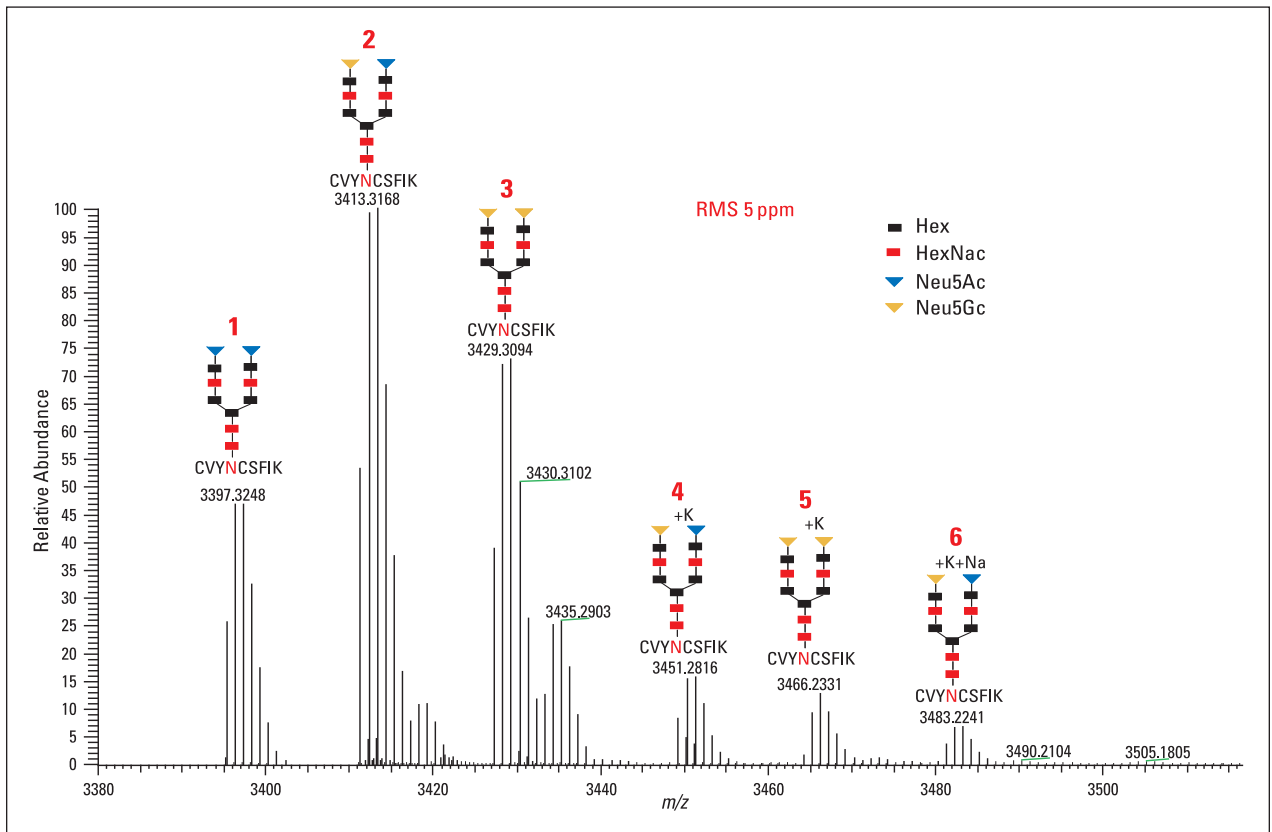


Figure 4: Deconvoluted full MS spectrum of bovine α 1-acid glycoprotein bi-antennary peptide $_{91}$ CVYNCSEFIK $_{99}$

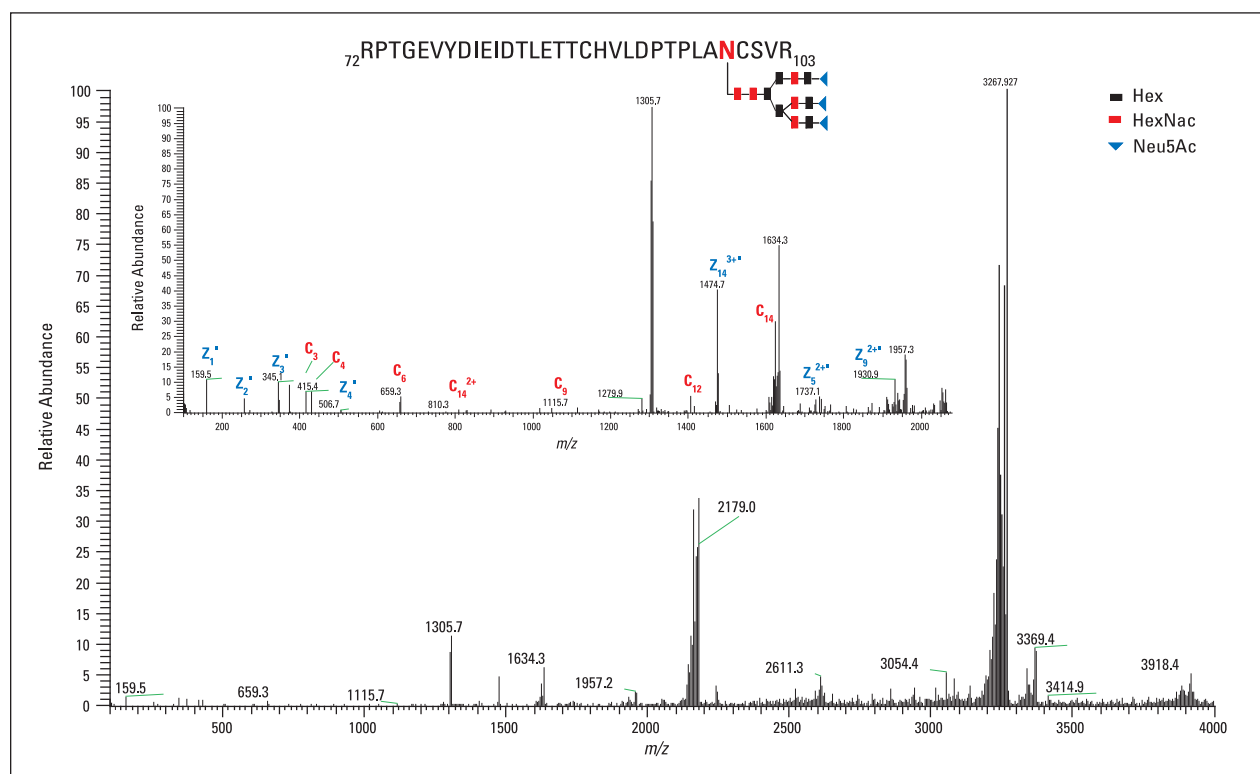
Peptides	Type of LC Column		
	Graphite	C18	C8
¹⁰³ QNGTLSK ₁₀₉	•		
⁵³ NPEYNK ₅₈	•		
⁹¹ CVYNCSEFK ₉₉	•	•	•
¹²⁸ TFMLAASWNGTK ₁₃₉	•	•	•
¹⁹ QSPECANLMTVAPITNATMDLLSGK ₄₃			•

Table 1: Bovine α 1-acid glycoprotein glycopeptides detected by nano LC-MS/MS

(Table 1) without any prior enrichment. Only the largest and most hydrophobic peptides were not detected using any of the phases. Similar results were obtained for bovine fetuin digest. All bovine fetuin glycopeptides could be detected using C₁₈² or C₈ chromatography. However, they were mostly present as lower-charge species, resulting in poorer MS/MS ETD spectra without enough information for their unambiguous identification. Previously, Alley and co-workers reported that fetuin glycopeptides could not be observed after separation on a graphite HPLC Glycan Chip.¹¹ Our studies indicated that larger hydrophobic peptides elute much later in the gradient. Nevertheless, three out of four fetuin peptides were identified after separation on the porous graphite column. Only the largest O-glycosylated 246-306 peptide was not detected. Figure 5 shows an example of an ETD spectrum of 5+ precursor at m/z 1307 of bovine fetuin tri-antennary peptide ⁷²RPTGEVYDIEIDTLETTCHVLDPTPLANCSVR₁₀₃, which was successfully identified after separation on porous graphite column. After optimization, all nano LC-MS/MS analyses of glycopeptides were performed using a porous graphite column and 1 pmol of glycoprotein digest.

MS/MS Analysis of Glycopeptides

To identify glycopeptides, we utilized a strategy described by Peterman and Mulholland², where in-source CID generated characteristic oxonium ions at m/z 204 and/or 366 and were further fragmented by a dedicated MS³ event. This allowed for a highly sensitive and selective detection of the eluting glycosylated peptide ion(s) at a given retention time. High-resolution, accurate-mass full-scan MS was measured in the Orbitrap mass analyzer, as shown in Figure 6, followed by data-dependent MS/MS alternating CID and ETD scans with fragments analyzed in either the ion trap or Orbitrap mass analyzers. The resulting CID spectra of the 3+ precursors (Figure 6c) were used for glycan structure elucidation and the ETD spectra of the 4+ precursors (Figure 6b) were used for glycopeptide identification as demonstrated in Figures 7 and 8 for the bovine α 1-acid glycoprotein peptide ¹⁰³QNGTLSK₁₀₉. Figure 7, inset, shows the CID spectrum of the precursor [M+3H]³⁺ at m/z 990.395 measured in the Orbitrap mass analyzer. The oxonium fragment ion at m/z 366 confirmed this precursor as a glycopeptide. The spectrum was deconvoluted and glycan composition was assigned as shown in Figure 7. This glycoform contains one each of N-acetylneuraminic (Neu5Ac) and N-glycolyeuraminic (Neu5Gc) acids at the glycan branch end as determined by the presence of 657/673 fragment pair. The product ion at m/z 950.4805 corresponds to [M-GlcNAc+H]⁺. All measured masses were within 5 ppm of their theoretical values which helped unambiguously assign the glycan portion as a bi-sialated glycopeptide structure.

Figure 5: Ion trap MS/MS ETD spectrum of bovine fetuin tri-antennary peptide ⁷²RPTGEVYDIEIDTLETTCHVLDPTPLANCSVR₁₀₃ (5+, m/z 1307). Inset: Magnified region for scan range 100-2000 m/z .

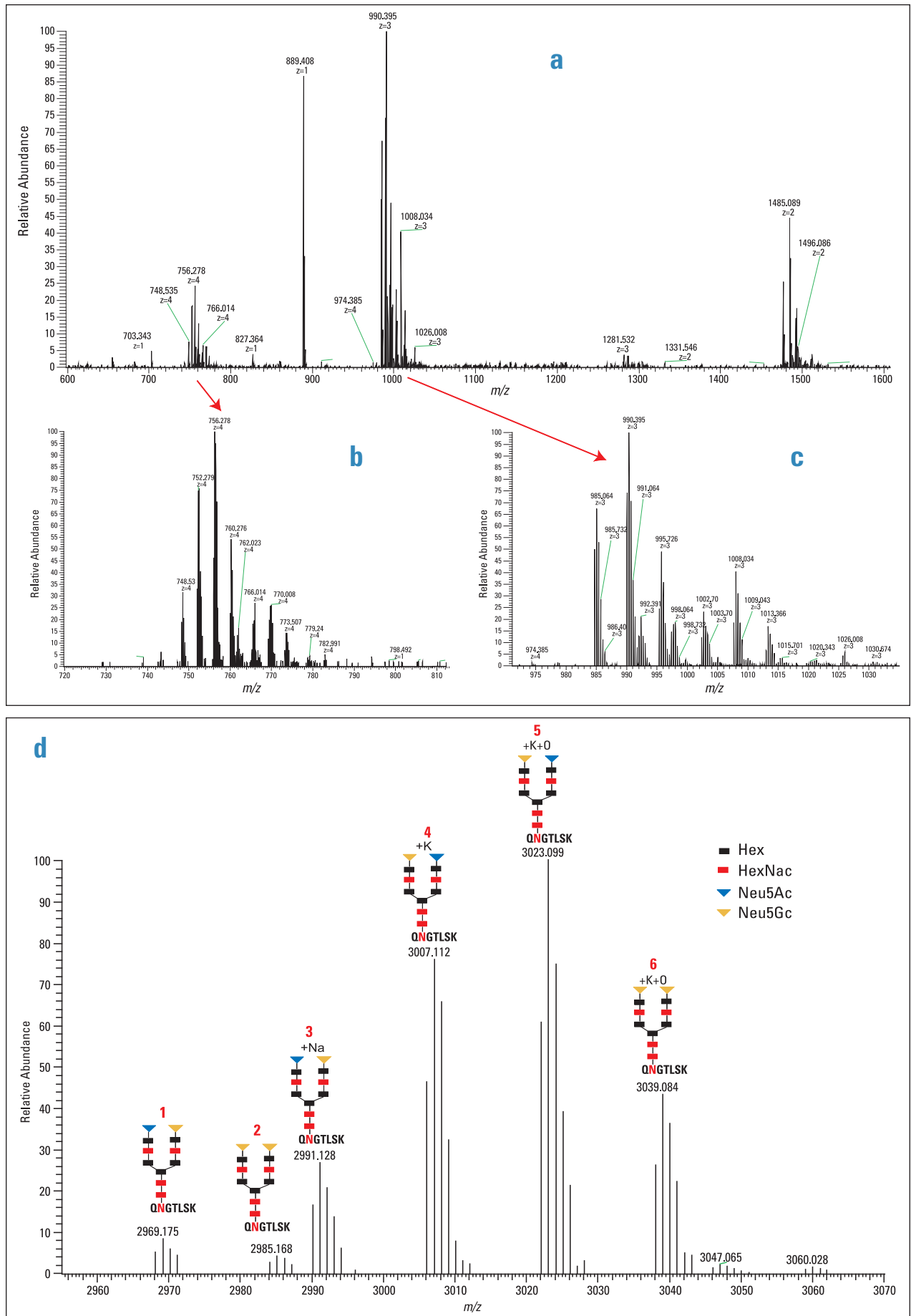


Figure 6: a) MS full scan; b, c) zoomed in charge states 4+, 3+ showing highly heterogeneous glycoforms; d) deconvoluted full MS spectrum of bovine α 1-acid glycoprotein bi-antennary peptide $_{103}\text{QNGTLSK}_{109}$.

Higher-charged 4+ metal-adducted precursor ions were further selected for ETD analysis. From the ETD MS/MS spectrum of the precursor $[M+K+O+3H]^{4+}$ as shown in Figure 8, the glycosylation site was clearly identified at

Asn 104 based on an almost complete series of c/z^* ions. No significant loss of carbohydrate was detected and, as expected, several of the observed glycan-containing fragments retained potassium ions. The high-resolution, high-mass-

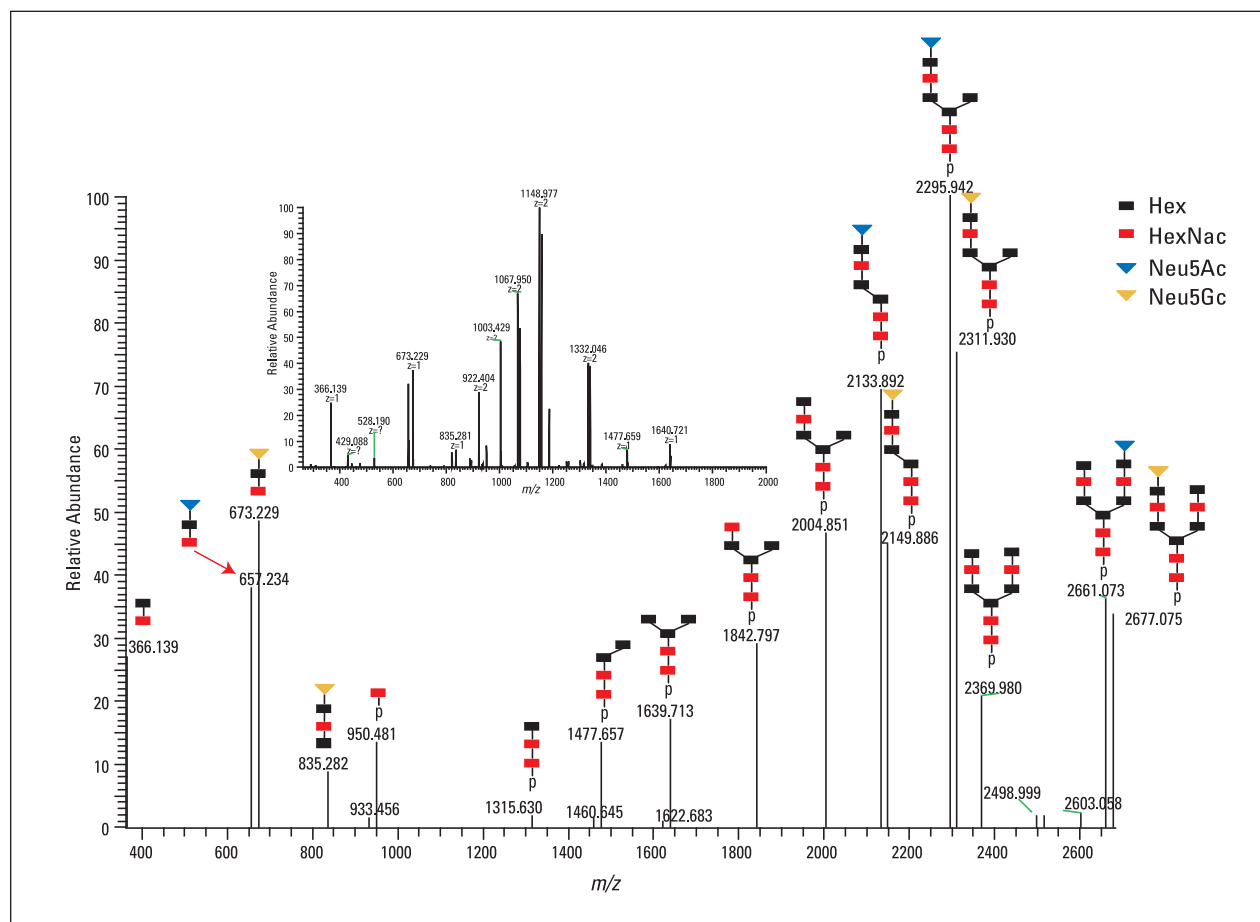


Figure 7: Deconvoluted Orbitrap CID MS/MS spectrum of bovine α 1-acid bi-antennary glycopeptide $_{103}\text{QNGTLSK}_{109}$. Insert shows original Orbitrap CID spectrum of 3+ parent at m/z 990.395 (Figure 6d, structure 1).

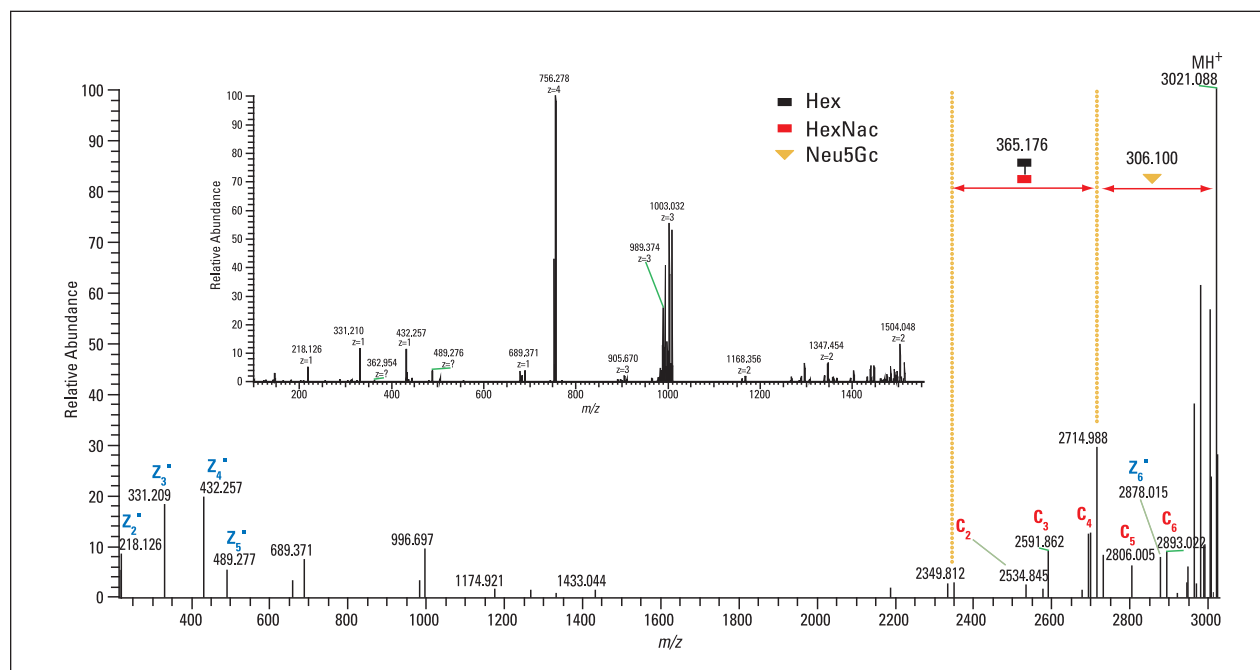


Figure 8: Deconvoluted Orbitrap ETD MS/MS spectrum of bovine α 1-acid bi-antennary glycopeptide $_{103}\text{QNGTLSK}_{109}$. Insert shows original Orbitrap ETD spectrum of $[M+K+O+3H]^{4+}$ at m/z 756.278 ion (Figure 6d, structure 5).

accuracy and low chemical noise of the Orbitrap mass analyzer significantly benefited ETD analysis of glycopeptides with charge states 4+ and above, allowing straightforward deconvolution and interpretation of spectra (Figure 8).

Conclusions

- The Hypercarb porous graphite column demonstrated excellent separation for glycopeptide analysis, especially for short, hydrophilic peptides containing bi- or tri-antennary glycan chains. It allowed for their sensitive detection without any prior enrichment.
- Formation of metal adducts promoted evolution of higher-charge species, aiding ETD fragmentation of glycopeptides.
- ETD preserved labile glycans, facilitating the identification of both the peptide of interest and the site of modification.
- Combining peptide structural information obtained by ETD and the glycan composition information obtained by CID enabled confident identification and characterization of glycopeptides within a single LC-MS analysis using an LTQ Orbitrap XL ETD mass spectrometer.

References

1. Morelle, W., Canis, K., Chirat, F., Faid, V. and Michalski, J.-C. (2006) The use of mass spectrometry for the proteomic analysis of glycosylation. *Proteomics*, 6, 3993-15.
2. Peterman, S.M. and Mulholland, J.J. (2006) A novel approach for identification and characterization of glycoproteins using a hybrid linear ion trap/FT-ICR mass spectrometer. *J. Am. Soc. Mass Spectrom.*, 17(2), 168-79.
3. Kaji, H., Isobe, Toshiaki, (2008), Liquid Chromatography/Mass Spectrometry (LC-MS)-Based Glycoproteomics Technologies for Cancer Biomarker Discovery. *Clinical Proteom.*, 4:14-24
4. Syka J.E., Coon J.J., Schroder M.J., Shabanowitz J, Hunt D.F. (2004) Peptide and protein sequence analysis by electron transfer dissociation mass spectrometry. *Proc. Natl. Acad. Sci. USA*; 101, 9528-33.
5. Alley Jr., W.R., Merchref, Y. and Novotny, M.V. (2009) Characterization of glycopeptides by combining collision-induced dissociation and electron-transfer dissociation mass spectrometry data. *Rapid Commun. Mass Spectrom.*, 23, 161-170.
6. McAlister, G.C., Phanstiel, D., Good D.M., Berggren, W.T. and Coon, J.J. (2007) Implementation of electron-transfer dissociation on a hybrid linear ion trap-orbitrap mass spectrometer. *Molecular & Cellular Proteomics*, 2007, 6, 1942-1951.
7. Newton, K.A., Amunugama, R. and McLuckey, S.A. (2005) Gas-phase ion/ion reactions of multiply protonated polypeptides with metal containing anions. *J. Phys. Chem. A.*, 109(16), 3608-16.
8. Medzihradzky, K.F., Guan, S., Maltby, D.A. and Burlingame, A.L. (2007) Sulfopeptide fragmentation in electron-capture and electron-transfer dissociation. *J. Am. Soc. Mass. Spectrom.*, 18(9), 1617-24.
9. Snovida, S.I., Chen, V.C., Krokhin, O. and Perreault, H. (2006) Isolation and identification of sialylated glycopeptides from bovine α 1-acid glycoprotein by off-line capillary electrophoresis MALDI-TOF mass spectrometry. *Anal. Chem.*, 78, 6556-635
10. Treuheit, M.J., Costello, C.E. and Halsall, H.B (1992) Analysis of the five glycosylation sites of human α 1-acid glycoprotein. *Biochem. J.*, 283, 105-12.
11. Alley Jr., W.R., Merchref, Y. and Novotny, M.V. (2007) Using graphitized carbon for glycopeptides separations prior to mass spectral detection. *Proceedings of the 55th ASMS conference*, Indianapolis.

The Use of Porous Graphitic Carbon LC-MS for the Analysis of Underivatised Carbohydrates from Wheat Stems

Sarah Robinson, Thermo Fisher Scientific, Hemel Hempstead, UK

Introduction

The stems of wheat (*Triticum aestivum*) contain pith, which varies in quantity between different cultivars and at different stages of the growth cycle. It is known that stored in the pith is a pool of endogenous water soluble carbohydrate metabolites, and that these carbohydrates are translocated into the plant's grains.¹ It has further been suggested that some wheat genotypes, which contain high concentrations of soluble carbohydrates in their stems, may be able to deposit more carbohydrates into the grains of the plant and significantly increase the grain yield.²

The separation and detection of such a pool of oligosaccharides is not easy owing to the fact that these analytes are very polar, potentially highly branched, isomeric structures which contain no chromophore and which are poorly or completely unretained on reversed phase HPLC columns. Many workers tackle detection issues via derivatisation of the reducing terminal of their carbohydrate analytes, however, this presupposes that all carbohydrates are reducing.³ This additional step also demands extra time and sample handling, and involves inevitable losses, as well as changing the original structure of the analyte.

Here we present a rapid, robust and efficient chromatographic separation method that utilises the highly selective stationary phase of porous graphitic carbon in an on-line coupling of liquid chromatography with electrospray mass spectrometry (PGC-LC-MS). Additionally, we describe the development, characterization and use of a nanoscale LC column coupled with a nanospray ionisation source which enabled us to miniaturize the system and obtain much improved sensitivity.

Goal

To demonstrate the separation of a complex pool of branched, isomeric and underivatised oligosaccharides utilizing porous graphitized carbon liquid chromatography coupled with mass spectrometric detection.

Experimental

Sample Preparation

Post-harvesting, frozen wheat stems were cut into ~ 2 cm pieces and boiled for 30 min in ethanol. The ethanol extract was dried and the stem pieces further boiled in water for 30 min. The ethanol and water extracts were mixed and washed with hexane until all colouration had been removed. Each extract was filtered through an inert 0.22 µm syringe filter.

HPLC and nano-HPLC Methodology

Thermo Scientific Surveyor LC system

Mobile phase A: HPLC grade water

Mobile phase B: acetonitrile

Mobile phase C: 2-propanol

HPLC column: Thermo Scientific Hypercarb
100 x 4.6 mm, 5 µm (part number 35005-104630)

Flow rate: 600 µL/min

Nano-HPLC column: Thermo Scientific Hypercarb
100 x 0.1 mm, 5 µm (part number 35005-100165)

Flow rate: Flow split from 400 µL/min to 0.15 µL/min

The eluent gradient is presented in Table 1.

Mass Spectrometry

Thermo Scientific LCQ Deca XP ion trap mass spectrometer

Start	Flow	%A	%B	%C	%D
00.00	600	94	3	3	-
10.00	600	92	4	4	-
20.00	600	85	6	9	-
30.00	600	82	8	10	-

Table 1: Eluent gradient program for the HPLC system. Flow rate is reported as µL/min.

Ion source, polarity: ESI, positive ion mode

Spray voltage: 6 kV

Sheath gas: 70 units

Auxillary gas: 60 units

Capillary temperature: 350 °C

m/z 200 – 2000 at 5500 amu/s

Nanoscale Experiments

Nano-ion source & polarity: nano-ESI (front coated tip), positive ion mode

Nano-spray Voltage: 3.1 kV

Sheath and Aux gas: 0 units

Capillary temperature: 200 °C

Results and Discussion

A chromatographic approach that utilized a ternary gradient afforded better control of the separation of the oligosaccharide mixture. In the early part of the chromatographic separation mono, di, tri and tetrasaccharides were removed in a relatively steep aqueous/acetonitrile gradient. After these analytes were eluted the gradient was made gentler and the 2-propanol eluent was gradually increased in order to remove the larger

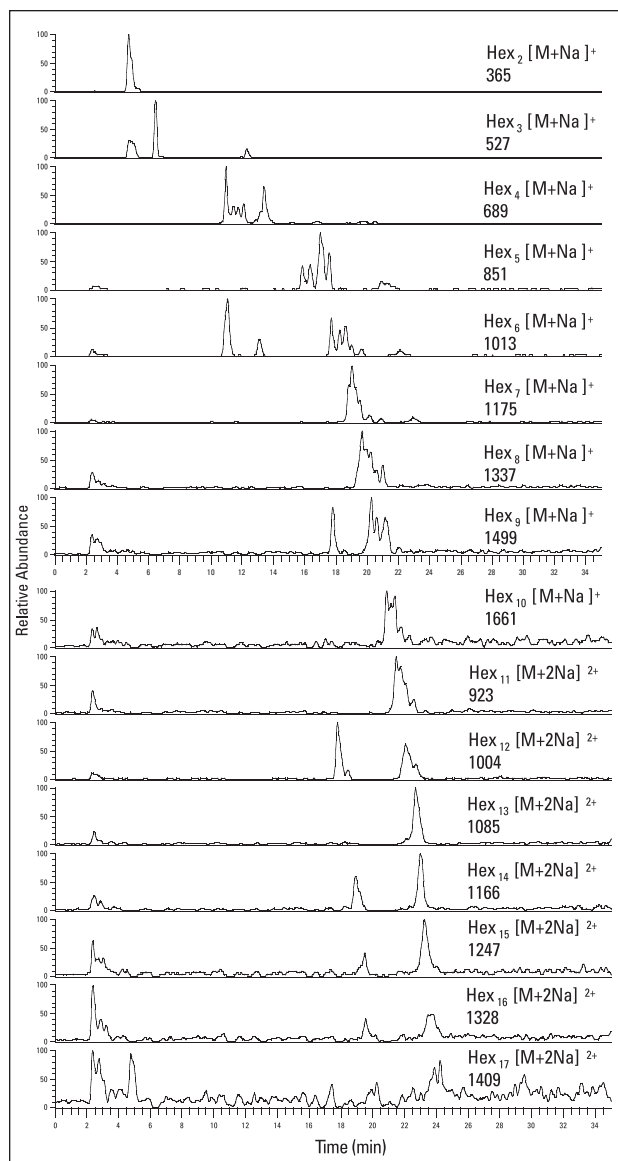


Figure 1: PGC-LC-MS selected ion chromatograms of underivatized oligosaccharides extracted from the stems of a wheat cultivar.

Reprinted with permission from *Anal. Chem.* 2007, 79, 2437-2445. Copyright 2009 American Chemical Society.

and very strongly retained oligosaccharides from the column. This method development ultimately allowed the successful separation of the complex mixtures of oligosaccharides that had been extracted from wheat stems and which ranged in size from dp 2 to dp 20, in under 30 minutes.

A series of selected ion chromatograms of the oligosaccharides extracted from the stems of one cultivar type are presented in Figure 1. Although ions consistent with Hex₁₈, Hex₁₉ and sometimes Hex₂₀ species were observed in the full scan mass spectra, their ion intensities were not significantly different from background, so that their ions were not distinguishable in the SIC. In the mass spectra we observed sodiated singly charged, doubly charged and dimeric (two analyte molecules with one charge-bearing cation) species of the oligosaccharide analytes in the extracts from wheat stems (Figure 2).

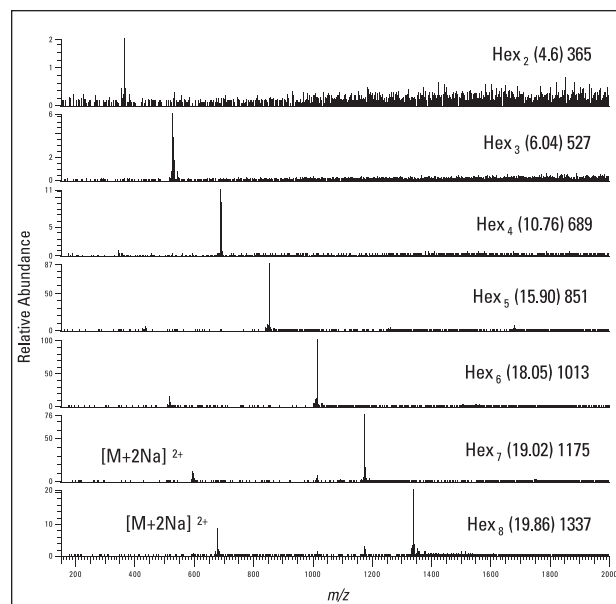


Figure 2: PGC-LC-MS positive ion mass spectra of underivatized oligosaccharides extracted from the stems of a wheat cultivar. Retention times are marked in brackets, m/z value of sodiated or disodiated molecules follows.

Reprinted with permission from *Anal. Chem.* 2007, 79, 2437-2445. Copyright 2009 American Chemical Society.

It was noted that the elution order of the oligosaccharides was not necessarily in the order of increasing oligosaccharide size; sometimes larger oligosaccharides co-eluted with a smaller oligosaccharide. For example in Figure 1, a Hex₆ chromatographic peak (t_R : 11 min) can be observed to co-elute with a Hex₄ chromatographic peak (t_R : 11 min), while further Hex₆ peaks elute later in the chromatographic run. Since planar molecules are more strongly retained on PGC than less planar molecules (as they do not induce as strong dipole interactions with the PGC surface), we propose that the elution order of differently sized oligosaccharides is further evidence that these analytes are isomeric structures.

There are many reported benefits of using miniaturized systems, for example the use of nanoscale electrospray can overcome sensitivity problems found when analysing neutral oligosaccharides in conventional microscale electrospray.⁴ In light of these observations, and more importantly the recent availability of nanoscale PGC columns, we decided to compare the limit of detection (LOD) of the on-line PGC-LC-MS separation with the LOD obtainable using an on-line nanoscale system. Based on the column dimensions it could be predicted that the linear velocity of the mobile phase would be 1.9 times higher in the 4.6 mm column. After optimisation we could reproduce a similar chromatographic separation of oligosaccharides extracted from wheat stems in 50 min (compared with 30 min using the 4.6 mm column) (Figure 3). Our LOD comparative study utilized a dilution series of a standard fructan trisaccharide compound, 1-kestose. The solutions were analysed using the HPLC and the nanoHPLC-MS method and samples were analysed in the order of decreasing concentration. From the SIC of each sample run in triplicate, the average peak height was calculated. An approximation of the noise level in the system was made by measuring the noise level in the baseline close to the analyte chromatographic peak. A signal three times the noise was used as an approximation to the detection limit.

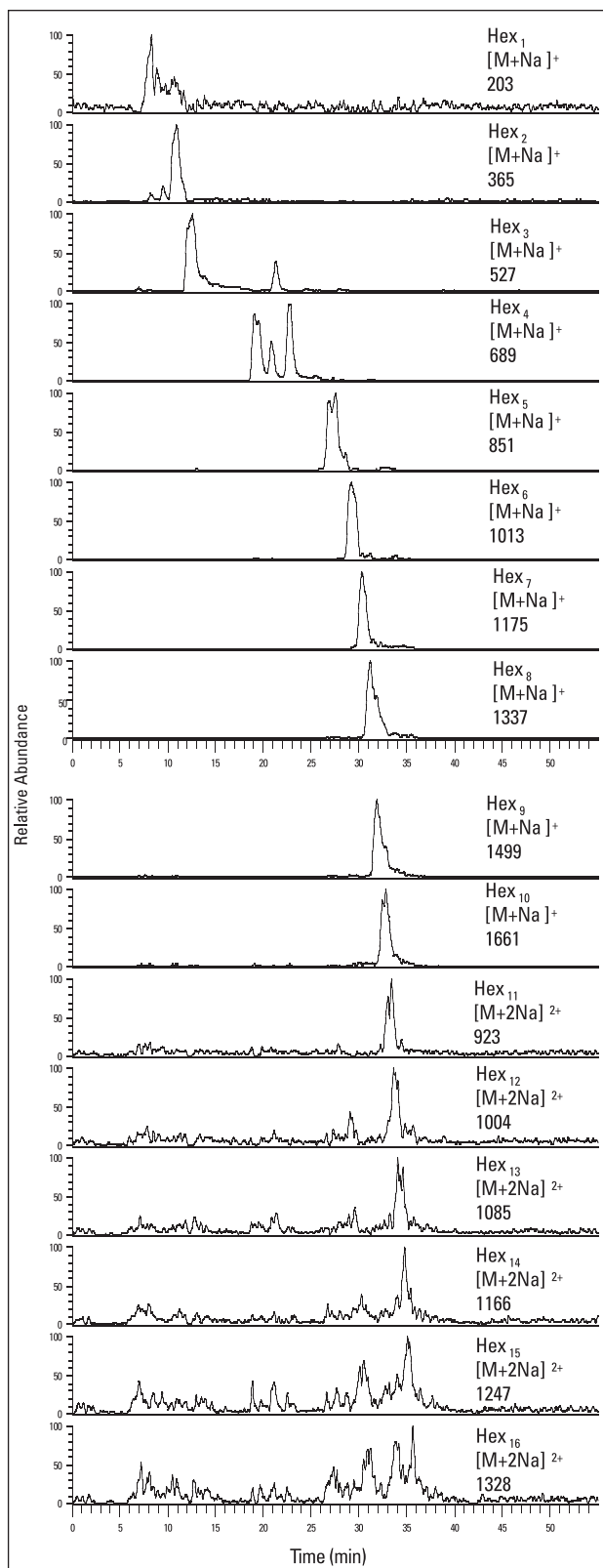


Figure 3: PGC-nanoLC-MS selected ion chromatograms of underivatized oligosaccharides extracted from the stems of a wheat cultivar.

Reprinted with permission from *Anal. Chem.* 2007, 79, 2437-2445. Copyright 2009 American Chemical Society.

The lowest concentration from the dilution series injected that could be detected in the PGC-LC-MS and PGC-nanoLC-MS analysis of 1-kestose was 5 μM and 50 pM respectively. From the peak height and the noise measured in the single ion chromatogram of these analyses the *concentration limit of detection* for this analyte in this system was calculated as 14 nM and 14 pM respectively. Thus, it may be concluded that there is a 1000 fold improvement in the *concentration LODs* when using the 0.1 mm column compared with the 4.6 mm column.

In addition to calculating the *concentration LOD* of each system, the *amount LOD* for the two systems was calculated by multiplying the concentration LODs by the injection volumes of 20 nL and 10 μL used for the 0.1 mm and 4.6 mm columns respectively. It was concluded that there is a 500,000 fold increase in absolute amount sensitivity when using the 0.1 mm column compared with the 4.6 mm column.

Conclusion

We have developed and optimised an on-line LC-MS method, using a PGC stationary phase, for the separation of a complex mixture of non-reducing oligosaccharides extracted from the stems of wheat in 30 minutes. Our system displays high chromatographic resolution and selectivity for a broad size range of isomeric oligosaccharides in a relatively short analysis time. In addition, the system is robust and automation has allowed very high throughput of samples.

We have shown that significantly smaller quantities of analyte are required for detection when using a nanobore PGC LC column and nanoESI source compared with those required for use with the microbore PGC LC column and microESI source. The amount LODs calculated from the nanoscale experiments also suggest that analytes are detected at the zeptomol level. Nanoscale analysers are also 'greener' as they create significantly less organic solvent waste.

Our method has been applied to the analysis of wheat cultivar crosses to study further the link between stem carbohydrate and grain yield, but also this system could be applied to the analysis of other highly polar analytes that have previously been difficult to analyse by other separation methods.

References and Acknowledgements

The full text article that further describes the data presented in this application note may be found with the following reference:

Robinson, S., Bergstrom, E., Seymour, M., Thomas-Oates, J.E. *Anal. Chem.* 2007, 79, 2437-2445.

1. Wardlaw, I. F., Porter, H. K. *Aust. J. Biol. Sci.* 1967, 20, 309-18.
2. Ford, M. A., Blackwell, R. D., Parker, M. L., Austin, R. B. *Ann. Bot.* 1979, 44, 731-38.
3. Mechref, Y.; Novotny, M. V. *Chem. Rev.* 2002, 102, 321-69.
4. Bahr, U., Pfenninger, A., Karas, M. *Anal. Chem.* 1997, 69, 4530-35.

Quantitation of Acrylamide in Food Samples on the TSQ Quantum Discovery by LC/APCI-MS/MS

Kevin J. McHale, Witold Winnik, Gary Paul, Thermo Fisher Scientific, Somerset, NJ, USA

Introduction

Acrylamide has been identified as a potential human carcinogen. This is important not only because acrylamide is a common industrial chemical, but acrylamide has been shown to be present at significant levels in food samples,¹ particularly cooked foods high in carbohydrates. This has led many government health agencies around the world to assess the risk of short- and long-term exposure to acrylamide in humans.

This has led to the development of LC-MS/MS methodology for the quantitative analysis of acrylamide in foodstuffs.¹⁻⁵ While a GC/MS protocol for the analysis of acrylamide exists, this method requires extensive sample cleanup and chemical derivatization.⁶ The advantage of LC-MS/MS is that chemical derivatization is not necessary prior to acrylamide analysis.

To date, most LC-MS/MS methods for the assay of acrylamide have utilized an electrospray ionization (ESI) source for the production of acrylamide ions.¹⁻⁴ Yet it is well-known that ESI-MS is problematic when highly aqueous solutions, such as those required for the reversed-phase LC separation of acrylamide, are used.⁷ On the other hand, water does not pose a problem for the formation of a stable corona discharge used in APCI. One published report has demonstrated that APCI is a viable ion source for the production of acrylamide ions for LC-MS/MS detection.⁵ Furthermore, a study comparing ESI and APCI ion sources for the LC-MS/MS analysis of acrylamide showed that under the same chromatographic conditions, APCI-MS/MS yielded an improved detection limit.⁸

This report presents data acquired on the Thermo Scientific TSQ Quantum Discovery for the analysis of acrylamide. A simple LC-MS/MS method using the APCI source is used to measure acrylamide, via selective reaction monitoring (SRM), over a wide concentration range. A small selection of food samples was analyzed for acrylamide content following extraction with water. To preclude the need for a time-consuming solid-phase extraction procedure, a column-switching method was employed to selectively “fractionate” acrylamide from polar matrix interferences prior to LC-MS/MS detection.

Goals

1. **Development**—A sensitive and rugged LC/APCI-MS/MS assay for the analysis of acrylamide
2. **Application**—An on-line column-switching technique to aqueous food extracts as an alternative to solid-phase extraction (SPE) cleanup
3. **Measurement**—Acrylamide content in selected food samples

Experimental

Chemicals and Reagents: Acrylamide (> 99.0%) was purchased from Fluka (Buchs SG, Switzerland). 2,3,3-d3-acrylamide (98%) was obtained from Cambridge Isotope Laboratories (Andover, MA, USA). HPLC grade water was acquired from Burdick and Jackson (Muskegon, MI, USA). All chemicals were used as received without further purification.

Sample Preparation: Standards were prepared by dilution of a stock solution of 1.0 mg/mL acrylamide or 1.0 mg/mL d3-acrylamide in water. The stock solutions were stored at 4 °C for a period of no longer than two weeks.

Two brands of potato chips and two brands of breakfast cereals were purchased and stored at room temperature until processed. After homogenizing approximately 50 grams of a food sample, two grams were weighed into a 35 mL polypropylene centrifuge tube. Aqueous extraction of acrylamide was initiated by the addition of 20 mL water containing 1000 ng d3-acrylamide as the internal standard (final concentration = 50 ng/mL). The sample was vortexed for 30 s then subsequently centrifuged at 18,000 g for 15 minutes. Ten milliliters of the supernatant was decanted into a clean 35 mL centrifuge tube and centrifuged at 18,000 g for 10 minutes. Prior to analysis, 0.49 mL of the aqueous extract was filtered through a 0.45 µm centrifuge filter (Millipore Corp., Bedford, MA, USA) at 9,000 g for 5 minutes.

Sample Analysis: LC experiments were conducted with the Thermo Scientific Surveyor HPLC system. A Thermo Scientific Hypercarb 2.1 × 50 mm (part number 35005-052130) column was utilized as the analytical LC column. Separations of acrylamide were achieved under isocratic conditions using 100% water as the mobile phase at a flow rate of 0.4 mL/min. The injection volume for all LC experiments was 10 µL.

To eliminate the need for solid phase extraction (SPE) purification prior to the analysis of the food sample extracts, a column-switching LC method was employed. Briefly, the sample extract was loaded onto a 2.1 × 50 mm Thermo Scientific Aquasil C18 column (part number 77505-052130), which was positioned before a 6-port switching valve. The eluent from the C18 column was diverted to waste except for the period when acrylamide eluted from the C18 column, whereby the valve was switched to the Hypercarb column for MS/MS detection. This column-switching method required a second Thermo Scientific Surveyor MS pump, which also delivered 100% water at 0.4 mL/min. Both Surveyor MS pumps and the 6-port switching valve were controlled using Thermo Scientific Xcalibur version 1.3 software.

The experimental conditions for the TSQ Quantum Discovery were as follows:

Source: APCI

Ion polarity: Positive

Vaporizer Temperature: 375 °C

Discharge Current: 5 μ A

Ion Transfer Capillary Temperature: 250 °C

Source CID Offset: 6 V

Scan Mode: Selective Reaction Monitoring

Q2 Pressure: 1.0 mTorr argon

SRM Transitions: m/z 72 \rightarrow 55 for acrylamide;

m/z 75 \rightarrow 58 for d3-acrylamide

Collision Energy: 13 eV

Scan Width: 1.0 u

Scan Time: 0.3 s (each SRM transition)

Q1, Q3 Resolution: Unit (0.7 u FWHM)

Results and Discussion

Prior to the acquisition of acrylamide standards, it was important to determine if there was any detectable native acrylamide contribution originating from the deuterated internal standard. As shown in Figure 1, there is no acrylamide signal observed for the m/z 72 \rightarrow 55 SRM transition at the same retention time as the 50 ng/mL d3-acrylamide standard.

The limit of quantitation (LOQ) for acrylamide on the TSQ Quantum Discovery was 0.25 ng/mL acrylamide or 2.5 pg on column (Figure 2). This compares favorably to LOQs previously reported by other research groups, including an 8-fold improvement over the mass LOQ by LC/ESI-MS/MS (20 pg)¹ and a 40-fold improvement over the concentration LOQ on the TSQ 7000 (10 ng/mL),⁵ which used an LC/APCI-MS/MS method.

The calibration curve for acrylamide from 0.25 ng/mL to 2500 ng/mL is displayed in Figure 3. This calibration curve was generated using the column-switching LC method just prior to the acquisition of the food extracts data. A linear regression fit to these data using 1/x weighting yielded the following equation: $y = 5.5997 \times 10^{-4} + 0.0206125x$. The correlation coefficient for this curve was $r^2 = 0.9999$, indicating excellent linearity across the four orders of magnitude dynamic range. Table 1 summarizes the statistical results for the acrylamide calibration curve. At the LOQ, the accuracy, as a percent relative error, is 1.1% and the precision, as a percent coefficient of variance (%CV), is 12.1% for five replicate injections. Above the LOQ, the relative error varied from -2.9 to +2.4% and the %CV ranged from 0.5 to 6.7%.

Results obtained from the aqueous extract of Potato Chip 2 are presented in Figure 4. By utilizing a C18 column positioned before a switching valve to selectively elute acrylamide onto the Hypercarb column, background interferences are reduced. Unlike most of the other acrylamide reports where SPE cleanup was used following extraction of the sample with water,¹⁻⁴ the column-switching LC method employed here provides an on-line means of acrylamide fractionation. This has the advantage of minimizing sample losses during SPE and greatly reduces sample preparation time.

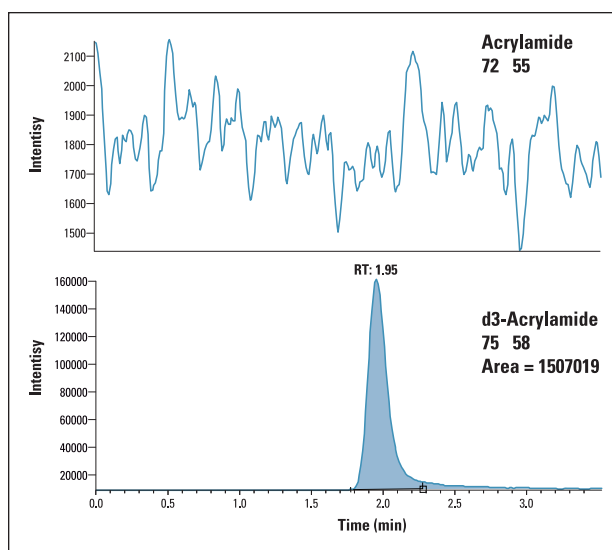


Figure 1: SRM chromatograms for 50 ng/mL d3-acrylamide

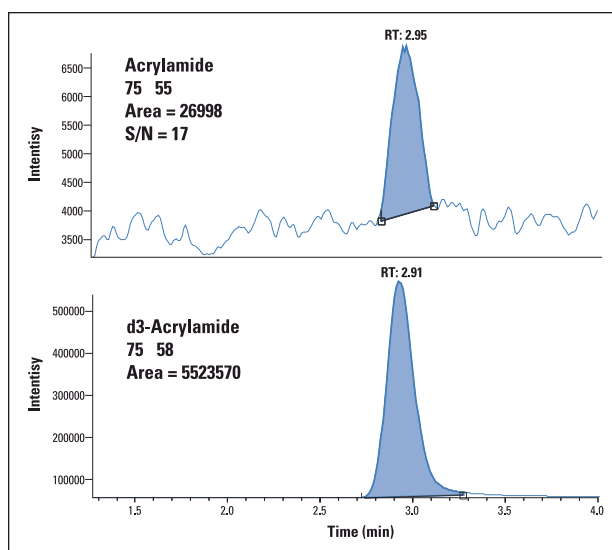


Figure 2: SRM chromatograms for 0.25 ng/mL acrylamide (LOQ) with 50 ng/mL d3-acrylamide

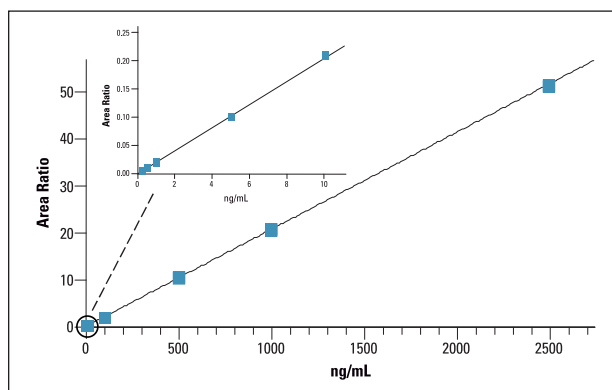


Figure 3: Calibration curve for acrylamide using column-switching LC method with APCI-MS/MS detection

Nominal (ng/mL)	Mean Conc. (ng/mL)	% Rel. Error	% CV	Number of Replicates
0.250	0.253	1.1	12.1	5
0.500	0.485	-2.9	6.7	5
1.00	1.00(4)	0.4	4.6	5
5.00	4.86	-2.7	0.9	5
10.0	10.2	2.1	0.7	5
100	101	0.7	0.5	5
500	512	2.4	0.8	3
1000	1006	0.6	0.6	3
2500	2481	-0.8	0.6	3

Table 1: Statistical data for the calibration curve of acrylamide

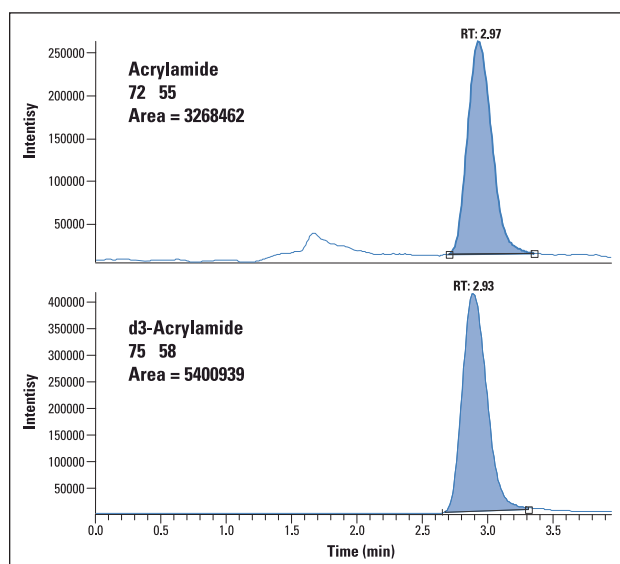


Figure 4: SRM chromatograms of the Potato Chip 2 sample aqueous extract

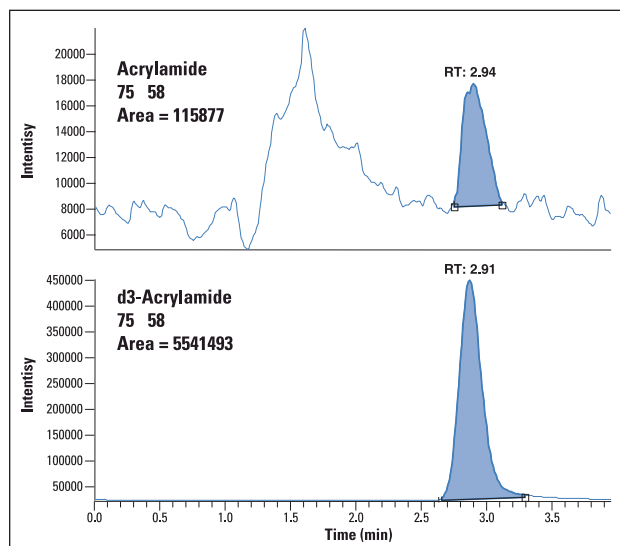


Figure 5: 1 ng/mL acrylamide standard analyzed directly after duplicate injections of the aqueous extract of the Potato Chip 2 sample

To monitor the consistency and reproducibility of the column-switching LC-MS/MS method, a 1 ng/mL acrylamide standard was analyzed immediately following each food sample. An example of this quality control standard analyzed after the Potato Chip 2 sample is shown in Figure 5. Although the baseline for the m/z 72 \rightarrow 55 SRM transition is somewhat elevated near the retention time for acrylamide, the calculated concentration for this standard is 0.99 ng/mL, equating to a relative error of -1.0%.

Table 2 reports the results for four different food samples that were assayed for acrylamide using the column-switching LC method and MS/MS detection. The acrylamide concentrations in each food sample were calculated by multiplying the measured solution concentration from duplicate injections by the extraction volume and dividing by the food sample mass that was extracted. The determined acrylamide concentrations correlated well to those reported elsewhere for these classes of food.¹⁻⁵

	Cereal 1	Cereal 2	Potato Chip 1	Potato Chip 2
Injection 1	17.17 ng/mL	55.93 ng/mL	57.11 ng/mL	29.18 ng/mL
Injection 2	17.00 ng/mL	56.18 ng/mL	56.52 ng/mL	29.14 ng/mL
Mean	17.09 ng/mL	56.06 ng/mL	56.82 ng/mL	29.16 ng/mL
Extraction Vol.	20.0 mL	20.0 mL	20.0 mL	20.0 mL
Mass Sample	2.003 g	2.007 g	2.021 g	1.995 g
Acrylamide Conc.	171 ng/g	559 ng/g	562 ng/g	292 ng/g

Table 2: Results of acrylamide assay from food samples

Conclusions

An LC-MS/MS method has been developed for the measurement of acrylamide on the TSQ Quantum Discovery. Using APCI for the analysis of acrylamide from 100% water, an LOQ of 0.25 ng/mL acrylamide or 2.5 pg on column was achieved. Incorporation of a column-switching LC method prior to MS/MS detection of acrylamide eliminated the need to purify food sample extracts by SPE. The method was successfully demonstrated for the analysis of four brands of food samples using TSQ Quantum Discovery in conjunction with a column-switching LC method.

References

- Tareke, E.; Rydberg, P.; Karlsson, P.; Eriksson, S.; Tornqvist, M. *J. Agric. Food Chem.*, 2002, 50, 4998-5006.
- Rosen, J.; Hellenas, K. *Analyst*, 2002, 127, 880-882.
- Musser, S. M. <http://www.cfsan.fda.gov/~dms/acrylami.html>
- Becalski, A.; Lau, B.P.; Lewis, D.; Seaman, S.W. *J. Agric. Food Chem.*, 2003, 51, 802-808.
- Brandl, F.; Demiani, S.; Ewender, J.; Franz, R.; Gmeiner, M.; Gruber, L.; Gruner, A.; Schlummer, M.; Smolic, S.; Stormer, A.; Wolz, G. *Electron. J. Environ. Agric. Food Chem.*, 2002, 1(3), 1-8.
- Castle, L.; Campos, M.J.; Gilbert, J. *J. Sci. Food Agric.* 1993, 54, 549-555.
- Ikonomou, M.G.; Blades, A.T.; Kebarle, P. *J. Am. Soc. Mass Spectrom.*, 1991, 2, 497-505.
- McHale, K.J.; Winnik, W.; Paul, G. *Proceedings of the 51st ASMS Conference on Mass Spectrometry and Allied Topics*, Montreal, 2003.

Fast LC Separation of Triazine Herbicides at Elevated Temperature

Dave Thomas, Thermo Fisher Scientific, San Jose, CA USA

Introduction

Temperature is a key variable in high performance liquid chromatography (HPLC), influencing solute diffusion rates, mobile phase viscosity, and solubility. For example, as column temperature increases, analyte diffusion increases. Increased analyte diffusion generally leads to an increase in the optimum linear velocity of the separation, so that equivalent chromatographic efficiency and resolution can be achieved at a higher flow rate. Furthermore, elevating the temperature reduces the operating backpressure. The net result is that separations can be performed faster without exceeding the pressure limitations of the instrument.

This application uses a porous graphitic carbon stationary phase thermostatted in a high temperature column oven to separate triazine herbicides 5 to 10 times faster than is typical with conventional HPLC. The triazines and degradation products are separated on the Thermo Scientific Accela High Speed Liquid Chromatograph in 2 minutes on a Hypercarb 3 μm , 1 x 100 mm column operated at 160 $^{\circ}\text{C}$. This application note also documents the performance of the high temperature liquid chromatographic method, including precision of retention time and peak area, resolution, and spike recovery from several environmental water matrices.

Goal

Increase throughput of the HPLC method for triazine herbicides by employing ultra high-speed liquid chromatography at elevated temperature on a heat stable Hypercarb column.

Experimental

Chromatographic Conditions

Column:	Thermo Scientific Hypercarb 3.0 μm , 1 x 100 mm (part number 35003-101046)		
Mobile phase:	A: water	B: acetonitrile	
Gradient:	Time	%A	%B
	0.00	75	25
	1.00	70	30
	2.20	10	90
	2.30	75	25
	4.00	75	25
Flow rate:	500 $\mu\text{L}/\text{min}$		
Detector:	PDA, 238 nm, 10-mm flow cell, 11 nm bw, 20 Hz, 0s rise time		
Column temp.:	160 $^{\circ}\text{C}$ (housed in Selerity temperature controller)		
Injection:	5 μL sample loop, 2 μL partial loop injection		
	Syringe Speed: 4 $\mu\text{L}/\text{sec}$		
	Flush Speed: 100 $\mu\text{L}/\text{sec}$		
	Flush Volume: 400 μL		
	Wash Volume: 200 μL		
	Flush/Wash source: Bottle with 90:10 methanol:water		

Instrumentation

Thermo Scientific Accela HPLC system with PDA Detector
Thermo Scientific ChromQuest 5.0 Chromatography Data System (CDS)
Polaratherm Series 9000 Total Temperature Controller (Selerity Technologies)

Chemicals

Water, LC/MS-grade	Fisher Scientific W6
Acetonitrile, LC/MS-grade	Fisher Scientific A998
Methanol, LC/MS-grade	Fisher Scientific A456
Atrazine	Supelco 49085
Ametryn	ULTRA PST-024
Cyanazine	ULTRA PST-1360
Deisopropylatrazine, 1000 mg/L	SPEX CertiPrep S-1135
Desethylatrazine, 1000 mg/L	SPEX CertiPrep S-1145
Propanil, 1000 mg/L	SPEX CertiPrep S-3155
Propazine	ULTRA PST-850
Prometryn	ULTRA PST-840
Simazine	ULTRA PST-1130
Simetryn	Chem Service PS-381

Consumables

Autosampler vials, 1.8 mL glass, yellow septa	Thermo Scientific A4954-010
Backpressure assembly	Upchurch P-788
Ferrules, high temperature	Selerity Technologies BM0054
Mixer, 50 μL in-line static	Thermo Scientific 109-99-032
Mobile Phase Preheater, 0.005" x 70 cm	Selerity Technologies AD104
Syringe filters, 0.45 μm Nylon	Thermo Scientific A5307-010
Sample Loop, 5 μL	Thermo Scientific 109-99-007

Mobile Phase

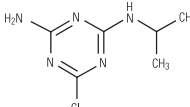
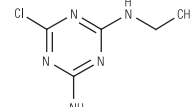
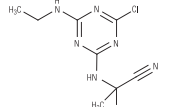
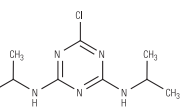
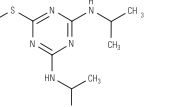
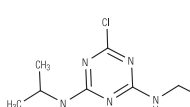
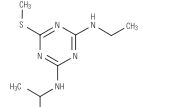
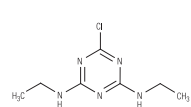
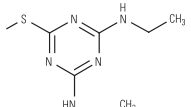
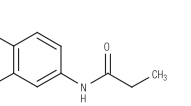
Proportioned mobile phase: Filled Solvent Reservoir Bottle A of the Accela pump with fresh HPLC-grade water and purged the solvent line with at least 30 mL of the water. Connected a fresh bottle of HPLC-grade acetonitrile to Reservoir B and purged as above.

Calibration Standards

Individual Stock Solutions, 1000 mg/L: Accurately weighed 10 mg (0.010 g) of each neat compound into a 10-mL volumetric flask, added 5 mL acetonitrile, and sonicated to dissolve. Brought to volume with acetonitrile and mix. Used desethyl atrazine, deisopropyl atrazine and propanil, purchased as solutions of 1000 mg/L in methanol, as received.

Combined Intermediate Standard 100 mg/L: Used a calibrated pipette to deliver 1000 μL of each individual stock solution to a 10-mL volumetric flask. Brought to volume with acetonitrile and mix.

Calibration Standards: Used a calibrated pipette to dilute the intermediate standard with mobile phase in volumetric glassware to 30, 10, 3, 1, 0.3, 0.1, and 0.03 mg/L.

CAS#	4-deethyl atrazine 6190-65-4	6-deisopropyl atrazine 1007-28-9	Cyanazine 21725-46-2	Propazine 139-40-2	Prometryn 7287-19-6
					
Formula	C ₈ H ₁₀ ClN ₅	C ₉ H ₈ ClN ₅	C ₉ H ₁₃ ClN ₆	C ₉ H ₁₆ ClN ₅	C ₁₀ H ₁₉ N ₅ S
MW (g/mol)	187.633	173.606	240.697	229.713	241.361
pKa			0.87	1.7	4.05
Log P _{o-w}	1.51	1.15	2.22	2.93	3.51
Water solubility, mg/L	3200	670	170	8.6	33
MeOH solubility, g/L			45 (ethanol)	6.2 (toluene)	160
CAS#	Atrazine 1912-24-9	Ametryn 834-12-8	Simazine 122-34-9	Simetryn 1014-70-6	Propanil 709-98-8
					
Formula	C ₈ H ₁₄ ClN ₅	C ₉ H ₁₇ N ₅ S	C ₇ H ₁₂ ClN ₅	C ₈ H ₁₅ N ₅ S	C ₉ H ₉ Cl ₂ NO
MW (g/mol)	215.687	227.334	201.66	213.307	218.082
pKa	1.7	4.1	1.62	4	2.29
Log P _{o-w}	2.61	2.98	2.18	2.8	3.07
Water solubility, mg/L	34.7	209	6.2	450	152
MeOH solubility, g/L	18	510	400		540

^a<http://toxnet.nlm.nih.gov>

Table 1: Useful properties of some triazine herbicides and degradation products^a

Analyte	k' ^a	R ^a	Linear range, mg/L	r ²	MDL ^b µg/L	Precision, Retention Time % RSD ^c	Precision, Peak Area % RSD ^c
deisopropylatrazine	2.4	1.1	0.03 – 10	0.9999	6	0.25	0.39
desethylatrazine	2.8	1.2	0.03 – 30	0.9999	16	0.22	0.89
cyanazine	5.6	7.2	0.03 – 30	0.9995	40	0.16	0.47
propazine	6.1	1.5	0.03 – 30	0.9996	23	0.13	0.82
atrazine	7.7	3.9	0.03 – 30	0.9995	14	0.10	0.87
simazine	9.2	3.9	0.03 – 30	0.9994	30	0.09	0.92
prometryn	10.4	3.0	0.03 – 30	0.9999	32	0.08	0.97
ametryn	11.9	4.3	0.03 – 100	0.9995	8	0.04	0.64
simetryn	13.1	3.7	0.03 – 100	0.9999	16	0.04	0.57
propanil	15.1	6.3	0.03 – 30	1.0000	25	0.02	0.42

^a Capacity factor (k') and Resolution (R) calculated according to Reference 1.

^b Detection limit MDL = $\sigma_{t_{s,99}}$ where $t_{\alpha,99} = 3.14$ for n = 7 replicates of the standard.

^c for n = 30 replicates.

Table 2: Performance of high temperature method for triazines performed on Hypercarb 3 µm, 1 x 100 mm column at 160 °C.

Samples

Samples of surface water (Salinas River, Monterey County, CA), ground water (domestic well, Santa Cruz county, CA), and drinking water (San Jose, CA tap water) were collected in accordance with established procedures, stored at 4–8 °C, and were filtered through a 0.45 µm nylon syringe filter into a glass autosampler vial before analysis.

System Preparation

To ensure good performance of this application, prepare the system as directed in Appendix A.

Results

Separation of seven triazine herbicides, two triazine degradation products often found in environmental samples, and propanil is shown in Figure 1. To optimize this separation, we adjusted the mobile phase composition to elute the first analyte with a capacity factor $k' > 2$, thereby improving

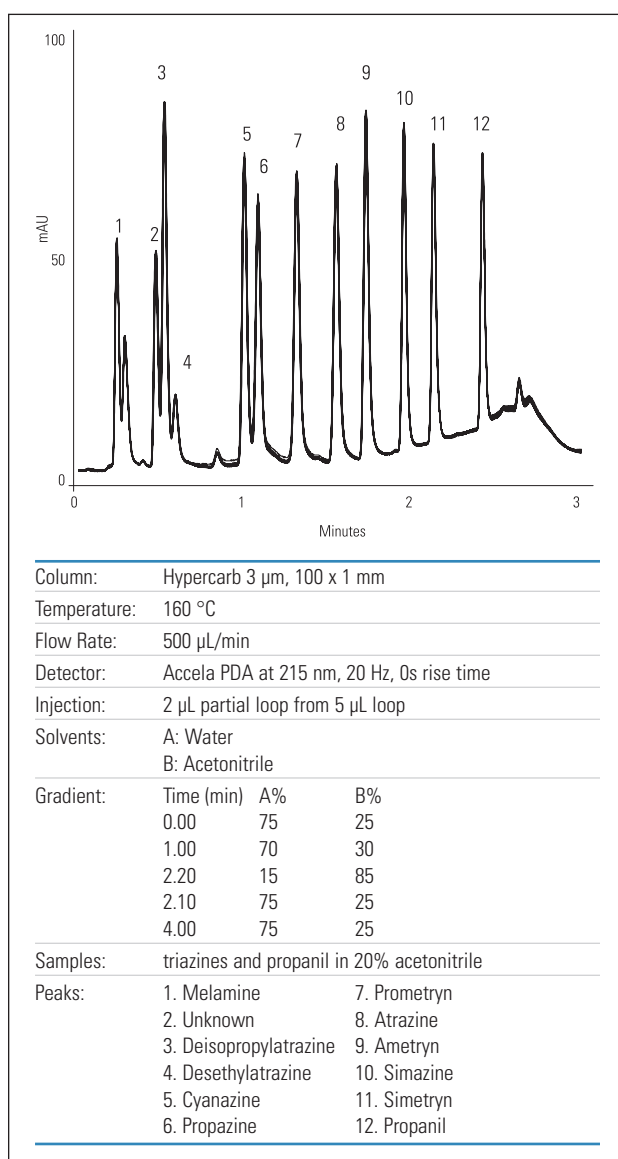


Figure 1: Separation of triazine herbicides, degradation products, and propanil on the Accela High Speed LC by reversed-phase chromatography with UV absorbance detection at 215 nm. Peaks: see Figure. Sample: overlay of 30 injections of triazines in HPLC-grade water with 20% acetonitrile.

resolution of the target analytes from sample matrix junk. Analytes spanning a wide range of polarity are well resolved by the combination of high temperature, solvent gradient, and the selectivity of the Hypercarb stationary phase. Note that because of the reduced viscosity of the mobile phase at 160 °C, this separation occurs at a linear flow rate of 15 mm/s – equivalent to a flow rate of over 10 mL/min on a 4.6 mm i.d. column. The system backpressure under these conditions is less than 4000 psi (272 bar).

Method performance is characterized by peak resolution, linear calibration range, limits of detection, and precision of retention time and peak area, as summarized in Table 2. MDLs for each analyte were determined by performing seven replicate injections of LC/MS-grade water fortified at a concentration of three to five times the estimated instrument detection limits, calculating the standard deviation of the measured concentration, and using the equation given in the figure caption. Note the good precision of retention time and peak area, as this reflects the temperature stability maintained by the high temperature oven.

We analyzed several environmental water samples to demonstrate the efficacy of this method with real matrices. Samples of surface, ground and municipal drinking water were analyzed before and after fortification with a known amount of each target analyte. Spike recovery was calculated as the amount of each analyte found in the spiked sample divided by the amount expected (i.e., the amount determined in the blank plus the amount added in the spike). Even with the dirtiest matrix, Salinas River water, the target analytes are well separated from the early eluting matrix peaks (Figure 2) and recovery of the spiked analytes exceeds 80% (Table 3).

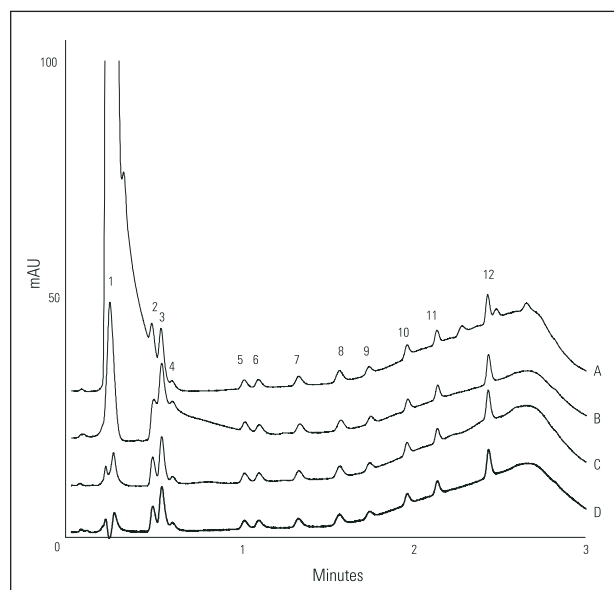


Figure 2: Chromatograms of four environmental water samples spiked with 200 µg/L each of triazines and propanil. Chromatograms obtained on the Accela High Speed LC by reversed phase chromatography with UV absorbance detection at 215 nm. Peaks: see Figure 1. Samples: top trace A, surface water (Salinas River); trace B, ground water (Simoes' well); trace C, drinking water (San Jose tap); bottom trace D, HPLC-grade water. Conditions: see text for details.

Analyte	HPLC water	Drinking water	Ground water	Surface water
deisopropylatrazine	94.0	104	104	93.0
desethylatrazine	93.0	110	98.5	85.0
cyanazine	92.5	102	94.0	97.0
propazine	97.0	106	104	101
atrazine	94.5	104	101	98.5
simazine	98.0	102	100	103
prometryn	104	117	116	110
ametryn	97.0	104	101	98.5
simetryn	99.0	98.5	104	100
propanil	101	103	104	80.0

Table 3. Percent recovery of analytes spiked into selected environmental water matrices. n = 3 replicates.

Conclusion

A separation performed at 160 °C on the Accela high speed chromatography system equipped with a heat stable Hypercarb column and high temperature column oven resolves 11 triazine herbicides in about two minutes with retention time and peak area precision better than 1% RSD for thirty replicates.

References

1. United States Pharmacopeia 30-National Formulary 25, United States Pharmacopeia, Rockville, Maryland 20852-1790, USA.

Suppliers

Chem Service, West Chester, PA, USA (<http://www.chemservice.com>)

Selerity Technologies, Inc., Salt Lake City, UT, USA

Sigma-Aldrich, St. Louis, MO, USA (<http://www.sigmaaldrich.com>)

Supelco, Bellefonte, PA, USA (<http://www.sigmaaldrich.com>)

Thermo Fisher Scientific, Waltham, MA, USA (<http://www.thermofisher.com>)

ULTRA Scientific, No. Kingstown, RI, USA (<http://www.ultrasci.com>)

Appendix A

System Preparation

Pump: Always plumb the Accela system with precut and polished 0.005" i.d. high-pressure tubing and high pressure fittings as shown in Figure 15 of the Accela Pump Hardware Manual (Document 60157-97000 Revision B). For all tubing connections that you make, ensure that the tubing end is square-cut and burr-free. Firmly push the tubing into the injection valve port as you tighten the high-pressure fitting in order to maximize peak efficiency. Prime the pulse dampener and purge the solvent lines as instructed in Chapter 4 of the Accela Pump manual. Verify that the pump is performing well by monitoring the pressure pulsation and by testing the pump proportioning accuracy as described in Chapter 5 of the pump manual. If your Accela pump does not include an inline 35 µL dynamic mixer, then install a 50 µL static mixer between the inline high pressure filter and the Accela AS mobile phase preheater.

AS: Open the Instrument Configuration and verify that the Accela AS Configuration entry for "Dead volume" is correct (the calibrated volume in µL written on the transfer tubing between the injection port and injection valve). Verify that the entry for "Loop size" is correct for the currently installed sample loop. Fill the Flush reservoir with 90:10 (v/v) methanol:water and flush the syringe with solvent to purge any air bubbles from the syringe and tubing. Use the Wash/Flush conditions specified under "Conditions" to ensure low carryover between injections. Consult the Accela Getting Connected manual (Document 60057-97001 Revision A) for details.

Polaratherm Column Oven: Install the Total Temperature Controller according to the Polaratherm Series 9000 Installation and Operation Manual. Install the Hypercarb, 3 µm 1 x 100 mm column, by using a 70-cm length of precut and polished 0.005" i.d. high-pressure tubing with mobile phase preheater. It is important to use a heat stable Hypercarb column as this does not contain any PEEK components that will degrade at the temperatures used in this method. Use the high temperature graphite/Vespel ferrules and fittings described in the Series 9000 manual. Ensure that the tubing is fully pushed into the column inlet when you tighten the high-pressure fitting.

Detector: Use a 10 mm light-pipe flow cell. Install a 250 psi backpressure regulator after the flow cell outlet to suppress bubble formation in the flow cell. Verify that the deuterium lamp has been used for less than 2000 hours.

Use Direct Control or a downloaded method to equilibrate the Accela system under the conditions shown above. Create a method based on these operating conditions and then create a sequence to make several injections of HPLC grade water. The system is ready to run standards and samples when the peak-to-peak baseline oscillation is between 50 – 200 µAU/min (average of 10 1-min segments) and no significant peaks elute in the retention time window of the analytes.

Analysis of Polar Metabolites of Atrazine in Ground Waters Using Hypercarb as SPE Sorbent Coupled On-Line with Hypercarb LC Column

Valérie Pichon, Christophe Flinois, Marie-Claire Hennion, Laboratoire Environnement et Chimie Analytique (UMR PECSA 7195) Ecole Supérieure de Physique et Chimie Industrielles (ESPCI ParisTech), Paris, France

Introduction

Chlorotriazine herbicides have been extensively used as pre- and post-emergence weed control agents on crops, mainly corn and soybean. The potential for contamination of water and sediments by the widely used herbicide atrazine is high. This is due to its relatively high solubility, its weak adsorptivity (as measured by the partition coefficient between soil organic carbon and water) and its relatively long hydrolysis half-life in some soils. These characteristics easily explain that it is the most frequently reported pesticide in agricultural areas. Its use has then been limited in several countries but without solving the problem of its degradation products found in ground and surface water. Its degradation after spreading depends on several factors such as hydrolysis, photolysis and microbial activity. The main degradation products in ground and surface waters and in soils are dealkylated metabolites and therefore deethyl- (DEA) and deisopropyl-atrazine (DIA).

The European Union has set pesticide standards for drinking waters at a maximum permissible concentration for a particular pesticide at 0.1 µg/L and the sum of all pesticides at 0.5 µg/L. The new regulation establishes not only a maximum concentration of pesticides in drinking water but also includes their degradation products after drinking water treatment. In order to estimate the efficiency of a degradation process that will generate very polar degradation products, and to control the contamination level of ground water that can be used for the production of drinking water, it is necessary to develop analytical methods suitable for the trace analysis of these very polar organic contaminants.

The objective of this study was to provide a sensitive method for the detection and quantification of several polar dealkylated degradation products of atrazine, i.e. DEA, DIA, didealkylatrazine (DDA), ammeline (2,4-diamino-6-hydroxy-1,3,5-triazine) and ammelide (2-amino-4,6-dihydroxy-triazine) at the trace level in water samples. Their structures are presented in Figure 1. The analysis of such organic contaminants in complex matrices at low levels of concentration requires a procedure of pretreatment in order to extract and concentrate them before their LC/UV or LC/MS analyses. Solid-phase extraction has proven to be a very efficient technique and its application to the analysis of triazines and their metabolites has been already reviewed.¹ On-line coupling of solid-phase extraction with liquid chromatography was shown to be a technique of choice for the trace-level determination of organic compounds because of its speed, easy automation and reliability.² With this approach, the monitoring of organic pollutants in drinking

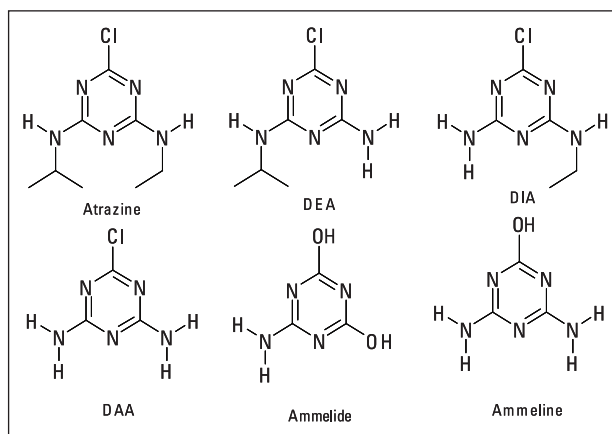


Figure 1: Structure of the studied compounds

water at 0.1 µg/L is commonly achieved using a sample volume of 50-150 mL depending on the sensitivity of the detection device. Several studies reported the use of C18 silica or apolar copolymers of styrene divinylbenzene (PS-DVB) as extraction sorbent packed in a precolumn for the on-line extraction of triazines from water samples.³ However, the high polarity of the metabolites cited below causes the breakthrough of most of them during the extraction process on these sorbents. The interest in using carbonaceous sorbents for very water-soluble compounds has been reviewed.⁴ The most widely used carbon-based SPE sorbent is graphitized carbon black (GCB). In spite of its low surface area (120 m²/g), its potential for trapping polar compounds with a higher efficiency than C18 silica sorbent has been largely demonstrated.⁴⁻⁷ Porous Graphitic Carbon (PGC, Hypercarb, Thermo Scientific) characterized by a crystalline structure made of large graphitic sheets held together by weak Van der Waals forces has also been largely used for the extraction of polar pollutants from water.⁴ Most applications using carbonaceous sorbents have been carried out following an off-line procedure.⁸⁻¹⁰ Their on-line coupling with classical reversed-phase C18 silica analytical columns is difficult because polar analytes may be too strongly retained on PGC and the high water content of the mobile phase required for the separation of these polar compounds on C18 silica is unable to elute the analytes from PGC.⁴ A solution is to couple this sorbent with a Hypercarb column because in this case, a higher amount of organic solvent can be used in the mobile phase for the separation of polar compounds. With this system, the direct determination of the polar compounds at 0.1 µg/L can be achieved. The PGC/PGC coupling was automated and used for the monitoring of polar metabolites DEA and DIA in ground

waters with a 100 mL sample.^{11,12} The application of PGC for the most polar metabolites, i.e. ammeline and ammelide has only been applied following an off-line procedure.¹⁰

Goal

The development of a miniaturized on-line coupling of a Hypercarb precolumn for the extraction of atrazine and their polar dealkylated metabolites from water, with a LC separation using a microbore Hypercarb column for increasing the sensitivity in UV detection and for facilitating the coupling with electrospray mass spectrometry detection.

Experimental

Chemicals and Reagents

Atrazine, simazine and their metabolites were obtained from C.I.L. (Saint-Foy-la-Grande, France). Stock standard solutions of 100 mg/L were prepared by weighing the solutes and dissolving them in methanol or in a water-methanol (50:50) mixture for some degradation products of triazines. The stock solutions were stored at 4 °C. A standard solution of 5 mg/L was obtained by dilution in methanol from the stock solution. HPLC-grade acetonitrile and methanol were purchased from Mallinckrodt Baker (Deventer, Netherlands). High purity water was obtained from a Milli-Q purification system (Millipore, Saint-Quentin en Yvelines, France).

Online SPE/LC/UV Set-up

LC analysis were performed with a Varian LC System Workstation including a Varian Star 9012 solvent-delivery system and a Model 9065 Polychrom diode-array detector (190-366 nm). A Thermo Scientific Hypercarb analytical column (100 x 3 mm, 5 µm, part number 35005-103030) was connected to a Valco valve (VICI, Houston, TX, USA). The elution gradient was based on acetonitrile (ACN) and water. The gradient was 10% to 35% ACN from 0 to 35 min, 100% ACN at 45 min. The flow rate was set at 0.45 mL/min. The UV detection was set to 220 nm. Trace enrichment was performed on small-size precolumn using an automated programmable sample preparation unit (Prospekt, Spark Holland, Emmen, Netherlands) allowing direct elution of compounds trapped on the Hypercarb precolumn (10 x 2 mm, 5 µm) to the LC column.

Online SPE/µLC/UV/MS Set-up

The instrumentation for microLC consisted of 1100 Series pump (Agilent Technologies, Waldbronn, Germany) connected to an Accurate 1/10 microflow splitter (LC Packings, Amsterdam, The Netherlands). UV detection was performed with a SPD-M10A photodiode array detector (Shimadzu) equipped with a microcell with an internal volume of 35 nL (LC Packings).

Analytical micro LC separations were performed on a Hypercarb column (100 x 1 mm, 5 µm, part number 35005-101030). The elution gradient is based on acetonitrile (ACN) and water containing 0.03% trifluoroacetic acid (TFA). The gradient was 0% to 5% ACN from 0 to 5 min, 30% ACN at 15 min and 80% ACN at 30 min. The flow rate was set at 50 µL/min after the microflow splitter and was introduced without any split in the ESI/MS. The UV detection was set to 220 nm.

Micro-LC/ESI/MS-MS analyses were carried out on a VG Quattro (Fisons Instruments, VG Biotech, Altrincham, United Kingdom) triple quadrupole equipped with an electrospray ion source. Data analysis was controlled by MassLynx 3.3 V. Full scan spectra were acquired in the positive ion peak centroid mode over the mass range of m/z 50-1200 in 4.5 s. The energy of collision applied was set to 50 eV. The transitions were monitored with 0.3 or 0.5 sec, EI: 3.9 V.

Trace enrichment was performed on Hypercarb precolumn (10 x 2.1 mm) introduced in a precolumn holder. The precolumn was connected to a preconcentration pump (Shimadzu LC 5A) and to the analytical column via a six-port switching valve (Rheodyne, Berkeley, CA, USA). The conditioning solvents and the samples were selected using a low pressure valve (Rheodyne) that was connected to the preconcentration pump.

SPE Procedure

Using the Prospekt system connected to LC/UV, the Hypercarb precolumns were conditioned by passing 5 mL of acetonitrile, 5 mL of methanol and 5 mL of pure water. Water samples were percolated and the sorbents were washed with 1 mL of pure water. The flow rate was set at 2 mL/min. After switching the valve, the desorption was carried by the mobile phase by backflush elution at 0.45 mL/min for 10 min.

Using the Hypercarb precolumn connected to µLC/UV/MS, the carbonaceous SPE sorbent was conditioned with 5 mL of acetonitrile and 5 mL of pure water. Samples of water were then percolated through the precolumn. The flow rate was set at 0.5 mL/min. After switching the valve, the desorption was carried by the mobile phase by backflush elution at 50 µL/min for 10 min.

Results and Discussion

The studied compounds belong to a broad range of polarity with log Kow values between -1.2 for ammeline and 2.7 for atrazine. It has been already mentioned that the separation of the most polar metabolites, i.e. ammeline (AME) and ammelide (ADE), necessitates the use of a mobile phase containing only acidified pure water in order to decrease as much as possible the elution strength for their retention on C18 silica.⁹ A Hypercarb column has then, been selected for increasing the retention of these polar compounds. The use of a Hypercarb analytical column for the separation of some metabolites of atrazine has already been described but not for ADE and AME. Moreover, this mobile phase has to be compatible with the ESI-MS detection system. The separation on Hypercarb coupled to UV detection was achieved with a water/acetonitrile gradient. For LC/MS analysis, 0.03% trifluoroacetic acid was added to the water/acetonitrile mobile phase.

Initially, on-line coupling based on a conventional 3 mm i.d. column connected to UV detection was developed. To reach a high enrichment factor, 50 mL water sample was percolated through the Hypercarb precolumn. With these conditions, recoveries higher than 61% were obtained for DAA, DEA, DIA, atrazine and simazine. Because of ammelide and ammeline high polarity breakthrough occurs during the percolation step and recoveries lower than 10% were obtained. Recoveries are reported in Table 1.

Compounds	Log Kow	Recovery (%)	S.D
Ammelide	-0.7	< 10	-
Ammeline	-1.2	< 10	-
DAA	0	71.1	5.8
DEA	1.6	77.8	4.0
DIA	1.2	80.3	4.6
Atrazine	2.7	72.0	9.9
Simazine	2.3	71.3	5.7

Table 1: Extraction recoveries obtained for the percolation of 50 mL of pure water spiked at 0.5 µg/L with each compound, with the online PGC precolumn (10 x 2 mm) / PGC/UV system. S.D – standard deviation (n = 5).

Figure 2 shows the application of this on-line coupling to the analysis of a water sample spiked with 0.2 µg/L of each target analytes. In order to increase the sensitivity of the method the column diameter was reduced to 1 mm and MS detection was carried out in series with UV detection.

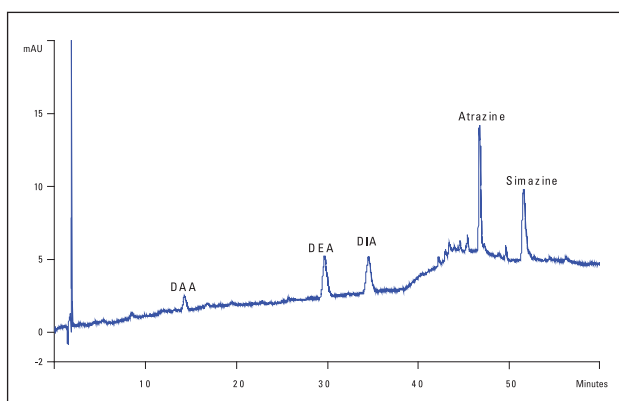


Figure 2: On-line analysis of water sample spiked with 0.2 µg/L of each analyte using the PGC/PGC/UV set up. UV detection at 220 nm

The sensitivity of this set-up allowed the reduction of the sample volume to 5 mL. This reduced percolated volume of sample facilitates recoveries closed to 100% for ammeline and ammelide. The use of a more sensitive detection system, i.e. MS detection, allows the analysis of all the metabolites in spring water spiked at 0.1 µg/L and the monitoring of these polar metabolites with a totally automated system. The performance of the method is illustrated in Figure 3.

Conclusion

A fully automated system consisting of a Hypercarb pre-column connected to µLC/UV/MS, using a Hypercarb analytical column, was set-up for the analysis of the polar dealkylated degradation products of atrazine, namely DEA, DIA, DDA, ammeline and ammelide. This methodology was applied to the detection of the metabolites present at trace levels (0.1 µg/L) in spring water.

References

1. H. Sabik, R. Jeannot, B. Rondeau, *J. Chromatogr. A*, 885 (2000) 217.
2. V. Pichon, *J. Chromatogr. A*, 88 5 (2000) 195.
3. V. Pichon, M.-C. Hennion, *J. Chromatogr. A*, 665 (1994) 269.
4. M.-C. Hennion, C. Cau-Dit-Coumes, V. Pichon, *J. Chromatogr. A*, 823 (1998) 147.
5. M.-C. Hennion, *J. Chromatogr. A*, 885 (2000) 73.
6. M. Berg, S.R. Müller, R.P. Schwarzenbach, *Anal. Chem.*, 67 (1995) 1860.
7. S.Y. Panshin, D.S. Carter, E.R. Bayless, *Environ. Sci. Technol.*, 34 (2000) 2131.
8. R. Jeannot, H. Sabik, E. Sauvard, E. Genin, *J. Chromatogr. A*, 879 (2000) 51.
9. V. Pichon, L. Chen, S. Guenu, M.-C. Hennion, *J. Chromatogr. A*, 711 (1995) 257.
10. G. Machtalère, V. Pichon, M.-C. Hennion, *J. High Resol. Chromatogr.*, 23 (2003) 437.
11. S. Guenu, M.-C. Hennion, *Anal. Method and Instrument.*, 2 (1995) 247.
12. S. Dupas, S. Guenu, V. Pichon, A. Montiel, B. Welté, M.-C. Hennion, *Intern. J. Environ. Anal. Chem.*, 65 (1996) 53.

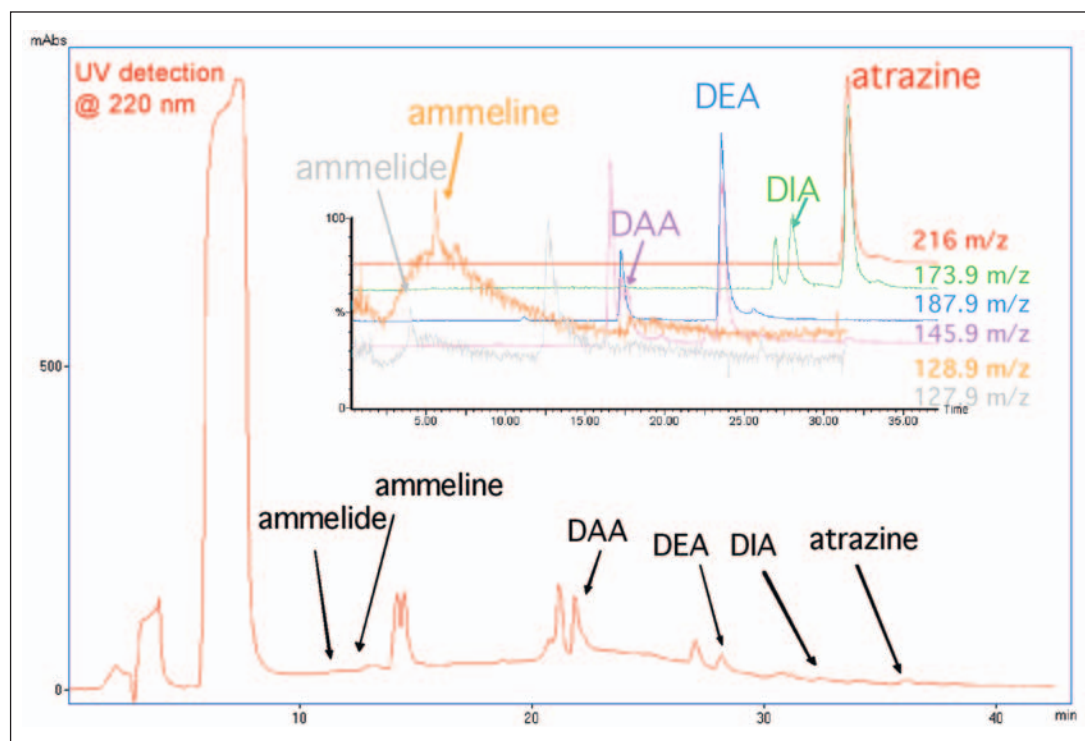


Figure 3: Analysis of 5 mL of spring water spiked at 0.1 µg/L with each analyte by the on-line PGC/µPGC/UV/MS system. Insert: MS signal (SIM mode)

Fast and Versatile Analysis of Desphenyl-Chloridazone and Methyl-Desphenyl-Chloridazone in Surface, Ground and Drinking Water Using LC-MS/MS and EQuan

N. Eßer, B. Preuß, F. Brille, Bergisches Wasser- und Umweltlabor der BTV GmbH, Wuppertal, Germany
O. Scheibner, Thermo Fisher Scientific, Dreieich, Germany

Introduction

Growing concerns about contaminants in water and food has resulted in governmental regulations with lower tolerance levels nearly every year. The number of samples has increased nearly at the same speed during the last few years. Thus the demand for shorter and less laborious techniques for residue analysis, with increased sensitivity levels, is higher than ever. The analysis of pesticides and other pollutant compounds such as pharmacological substances in water samples can be highly time-consuming due to the high volumes which need to be extracted. Direct injection of water samples is limited to a volume in the range of 100 μL , if one wishes to avoid affecting the peak shape. Automation of sample workup and use of fast HPLC methods for further method acceleration are the demands in modern residue analysis. The Thermo Scientific EQuan system provides a solution for these demands: injection of up to 5000 μL crude water sample onto an enrichment column with subsequent HPLC analysis results in full automation and high throughput. Methods for various pesticides, antibiotics and veterinary residues have been

described already, but still the automated analysis of highly polar compounds remains a major challenge since the reliable and quantitative trapping and re-elution during pre-concentration has not yet been satisfactorily resolved.

We describe a method for a fully automated analysis of metabolites of the well known herbicide Chloridazone, Desphenyl-Chloridazone and Methyl-Desphenyl-Chloridazone. Due to their polarity, quantitative trapping and sensitive HPLC analysis had not been achieved so far. Use of a Thermo Scientific Hypercarb trapping column (20 x 2.1 mm, 7 μm) in combination with a Hypercarb analytical column (100 x 2.1 mm, 3 μm) has resulted in a highly reliable and sensitive method for the direct analysis of surface, ground and drinking water.

Goal

The aim of our work was to establish a fast and versatile LC-MS/MS method using EQuan for both metabolites of Chloridazone providing a LOQ of less than 10 ng/L in all water samples.

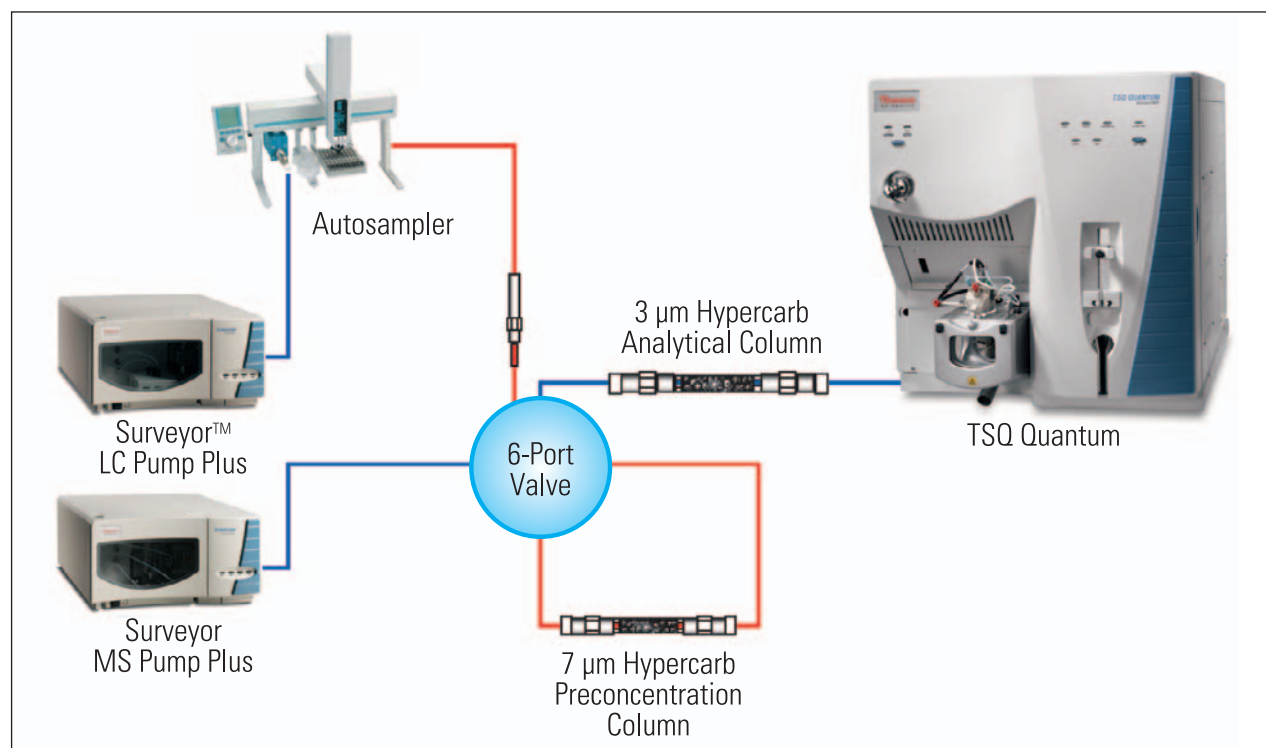


Figure 1: Schematic drawing of the EQuan system

Experimental

Sample Preparation

For the dilution series 10 g ultrapure water was passed through a syringe tip filter and spiked with the given levels of Desphenyl-Chloridazone and Methyl-Desphenyl-Chloridazone. Six levels with the following concentrations were prepared: 5, 6, 7, 8, 15 and 20 ng/L.

Samples were only passed through a syringe tip filter. No additional treatment of samples was necessary prior to measurement.

Instrumentation

Thermo Scientific Surveyor LC pump for sample concentration
Thermo Scientific Surveyor MS pump for sample analysis
CTC PAL autosampler for sample application
Thermo Scientific TSQ Quantum Access triple stage mass spectrometer.

Sample Pre-concentration

Hypercarb column 20 x 2.1 mm, 7 μ m
(part number 35007-022130)

A sample volume of 1 mL was transferred to the trap column with 20% methanol in water as solvent. Sample transfer and concentration was carried out with a flow rate of 500 μ L/min. The trap column was switched by means of the 6-port valve (Figure 1) into the flow of the analytical pump and followed by the introduction of an analytical gradient to both columns.

Chromatographic Conditions

Column: Hypercarb 100x2.1 mm, 3 μ m
(part number 35003-102130)

Mobile phase: A – Water +0.5% methanol; B – Methanol

Gradient: Time (min)	%A	%B
0	30	70
2	30	70
11	0	100
14	0	100
17	30	70
20	30	70

Flow rate: 200 μ L/min

The time for sample concentration was 1.9 min. The total cycle time for sample concentration, analysis and reconditioning was 20 minutes.

MS Conditions

Ionisation: ESI in positive mode
Spray voltage: 3500 V
Sheath gas pressure (N_2): 40 units
Auxiliary gas (N_2): 5 units
Ion transfer tube temperature: 350 °C
Collision gas pressure (Ar): 1.5 mTorr
Q1/Q3 peak resolution: 0.7 Da
Scan width: 0.01 u
Scan time: 0.6 s

The SRM transitions used are shown in Table 1. The product masses marked with * were used for quantification.

Analyte	Parent Ion (m/z)	Fragment Ions (m/z)	Collision Energy (V)
Desphenyl-Chloridazone	145.9	101.1	28
		117.1*	23
Methyl-Desphenyl-Chloridazone	159.9	88.2*	31
		117.0	23

Table 1: SRM conditions

Results and Discussion

The chromatogram of a real water sample spiked with 10 ng/L each of Desphenyl-Chloridazone and Desphenyl-Methyl-Chloridazone is shown in Figure 2. Thermo Scientific LCQuan 2.5 software was used to process the quantitative data. Figure 4 shows the calibration curves of Desphenyl-Chloridazone and Methyl-Desphenyl-Chloridazone and Table 2 summarizes the correlation coefficients, LODs and LOQs for both analytes.

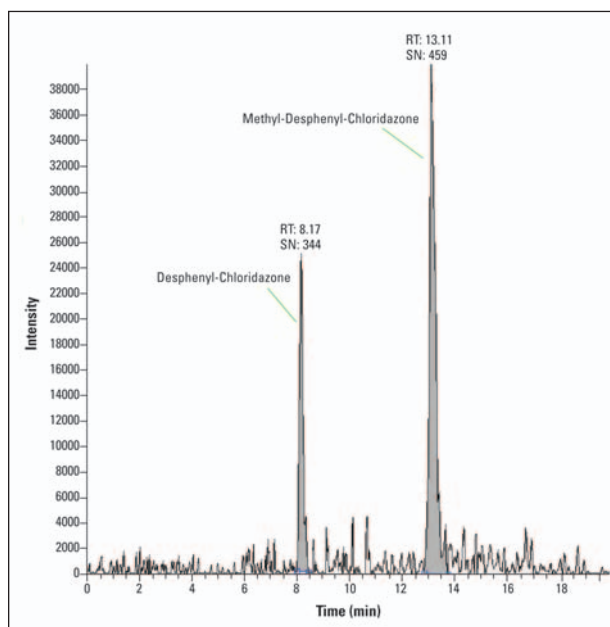


Figure 2: Chromatogram of a water sample spiked with a concentration of 10 ng/L each of Desphenyl-Chloridazone and Methyl-Desphenyl-Chloridazone

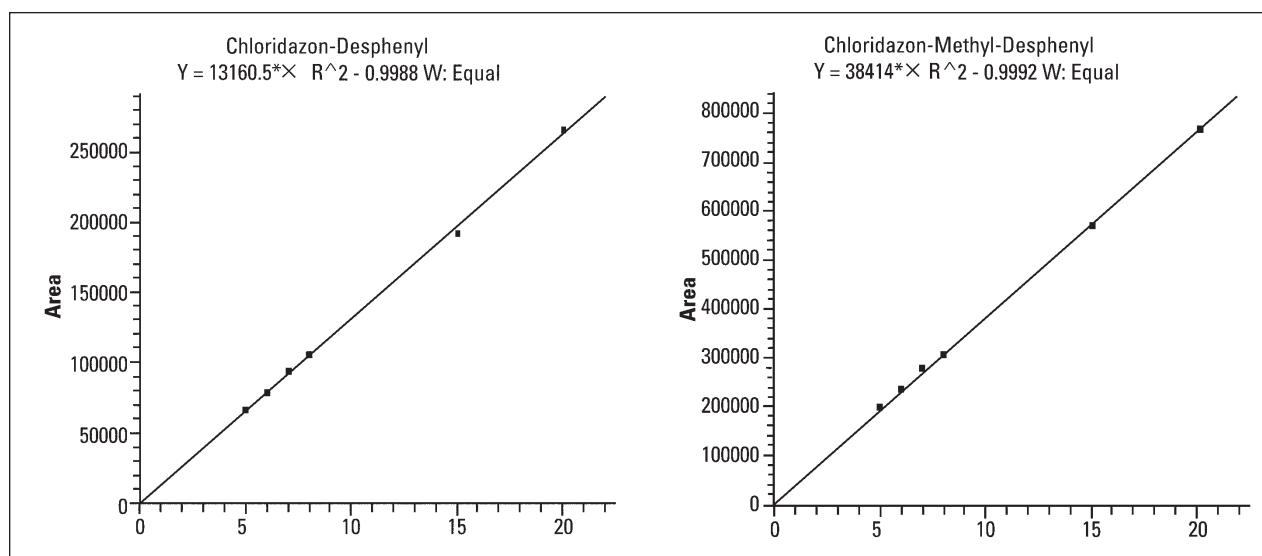


Figure 3: Calibration curves of Desphenyl-Chloridazone and Methyl-Desphenyl-Chloridazone

A concentration range from 5 to 20 ng/L was covered with pure standards, with focusing on the lower end of the range for quantitation in residue analysis from aqueous samples as specified in current legislation (Figure 3). A real sample containing 10 ng/L each of the two analytes shows peaks well suitable for quantitation which can be considered as limit of quantitation under such conditions. Less concentrated samples showed a limit of detection at less than 5 ng/L.

Analyte	Correlation Coefficient r^2	Limit of Detection (ng/L)	Limit of Quantitation (ng/L)
Chloridazone-desphenyl	0.9988	3.1	10
Chloridazone-methyl-desphenyl	0.9992	3.5	10

Table 2: LODs and LOQs for the two pesticide metabolites.

Conclusion

The online enrichment and analysis of highly polar compounds, especially polar metabolites of pesticides, is considered challenging due to insufficient trapping capabilities of available column materials. This application demonstrates that it is possible to build a system for online enrichment and automated LC-MS/MS analysis of polar metabolites of an important pesticide widely used in Europe.

A limit of quantitation of 10 ng/L, after pre-concentration from a sample volume of 1 mL, was demonstrated. Normally, sample volumes used for manual pre-concentration are much higher. The EQuan system provides capability to enlarge the sample volume up to 20 mL, thus opening the way to quantitation levels of 1 ng/L and below.

Determination of Leucine and its Isomers by LC-MS/MS Using a Porous Graphitic Carbon Column

Agnes Le Corre, Thermo Fisher Scientific, Paris, France
Lúisa Pereira, Thermo Fisher Scientific, Runcorn, UK

Introduction

Leucine and valine are used as biomarkers of maple syrup urine disease in neonatal blood spot screening. Maple syrup urine disease (MSUD) is caused by a gene defect. Infants with this condition cannot break down the branched-chain amino acids leucine, isoleucine, and valine. This leads to a build-up of these chemicals in the blood. The condition gets its name from the distinctive sweet odor of affected infants' urine. Beginning in early infancy, this condition is characterized by poor feeding, vomiting, lethargy, and developmental delay. MSUD affects an estimated 1 in 185,000 infants worldwide.

Traditionally, the monitoring of the concentration of leucine and its isomers (isoleucine and allo-isoleucine) in blood is performed with an amino acid analyser, which can take up to 2 hours to complete the analysis. LC-MS/MS is becoming an important tool in the semi-quantitative analysis of amino acids in neonatal screening. When applied to the screening and monitoring of MSUD, this methodology requires the chromatographic resolution of leucine, leucine isomers and hydroxyproline as these are all isobaric and produce the same m/z at 188 ($[M+H]^+$). Porous graphitic carbon (PGC, Hypercarb) can be used to retain and separate polar underivatized amino acids.¹ Furthermore, the flat and highly adsorptive surface of the graphite shows increased selectivity towards structurally related compounds such as structural isomers. This application note describes a LC-MS/MS method for the analysis of leucine, its isomers isoleucine and allo-isoleucine, valine and hydroxyproline, using a Hypercarb column to achieve chromatographic separation of the 5 compounds.

Goal

To develop a method for the LC/MS/MS analysis of leucine and isomers, with full chromatographic separation.

Experimental

Chromatographic Conditions

LC system: Thermo Scientific Surveyor

Autosampler: HTS Pal

Column: Hypercarb 100 x 4.6 mm, 5 μ m
(part number 35005-104630)

Mobile phase: water + 20 mM nonafluoropentanoic acid/Acetonitrile (75:25)

Flow rate: 1500 μ L/min (split 1/10)

Injection volume: 10 μ L

MS Conditions

MS system: Thermo Scientific TSQ Quantum Ultra

Ionisation Mode: +ESI

Selected reaction monitoring (SRM) transitions:

Compound	Precursor Ion	Product Ion	Collision Energy (eV)
Leucine			
Isoleucine	188.09	86.1	15
Allo-Isoleucine			
Hydroxy-Proline			
Valine	174.15	72.15	20
Isoleucine			
Allo-Isoleucine (Confirmation ion)	188.09	69.1	32

Table 1: SRM transitions used in the analysis

Sample Preparation

The calibration standards were prepared by successive dilutions with water/acetonitrile (75:25) mixture. Solutions were stored at +4 °C.

Results and discussion

The stereoselectivity of Hypercarb allows chromatographic resolution of the isobaric species in the analysis: leucine, isoleucine, allo-isoleucine and hydroxyproline. This is achieved using an isocratic mobile phase of water and acetonitrile with the addition of 0.1% nonafluoropentanoic acid, and illustrated in Figure 1.

In addition to retention time, the differentiation of leucine and its isomers can be done by monitoring alternative SRM transitions. At 15 eV, leucine, isoleucine and allo-isoleucine all produce a major product ion at m/z 86 (as shown in Figure 1B). However, when collision energy is increased to 32 eV, another product ion at m/z 69 is present in the spectra of isoleucine and allo-isoleucine but absent from the spectra for leucine. Therefore monitoring of SRM transition 188.09 – 69.1 will produce a signal for isoleucine and allo-isoleucine but not for leucine, as demonstrated in Figure 2.

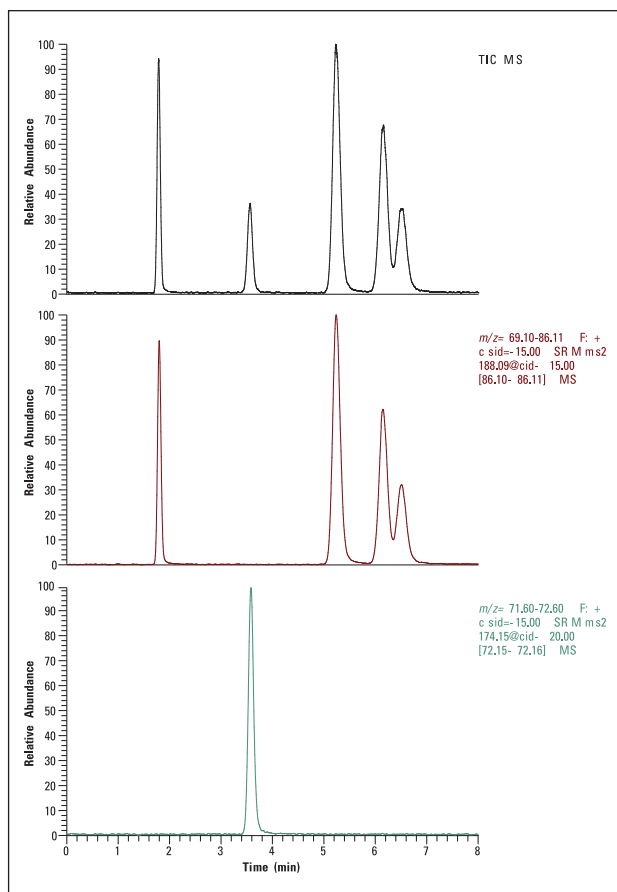


Figure 1: LC-MS/MS traces showing chromatographic separation of (1) Hydroxy-proline; (2) Valine; (3) Leucine; (4) Allo-isoleucine; (5) Isoleucine. (A) Total ion chromatogram; (B) SRM chromatogram for isobaric compounds of m/z 188; (C) SRM chromatogram for valine.

Conclusion

An eight minute method is demonstrated for the analysis of leucine and isomers. Chromatographic resolution of these underivatized amino acids, valine and hydroxyproline is achieved on a porous graphitic carbon column. The sensitivity of the method could be improved by reducing the column internal diameter and therefore reduce both the split ratio into the MS and sample dilution in the column. Future work should also include the investigation of the effect of changing the electronic modifier (nonafluoropentanoic acid) and investigate its effect on chromatographic resolution and method sensitivity.

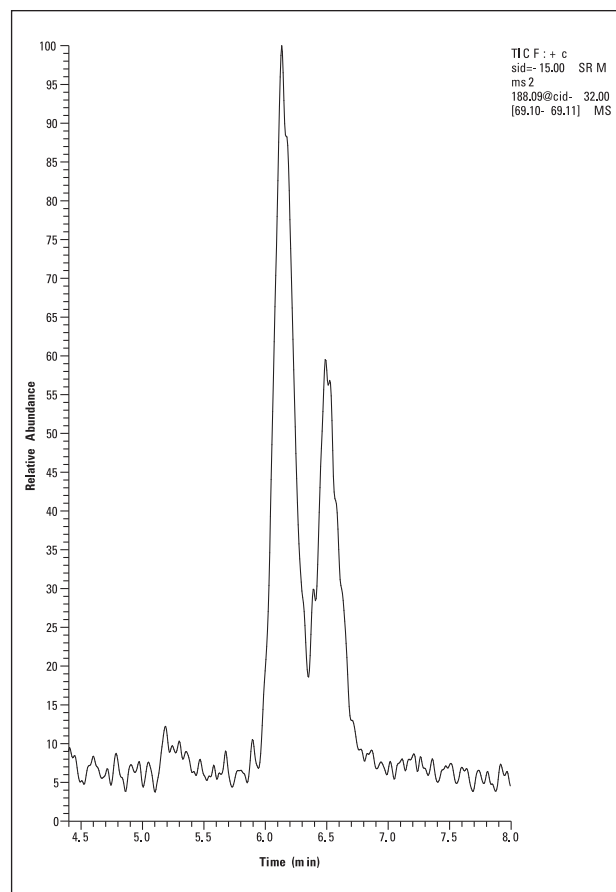


Figure 2: Differentiation of isoleucine and allo-isoleucine from isobaric leucine: SRM chromatogram for transition 188.09 – 69.10 at 32 eV collision energy. No peak for leucine is present.

References

1. P. Chaimbault, K. Petritis, C. Elfakir, M. Dreux, *J. Chromatogr. A*, 2000, 896, 253-263

Determination of Occupational Exposure to Toluene, Xylene and Styrene Through Metabolite Monitoring Using Isocratic HPLC

Lúisa Pereira, Brid Brosnan, Charlotte Blythe, Thermo Fisher Scientific, Runcorn, UK

Introduction

Toluene, xylene and styrene are widely used as an industrial feedstock and in the modern scientific workplace. Styrene is the precursor compound to polystyrene. Toluene is commonly used in the paint, plastics and printing industries. Xylene is consumed in the leather, printing and rubber industry.

Exposure to styrene, toluene or xylene has a detrimental effect upon the central nervous system. At low concentrations, symptoms of dizziness, headache, nausea and vomiting are experienced together with respiratory tract irritation.

Exposure can cause in-coordination and mental confusion and, as the central nervous system becomes further depressed, can result in unconsciousness and death. The monitoring and evaluation of the biological effects upon health of workers exposed to such chemicals is, therefore, vitally important.

Traditionally, exposure to these chemicals has been evaluated through measurement of their concentration in ambient air where workers are more likely to be exposed to, however, it has been found in recent years that biological monitoring (in blood or urine) affords a far more accurate estimate of exposure. For example, in the presence of ethanol, the adsorption of toluene into the blood is double that which occurs with exposure to toluene alone, thus illustrating that measurement of air concentration can result in misleading exposure estimates.¹

Upon inhalation/absorption into the body, all three chemicals undergo biological transformation. The metabolic reaction rates are fast, consequently, the products are rapidly excreted from the body. As such, levels of compounds in blood are low, thus the concentration of metabolites in urine is measured. The main metabolites are hippuric acid, o-, m-, p-methylhippuric acid, mandelic acid and phenylglyoxylic acid. These metabolites are polar, and isomeric in nature. Consequently, Thermo Scientific Hypercarb (porous graphitic carbon, PGC) presents itself as the ideal phase for the separation of such analytes. Indeed Schlatter *et al* highlighted the advantageous positional isomer separation performance of Hypercarb™ with respect to the analysis of cresol isomers in the urine of workers exposed to toluene.² As hippuric acid is present in the urine of individuals who have not been subject to toluene exposure, some authors believe that measurement of cresols provides a valid alternative to the monitoring of hippuric acid.

This application note highlights the use of Hypercarb for the effective separation of the associated compounds of styrene, toluene and xylene metabolism. Using a simple two component isocratic mobile phase all major metabolites (and an internal standard) are separated in under 11 minutes.

Goal

To detail the effective monitoring of excreted toluene, xylene and styrene metabolites using a PGC stationary phase in isocratic mode.

Experimental

LC Method

Column: Hypercarb 3 µm, 100 x 4.6 mm (part number 35003-104630)

Mobile Phase: H₂O / MeOH (50:50) +0.1% TFA

Flow Rate: 1 mL/min

Temperature: 25 °C

Detection: UV at 240 nm

Injection Volume: 10 µL

Results and Discussion

The separation achieved for the biological metabolites using the conditions described above is illustrated in Figure 1. The analysis is achieved in less than eleven minutes with all analytes possessing good peak shape (greatest asymmetry at 10% value measured for mandelic acid at 1.18).

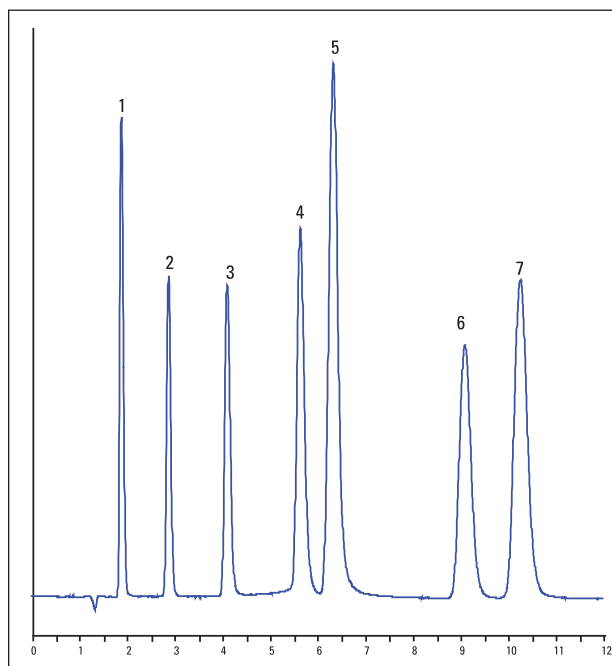


Figure 1: Metabolite separation: 1. Mandelic acid; 2. o-Methylhippuric acid; 3. Hippuric acid; 4. Phenyl-glyoxylic acid; 5. p-Hydroxybenzoic acid (internal standard); 6. m-Methylhippuric acid; 7. p-Methylhippuric acid.

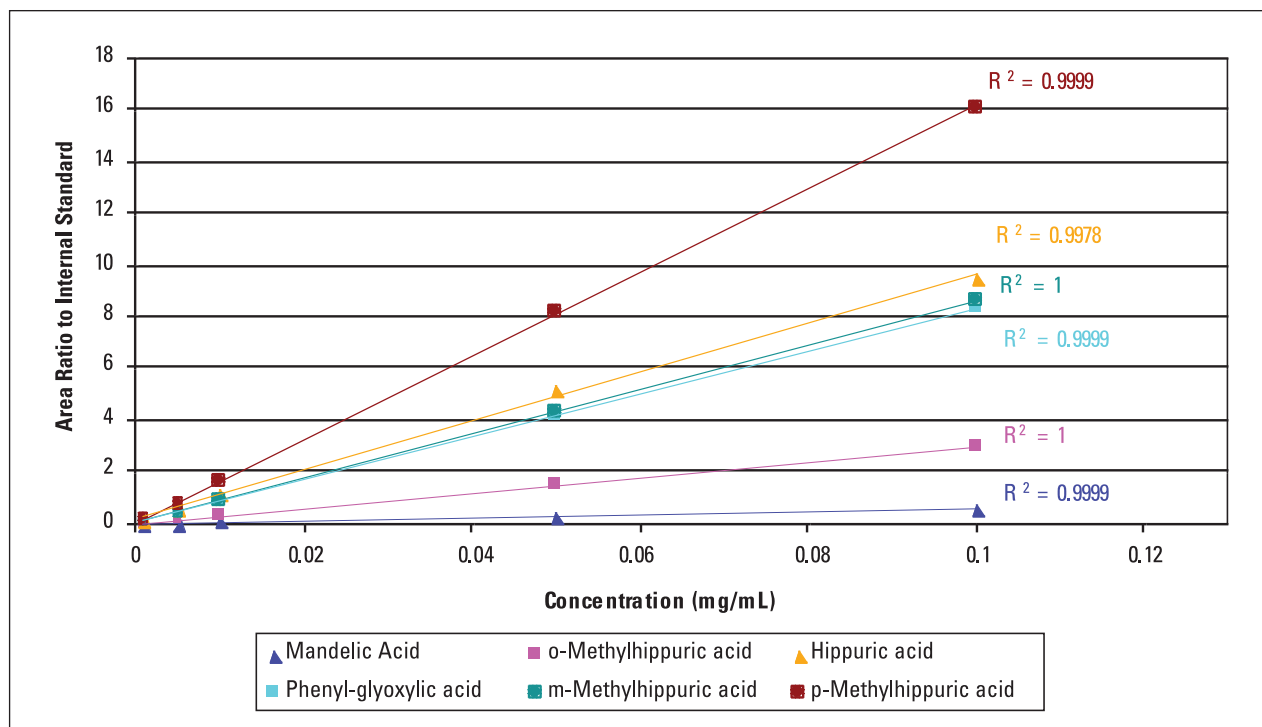


Figure 2: Linearity in the concentration range of 1 to 100 g/mL.

The suitability of the method for quantitative analysis was investigated through linearity and reproducibility assessment. The calibration curve displayed in Figure 2 shows that all analytes generate a true linear response over the concentration range of 1 – 100 µg/mL with the lowest R^2 coefficient value being recorded at 0.9978 for hippuric acid.

With respect to reproducibility of area, ratio of analyte area to internal standard (p-hydroxybenzoic acid) and repeatability of retention times (Table 1), the percentage relative standard deviation values recorded over twenty injections (equating to 240 column volumes) were low. The highest value observed was for the ratio of analyte area to internal standard area for 2-methylhippuric acid which was calculated at 1.15%.

Compound	%RSD Retention times	%RSD Area Ratio
Mandelic acid	0.28	1.09
o-Methylhippuric acid	0.47	1.15
Hippuric acid	0.63	1.05
Phenyl-glyoxylic acid	0.87	0.86
p-Hydroxybenzoic acid	0.76	
m-Methylhippuric acid	0.51	1.05
p-Methylhippuric acid	0.52	1.03

Table 1: Method reproducibility (n = 20 runs).

Conclusion

The use of Hypercarb for the effective separation of the associated compounds of styrene, toluene and xylene metabolism is demonstrated. Using a simple two component isocratic mobile phase all major metabolites (and an internal standard) are separated in under 11 minutes. The method is reproducible and linear in the concentration range of 1 to 100 g/mL.

References

1. Wallén M., Näslund P.H., Byfält Nordqvist M., *Toxicol Appl Pharmacol*, 1984; 76:414-419.
2. Schlatter J., Astier A., *Biomed. Chromatogr.* 1995, 9, 302-304.
3. Lauweys R.R., Hoet P., *Industrial Chemical Exposure Guidelines for Biological Monitoring*, 3rd Edition, Lewis Publishers.
4. International Agency for Research on Cancer (IARC). *IARC Monographs on the Evaluation of Carcinogenic Risk to Humans, Some Industrial Chemicals*. Lyon: IARC, 1994, Vol. 60, 233-246.

Porous Graphitic Carbon for Inorganic Ion Analysis in Drinking Water

A. Thompson, A. H. Marks Ltd, Wyke, Bradford, UK
L. Pereira, Thermo Fisher Scientific, Runcorn, UK

Introduction

The analysis of inorganic ions is routinely performed on a range of support materials, which include functionalised styrene-divinylbenzene copolymers, coated silica gels and even traditional ODS (C18) phases used in conjunction with ion pair reagents.

Hypercarb has been previously used for the analysis of inorganic ions. Elfakir and co-workers demonstrated the separation of hydrogenophosphate, sulphate, nitrate, and perchlorate with a volatile electronic interaction additive (formic, acetic, or perfluoro-carboxylic acid) in the aqueous mobile phase.^{1,2} Takeuchi *et al.* used sodium sulphate in the mobile phase to retain and separate iodate, bromide, nitrite, bromate, nitrate and iodide on a PGC column.³ Ion interaction chromatography with tetrabutylammonium hydroxide has also been used to separate inorganic ions on PGC.⁴ The same authors dynamically coated the surface of graphite with cetyltrimethylammonium (CTA) ions for the separation of seven common anions in water: F⁻, Cl⁻, NO₂⁻, Br⁻, NO₃⁻, HPO₄²⁻, SO₄²⁻.⁵ Using CTA-bromide as the coating agent, a permanently coated ion-exchange column was obtained which allowed separations of the anions without any coating agent in the mobile phase. This coating process was used in the work described in this application note.

In this application note it is demonstrated that by dynamically coating the Hypercarb surface with an ion exchanger a stable surface suitable for the ion chromatography of common inorganic anions is produced. We investigate the effect of coating coverage on the retention and resolution of anions whilst demonstrating good reproducibility, linearity, and excellent column coating lifetime. Two brands of bottled drinking water are analysed for inorganic anions using the methodology developed.

Goal

To study the suitability of porous graphitic carbon dynamically modified with cetyltrimethylammonium bromide for the selective ion chromatography of inorganic anions in drinking water.

Experimental

Column

Hypercarb 5 µm, 100 x 4.6 mm
(part number 35005-104630)

Ion exchanger – Cetyltrimethylammonium bromide (CTA) is adsorbed onto the surface of Hypercarb during coating process.

Hypercarb Coating Process

- Step 1. Column flushed with H₂O at 1 mL/min for 60 minutes.
- Step 2. Column flushed with CTA 0.5 mM in H₂O/MeCN (75:25), at 1 mL/min for 120 minutes.
- Step 3. Column flushed with H₂O at 1 mL/min for 60 minutes.

Ion Chromatograph

Dionex DX 300 Ion Chromatograph
Anion micromembrane suppressor, Dionex 4400 integrator
Rheodyne 7125 injector (20 µL loop)

Separation Conditions

Mobile Phase: 2 mM Na₂CO₃/1 mM NaHCO₃ + 2.5% MeCN
Flow Rate: 1.2 mL/min
Detection: Suppressed conductivity
Injection Volume: 20 µL

Results and Discussion

The separation of six inorganic anions commonly found in water was obtained in less than 15 minutes and is illustrated in Figure 1. Fluoride is retained away from the solvent front, allowing for easy quantification.

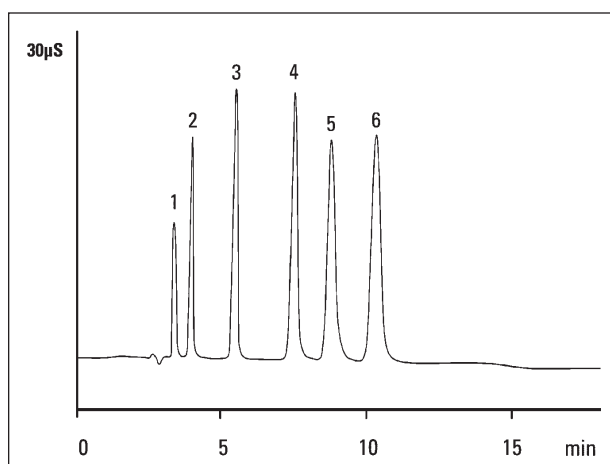


Figure 1: Separation of six anion mixture: 1. Fluoride; 2. Chloride; 3. Bromide; 4. Nitrate; 5. Phosphate; 6. Sulphate.

The degree of coating of the surface can be manipulated to offer changes in retention times and therefore the resolution of common anions, which provides the flexibility of tailoring the column performance to suit particular application needs. The concentration of CTA was increased whilst the remaining conditions for coating remained constant, giving increased adsorption of the ion exchanger onto the Hypercarb surface. The increased ion exchange capacity leads to increased retention times and therefore greater resolution of anions, as demonstrated in Figure 2.

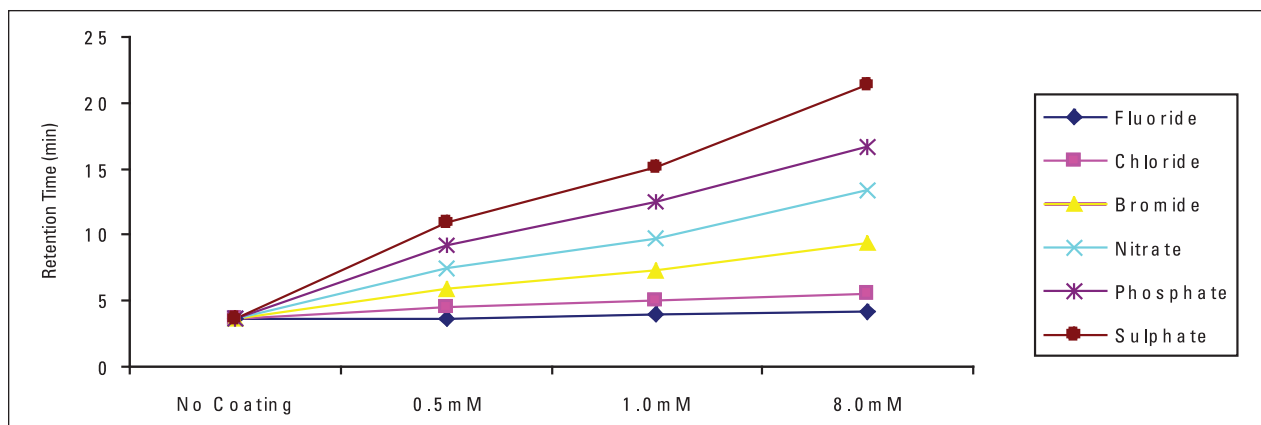


Figure 2: Effect of coating concentration on retention behavior.

The suitability of the method for quantitative analysis was investigated through a linearity assessment. Calibration curves (Figure 3) were generated by plotting the peak response area against the concentration of the standards injected. For fluoride and chloride 5 concentrations between 1 mg/L and 10 mg/L were used. For bromide, nitrate, phosphate and sulphate concentrations between 10 mg/L and 100 mg/L were used. All analytes generate a true linear response over the concentration ranges described, with the lowest R^2 coefficient value being recorded at 0.9978 for phosphate.

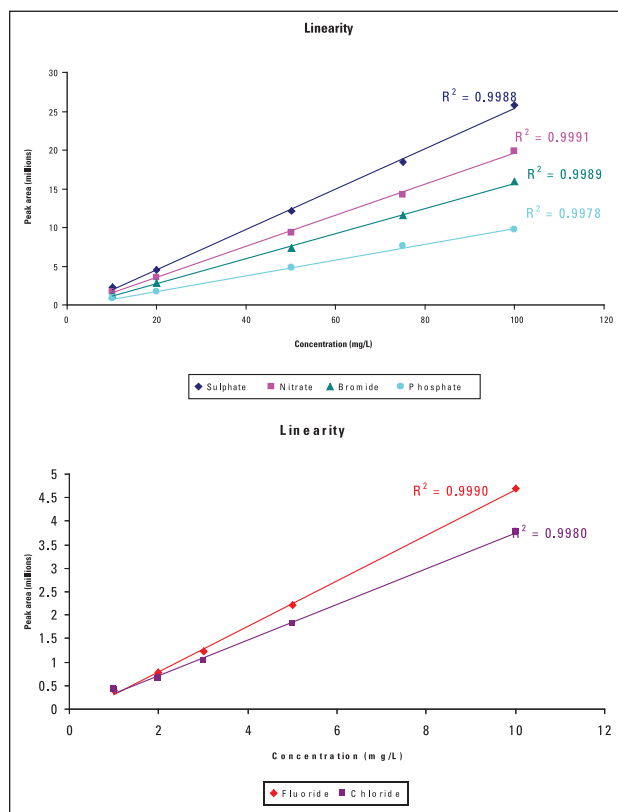


Figure 3: Linearity data in the concentration range of 10 to 100 mg/L for sulphate, nitrate, bromide and phosphate and 1 to 10 mg/L for fluoride and chloride.

To evaluate the reproducibility of area and repeatability of retention times, the percentage relative standard deviation (RSD) values were recorded over ten and twenty injections respectively (Table 1). The highest value observed for peak area RSD was 0.5% for fluoride and the highest RSD value for retention time was 1.1%.

The lifetime of the coated column was investigated by doing repeated injections of the anion mixture. Retention times remain constant for 445 runs, which equates to 16000 column volumes of mobile phase through the column (Figure 4). As the coating process involves the use of 25% organic, it ensures that using 5% organic during analysis will not be detrimental to column coating lifetime. The dynamic coating of the PGC surface is reversible. Flushing the column with 100% organic will remove all column coating, and the column can then be re-coated using original coating conditions or used as a conventional Hypercarb column.

Compound	%RSD Peak Area	%RSD Retention Time
Fluoride	0.51	0.21
Chloride	0.47	0.30
Bromide	0.26	0.57
Nitrate	0.20	0.75
Phosphate	0.57	0.47
Sulphate	0.27	1.09

Table 1: Reproducibility: 10 repeated measurements for peak areas and 20 repeated measurements for retention times.

The methodology developed was applied to the measurement of the level of inorganic anions present in two brands on bottled water, as demonstrated in Figure 5.

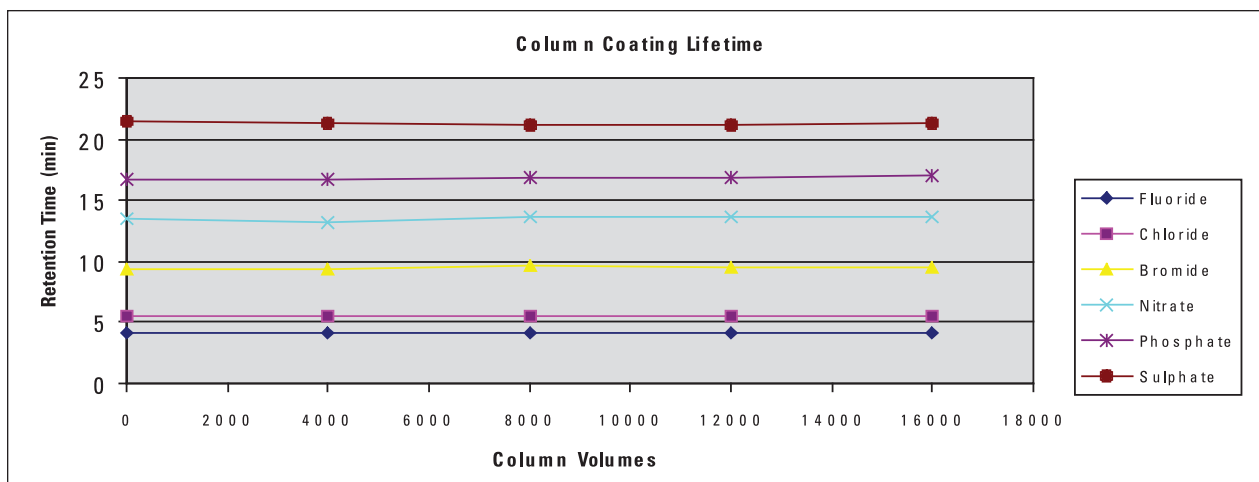


Figure 4: Column coating lifetime. Reproducible retention times for 16000 column volumes of mobile phase through the column or 445 injections. Column: Hypercarb 5 μ m, 100 x 4.6 mm (CTA 8 mM); Mobile phase: 2 mM Na_2CO_3 /1 mM NaHCO_3 + 5% MeCN; other conditions as described in the experimental section.

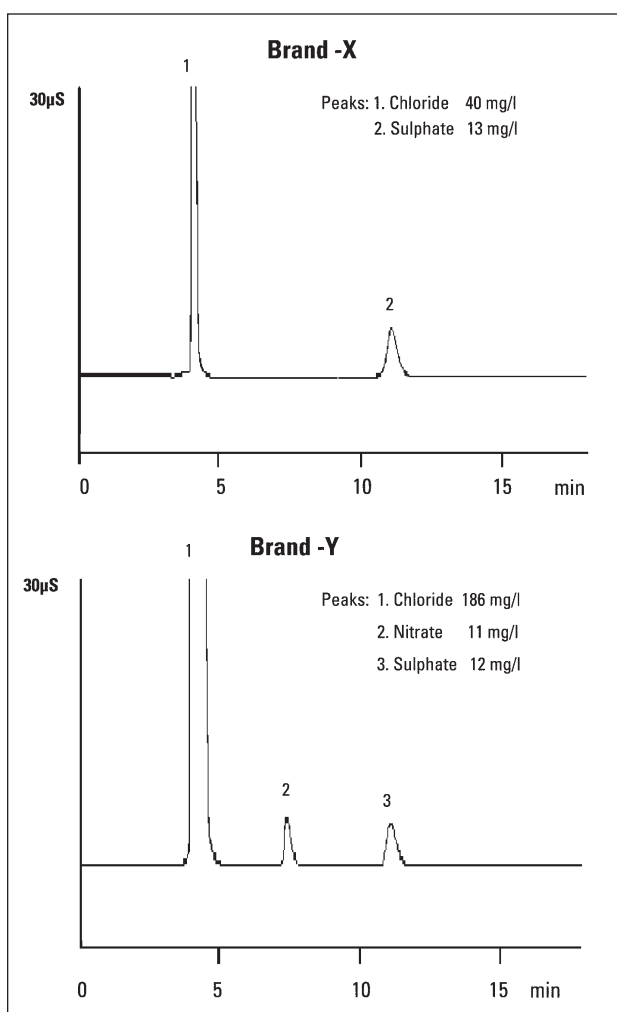


Figure 5: Analysis of bottled drinking water.

Conclusion

Dynamically CTA coated Hypercarb columns possess good stability, reproducibility, linearity and lifetime performance working with organic compositions up to 25%. This approach offers an alternative to the conventional methodology for the determination on inorganic anions in drinking water.

References

1. C. Elfakir, P. Chaibault, M. Dreux, *J. Chromatogr. A*, 829 (1998) 193
2. K. Petritis, P. Chaibault, C. Elfakir, M. Dreux, *J. Chromatogr. A*, 1999, 833, 147
3. T. Takeuchi, T. Kojima, T. Miwa, *J. High, Resol. Chromatogr.*, 2000, 23, 590
4. T. Okamoto, A. Isozaki, H. Nagashima, *J. Chromatogr. A*, 1998, 800, 239
5. H. Nagashima, T. Okamoto, *J. Chromatogr. A*, 1999, 855, 261-266

Applications Review

The table below provides an overview of the applications published between mid -1995 and 2008; these are organised in the following subsections: isomers (geometrical, positional and diastereoisomers), polar compounds (nucleotides/nucleosides/nucleobases, amino acids and peptides, carbohydrates and sugars, and other polar molecules), charged solutes and miscellaneous. The miscellaneous and other polar molecules subsections are further categorised into application areas such as food safety, environmental, pharmaceutical, etc.

Applications areas for PGC which are outside the scope of this review and therefore not covered include high temperature applications, chiral separations, PGC as a sorbent in solid phase extraction, electrically modulated chromatography and electrochromatography.

Applications Reference Guide (Modified from Reference 1.)

Application by Solute Type

Application Area	Analyte Group	Reference Number	
Isomers	Ionizable substituted benzenes	2, 3	
	Cresol	4	
	Substituted aromatics	5	
	p-Nonylphenol	6	
	Sulfobutyl ether- β -cyclodextrin	7	
	Schumannifidine	8	
	Tropane alkaloids	9	
	Estrogens	10	
	F2-Isoprostanes	11, 12	
	Branched oligosaccharides	13	
	Leucine, isoleucine, allo-isoleucine	14	
	Diastereoisomers	Xylose derivative	15
		Oligomers of methylidene malonate	16
Metabolites II, III, and VII, VIII		17	
Nucleotides/Nucleosides	Nucleobases, nucleosides, nucleotides	16	
	Purine bases	19	
	Nucleosides and their mono-, di- and triphosphates	20	
	Uracil, dihydrouracil	21	
	Tegafur, 5-fluorouracil, 5-fluorodihydrouracil	22	
Amino Acids and Peptides	Underivatized amino acids	23	
	Taurine derivatives	25	
	Di-, tri-, tetra-peptides	24, 27	
	Small peptides in wine	26	
	Phosphopeptides	27, 28	
	Glycopeptides	29	
Carbohydrates and Sugars	Mono-, disaccharides	29, 33, 42	
	Cyclodextrins	29, 46, 47, 7	
	Oligosaccharide alditols	29, 35, 36	
	N-linked oligosaccharides	29, 34, 35, 38, 41	
	Oligosaccharides	29, 36, 37, 39, 40, 42	
	Sugar phosphates	30	
	Sulphated disaccharides	31	
	Glycosaminoglycans	32	
	Carrageenans	43, 44, 45	
	Other Polar Species	Catecholamines/neurotransmitters	48, 49, 50, 51
<i>Biochemical</i>			
Glutathione and conjugates		52, 53	
Oligonucleotides		54	
Creatinine/creatinine		55	

Application Area	Analyte Group	Reference Number	
<i>Pharmaceutical</i>	Clopidogel and metabolites	56	
	Acarbose and metabolites	57	
	Metabolites in Escherichia coli K12	58	
	Arabinoside-CMP, cytarabine	59, 60	
	Cimetidine	61	
	Levetiracetam	64	
	Oxaliplatin	63	
	EDTA impurities	62	
<i>Food Safety</i>	Methylamines	65	
	Polar Phenolic	66	
	Acrylamide	67, 68	
	Acromelic acid A	69	
<i>Environmental</i>	Aniline	70	
	Glyphosate and Ampa	71	
	Cyanuric acid	72	
<i>Surfactants</i>	Alkylglycoside detergents	73	
	Polyethoxylated alcohols	74	
	Oligoglycerols	75	
	Oligomers of nonylphenyl ethylene	76	
	Polyglycerol fatty esters and fatty ethers	77	
<i>Natural Products</i>	Cyanoglycosides	78	
	Glucosinolates	79	
<i>Chemical Warfare</i>	Phosphonic acids	80	
<i>Other</i>	Guanidino compounds	81, 82	
	Diphosphine-bridged complexes	83	
Charged Solutes	Pertechnetate and perhenate ions	84	
	Organometallic-charged complexes	85, 86	
	Inorganic anions	87-89, 91, 92	
	Copper (II), copper (III)	90	
	Diquat, paraquat and difenzoquat	93	
Non-polar Solutes	Wax esthers	94	
	<i>Lipids</i>	Ceramides	94 -97
		Fatty acids methyl esters	94, 98-100
		Glycosphingolipids	101
		Triacylglycerols	107
	<i>Natural Products</i>	Digalactosyldiacylglycerol	102
		Triterpenic acids	103
		Taxol	104, 105
		Non-flavonoid polyphenols	106
		Ferrichrome and ferricrocin	107
<i>Pharmaceutical</i>	Morphine and metabolites	108	
	Pharmaceuticals and related substances	109-113	
	Steroids	114	
	Cyclosporins A and U	115	
	Tetracycline antibiotics	116	
	Phthalate metabolites	117	
<i>Clinical</i>	Boron-containing compounds	118	
	Flame retardants hydrolysis products	119	
<i>Environmental</i>	Benzo[]pyrene	120	
	PCBs	121-123	
	Halogenated contaminants and PAHs	124	
	Betamethasone and dexamethasone	125, 126	
<i>Food Safety</i>	Glucocorticoids and corticosteroids	127-129	
	Fenbutin oxide	130	
<i>Explosives</i>	Nitroaromatic and organic explosives	131-135	
	Nitrate ester, nitramine and nitroaromatic explosives	136	

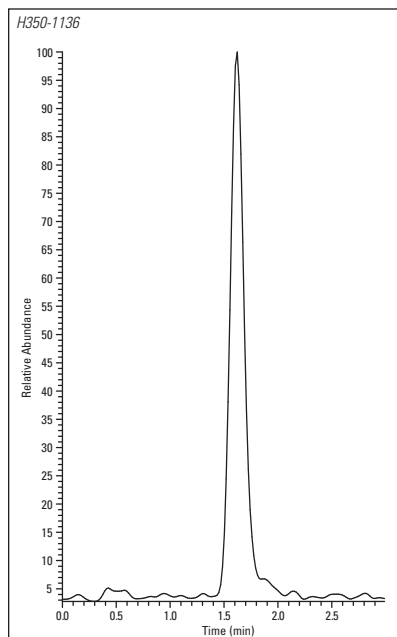
References

1. L. Pereira, *J. of Liq. Chromatogr. & Related Technol.*, **2008**, 31:11, 1687-1731
2. Q. Wan, P. Shaw, M. Davies, D. Barret, *J. Chromatogr. A*, **1995**, 697, 219-227
3. Q. Wan, P. Shaw, M. Davies, D. Barret, *Anal. Chem.*, **1996**, 68, 437-446
4. A. Schlatter, *Biomed. Chromatogr.*, **1995**, 9, 302-304
5. C. West, E. Lesellier, *J. Chromatogr. A*, **2005**, 1099, 175-184
6. J. Gundersen, *J. Chromatogr. A*, **2001**, 914, 161-166
7. R. Jacquet, R. Pennanec, C. Elfakir, M. Lafosse, *J. Sep. Sci.*, **2004**, 27, 1221-1228
8. P. Houghton, T. Woldermarium, *Phytochemical Anal.*, **1995**, 6, 85-88
9. S. Bieri, E. Varesio, O. Muñoz, J.-L. Veuthey, P. Christen, *J. Pharma. Biomed. Anal.*, **2006**, 40, 545-551
10. J. Reepmeyer, J. Brower, H. Ye, *J. Chromatogr. A*, **2005**, 1083, 42-51
11. K. Bohnstedt, B. Karlberg, L.-O. Wahlund, M. Jonhagen, H. Basun, S. Schmidt, *J. Chromatogr. B*, **2003**, 796, 11-19
12. K. Bohnstedt, B. Karlberg, H. Basun, S. Schmidt, *J. Chromatogr. B*, **2005**, 827, 39-43
13. Y. Okada, M. Semma, Y. Ito, *Carbohydrate Res.*, **2001**, 336, 203-211
14. D. Cooper, M. Morris, S. Kim, *Waters Application Brief (WAB22)*, **2002**
15. M. Chiron, N. Bonaventure, L. Boisauvert, V. Manzin, Poster presented at HPLC 2005 conference, 2005, Stockholm
16. A. Salvador, B. Herbreteau, P. Bretonb, D. Royc, P. Brigandc, N. Brub, M. Dreux, *Anal. Chim. Acta*, **1998**, 359, 57-64
17. Y.Q. Xia, M. Jemal, N. Zheng, X. Shen, *Rapid Commun. Mass Spectrom.*, **2006**, 20, 1831-1837
18. D. Gasparutto, J.-L. Ravanat, O. Gerot, J. Cadet, *J. Am. Chem. Soc.*, **1998**, 120, 10283-10286
19. L. Monser, *Chromatographia*, **2004**, 59, 455-459
20. J. Xing, A. Apedo, A. Tymiak, N. Zhao, *Rapid Commun. Mass Spectrom.*, **2004**, 18, 1599-1606
21. G. Remaudb, M. Boisdrón-Celle, C. Hameline, A. Morel, E. Gamelin, *J. Chromatogr. A*, **2005**, 823, 98-107
22. G. Remaudb, M. Boisdrón-Celle, A. Morel, E. Gamelin, *J. Chromatogr. B*, **2005**, 824, 153-160
23. P. Chaimbault, K. Petritis, C. Elfakir, M. Dreux, *J. Chromatogr. A*, **2000**, 896, 253-263
24. A. Adoubel, S. Guenu, C. Elfakir, M. Dreux, *J. Liq. Chrom. & Rel Technol.*, **2000**, 23, 2433-2446
25. P. Chaimbault, P. Alberic, C. Elfakir, M. Lafosse, *Anal. Biochem.*, **2004**, 332, 215-225
26. C. Desportes, M. Charpentier, B. Duteurtre, A. Maujeanc, F. Duchiron, *J. Chromatogr. A*, **2000**, 893, 281-291
27. E. Chin, D. Papac, *Anal. Biochem.*, **1999**, 273, 179-185
28. P. Vacratsis, B. Phinney, D. Gage, K. Gallo, *Biochemistry*, **2002**, 41, 5613-5624
29. K. Koizumi, *J. Chromatogr. A*, **1996**, 720, 119-126
30. C. Antonio, T. Larson, A. Gilday, I. Graham, E. Bergström, J. Thomas-Oates, *J. Chromatogr. A*, **2007**, 1172, 170-178
31. B. Barroso, M. Didraga, R. Bischoff, *J. Chromatogr. A*, **2005**, 1080, 43-48
32. N. Karlsson, B. Schulz, N. Packer, J. Whitelock, *J. Chromatogr. B*, **2005**, 824, 139-147
33. N. Nielsen, K. Granby, R. Hedegaard, L. Skibste, *Anal. Chim. Acta*, **2006**, 557, 211-220
34. N. Packer, M. Lawson, D. Jardine, J. Redmond, *Glycoconjugate J.*, **1998**, 15, 737-747
35. S. Itoh, N. Kawasaki, M. Ohta, M. Hyuga, S. Hyuga and T. Hayakawa, *J. Chromatogr. A*, **2002**, 968, 89-100
36. J. Yuan, N. Hashii, N. Kawasaki, S. Itoh, T. Kawanishi, T. Hayakawa, *J. Chromatogr. A*, **2005**, 1067, 145-152
37. B. Barroso, R. Dijkstra, M. Geerts, F. Lagerwerf, P. van Veelen, A. de Ru, *Rapid Commun. Mass Spectrom.*, **2002**, 16, 1320-1329
38. B. Schulz, N. Packer, N. Karlsson, *Anal. Chem.*, **2002**, 74, 6088-6097
39. S. Robinson, E. Bergström, M. Seymour, J. Thomas-Oates, *Anal. Chem.*, **2007**, 79, 2437-2445
40. N. Kawasaki, M. Ohta, S. Hyuga, O. Hashimoto, T. Hayakawa, *Anal. Biochem.*, **1999**, 269, 297-303
41. N. Kawasaki, M. Ohta, S. Hyuga, M. Hyuga and T. Hayakawa, *Anal. Biochem.*, **2000**, 285, 82-91
42. M. Davies, E. Hounsell, *J. Chromatogr.*, **1996**, 720, 227-233
43. A. Antonopoulos, B. Herbreteau, M. Lafosse, W. Helbert, *J. Chromatogr. A*, **2004**, 1023, 231-238
44. A. Antonopoulos, P. Favetta, M. Lafosse, W. Helbert, *J. Chromatogr. A*, **2004**, 1059, 83-87
45. A. Antonopoulos, P. Favetta, W. Helbert, M. Lafosse, *J. Chromatogr. A*, **2007**, 1147, 37-41
46. I. Clarot, D. Clédát, L. Boulkanz, E. Assidjo, T. Chianéa, P. Cardot, *J. Sep. Sci.*, **2000**, 38, 38-45
47. Kwatereczak, Bielejewska, *Anal. Chim. Acta*, **2005**, 537, 41-46
48. A. Törnkvist, P. Sjöberg, K. Markides, J. Bergquist, *J. Chromatogr. B*, **2004**, 801, 323-329
49. P. Koivisto, A. Törnkvist, E. Heldin, K. Markides, *Chromatographia*, **2002**, 55, 39-42
50. S. Rinne, A. Holm, E. Lundanes, T. Greibrokk, *J. Chromatogr. A*, **2006**, 1119, 285-293
51. D. Thiébaud, J. Vial, M. Michel, M.-C. Hennion, T. Greibrokk, *J. Chromatogr. A*, **2006**, 1122, 97-104
52. A. Sakhi, K. Russnes, S. Smeland, R. Blomhoff, T. Gundersen, *J. Chromatogr. A*, **2006**, 1104, 179-189
53. T. Lindemann, H. Hintelmann, *Anal. Chem.*, **2002**, 74, 4602-4610
54. D. Gasparutto, J.-L. Ravanat, O. Gérot, J. Cadet, *J. Am. Chem. Soc.*, **1998**, 120, 10283-10286
55. T. Smith-Palmer, *J. Chromatogr. B*, **2002**, 781, 93-106
56. A. Mitakos, I. Panderi, *Anal. Chim. Acta*, **2004**, 505, 107-114
57. Y. Daali, S. Cherkaoui, X. Cahours, E. Varesio, J.-L. Veuthey, *J. Sep. Science*, **2002**, 25, 280-284
58. A. Buchholz, R. Takors, C. Wandrey, *Anal. Biochem.*, **2001**, 295, 129-137
59. M.-H. Gouya, H. Fabre, M. Blanchin, S. Peyrottes, C. Périgaud, I. Lefebvre, *Anal. Chim. Acta*, **2006**, 566, 178-184
60. Y. Hsieh, C. Duncan, J.-M. Brisson, *Rapid Commun. Mass Spectrom.*, **2007**, 21, 629-634
61. N. Helali, L. Monser, *Chromatographia*, **2006**, 63, 425-430
62. H. Altorfer, *Pharmazie*, **2002**, 14, 637-639
63. H. Ehrsson, I. Wallin, *J. Chromatogr. B*, **2003**, 795, 291-294
64. J. Martens-Lobenhoffer, S. Bode-Boger, *J. Chromatogr. B*, **2005**, 819, 197-200
65. L. Monser, G. Greenway, *Anal. Chim. Acta*, **1996**, 322, 63-68
66. J. Vial, M.-C. Hennion, A. Fernandez-Alba, A. Aguera, *J. Chromatogr. A*, **2001**, 937, 21-29
67. H. Rosen, *Analyst*, **2002**, 127, 880-882
68. A. Claus, G. Weisz, D. Kammerer, R. Carle, A. Schieber, *Mol. Nutr. Food Res.*, **2005**, 49, 918 - 925

69. J. Bessarda, P. Saviuc, Y. Chane-Yenea, S. Monnetta, G. Bessarda, *J. Chromatogr. A*, **2004**, 1055, 99-107
70. R. Delépée, P. Chaimbault, J.-P. Antignac, M. Lafosse, *Rapid Commun. Mass Spectrom.*, **2004**, 18, 1548-1552
71. R. Phillips, *L.C.G.C. EUR*, **2003**, Suppl. S, 7-8
72. R. Cantú, O. Evans, F. Kawahara, L. Wymer, A. Dufo, *Anal. Chem.*, **2001**, 73, 3358-3364
73. C. Elfakir, M. Lafosse, *J. Chromatogr. A*, **1997**, 782, 191-198
74. P. Chaimbault, C. Elfakir, M. Lafosse, *J. Chromatogr. A*, **1998**, 797, 83-91
75. P. Chaimbault, S. Cassel, S. Claude, C. Debaig, T. Benvegnu, D. Plusquellec, P. Rollin, M. Lafosse, *Chromatographia*, **1999**, 50, 239-242
76. T. Cserhádi, E. Forgács, A. Szilágyi, *J. Pharma. Biomed. Anal.*, **1997**, 15, 1303-1307
77. S. Cassel, P. Chaimbault, C. Debaig, T. Benvegnu, S. Claude, D. Plusquellec, P. Rollin, M. Lafosse, *J. Chromatogr. A*, **2001**, 919, 95-106
78. V. Berenguer-Navarro, R. Giner-Galván, N. Grané-Teruel, G. Arrazola-Paternina, *J. Agr. Food Chem.*, **2002**, 50, 6960-6963
79. C. Elfakir, M. Dreux, *J. Chromatogr. A*, **1996**, 727, 71-81
80. J.-P. Mercier, P. Morina, M. Dreux, A. Tambute, *J. Chromatogr. A*, **1999**, 849, 197-207
81. Y. Inamoto, S. Inamoto, T. Hanai, M. Tokuda, O. Hatase, K. Yoshii, N. Sugiyama, T. Kinoshita, *J. Chromatogr. B*, **1998**, 707, 111-120
82. T. Hanai, Y. Inamoto, S. Inamoto, *J. Chromatogr. B*, **2000**, 747, 123-138
83. C.-H. Li, P. Low, H. Lee, T. Hor, *Chromatographia*, **1997**, 44, 381-385
84. C.-K. Lim, *Biomed. Chromatogr.*, **1989**, 3, 92-93
85. M. Emery, C.-K. Lim, *J. Chromatogr.*, **1989**, 479, 212-215
86. G. Gu, C.-K. Lim, *J. Chromatogr.*, **1990**, 515, 183-...
87. C. Elfakir, P. Chaimbault, M. Dreux, *J. Chromatogr. A*, **1998**, 826, 193-199
88. K. Petritis, P. Chaimbault, C. Elfakir, M. Dreux, *J. Chromatogr. A*, **1999**, 833, 147-
89. T. Takeuchi, T. Kojima, T. Miwa, *J. High, Resol. Chromatogr.*, **2000**, 23, 590-594
90. C. Merly, B. Lynch, P. Ross, J. Glennon, *J. Chromatogr. A*, **1998**, 804, 187-...
91. T. Okamoto, A. Isozaki, H. Nagashima, *J. Chromatogr. A*, **1998**, 800, 239-...
92. H. Nagashima, T. Okamoto, *J. Chromatogr. A*, **1999**, 855, 261-266
93. M. Ibáñez, Y. Picó, J. Mañes, *Chromatographia*, **1997**, 45, 402-407
94. F. Deschamps, K. Gaudin, E. Lesellier, A. Tchaplá, D. Ferrier, A. Baille, P. Chaminade, *Chromatographia*, **2001**, 54, 607-611
95. K. Gaudin, P. Chaminade, A. Baillet, *J. Chromatogr. A*, **2002**, 973, 69-83
96. C. West, G. Cilpa, K. Gaudin, P. Chaminade, E. Lesellier, *J. Chromatogr. A*, **2005**, 1087, 77-85
97. L. Quinton, K. Gaudin, A. Baillet, P. Chaminade, *J. Sep. Sci.*, **2006**, 29, 390-398
98. C. Viron, P. André, M. Dreux, and M. Lafosse, *Chromatographia*, **1999**, 49, 137-141
99. C. Viron, A. Saunois, P. Andre, B. Perly, M. Lafosse, *Anal. Chim. Acta*, **1999**, 20316, 1-11
100. K. Gaudin, T. Hanai, P. Chaminade, A. Baillet, *J. Chromatogr. A*, **2007**, 1157, 56-64
101. S. Roy, A. Delobel, K. Gaudin, D. Touboul, D. Germain, A. Baillet, P. Prognon, O. Laprèvote, P. Chaminade, *J. Chromatogr. A*, **2001**, 1117, 154-162
102. F. Deschamps, K. Gaudin, A. Baillet, P. Chaminade, *J. Sep. Sci.*, **2004**, 27, 1313-1322
103. C. Berangere, N. Caussarieu, P. Morin, L. Morin-Allory, M. Lafosse, *J. Sep. Sci.*, **2004**, 27, 964-970
104. V. Németh-Kiss, E. Forgács, T. Cserhádi, G. Schmidt, *J. Chromatogr. A*, **1996**, 750, 253-256
105. V. Németh-Kiss, E. Forgács, T. Cserhádi, G. Schmidt, *J. Pharma. Biomed. Anal.*, **1996**, 14, 997-1001
106. E. Leira, A. Botana and R. Cela, *J. Chromatogr.*, **1996**, 724, 67-78
107. M. Moberg, S. Holmstrom, U. Lundstrom, K. Markides, *J. Chromatogr. A*, **2003**, 1020, 91-98
108. D. Barrett, M. Pawula, R. Knaggs, P. Shaw, *Chromatographia*, **1998**, 47, 667-672
109. A. Karlsson, M. Berglin, C. Charron, *J. Chromatogr. A*, **1998**, 797, 75-82
110. L. Monser, F. Darghouth, *J. Pharma. Biomed. Anal.*, **2002**, 27, 851-860
111. L. Monser, F. Darghouth, *J. Pharmaceut. Biomed.*, **2003**, 32, 1087-1092
112. L. Monser, H. Trabelsi, *J. Liq. Chromatogr. Rel. Techn.*, **2003**, 26, 261-271
113. J. Xu, A.-F. Aubry, *Chromatographia*, **2003**, 57, 67-71
114. E. Forgács, T. Cserhádi, *J. Pharma. Biomed. Anal.*, **1998**, 18, 15-20
115. T. Nazir, L. Gould, C. Marriott, G. Martin, M. Brown, *Chromatographia*, **1997**, 46, 628-636
116. L. Monser, F. Darghouth, *J. Pharmaceut. Biomed.*, **2000**, 23, 353-362
117. A. Holm, K. Solbu, P. Molander, E. Lundanes, T. Greibrokk, *Anal. Bioanal. Chem.*, **2004**, 378, 1762-1768
118. E. Svantesson, J. Capala, K. Markides, J. Pettersson, *Anal. Chem.*, **2002**, 74, 5358-5363
119. K. Moller, C. Crescenzi, U. Nilsson, *Anal. Bioanal. Chem.*, **2004**, 378, 197-204
120. A. Al-Haddad, *Talanta*, **2003**, 59, 845-848
121. K. Echolsa, R. Gale, K. Feltz, J. O'Laughlin, D. Tillitt, T. Schwartz, *J. Chromatogr.*, **1998**, 811, 135-144
122. M. Pietrogrande, A. Benvenuti, S. Previato, F. Dondi, *Chromatographia*, **2000**, 52, 425-432
123. S. Chu, C.-S. Hong, B. Rattner, P. McGowan, *Anal. Chem.*, **2003**, 75, 1058-1066
124. J. de Boer, R. Law, *J. Chromatogr. A*, **2003**, 1000, 223-251
125. Y. Luo, C. Uboh, L. Soma, F. Guan, J. Rudy, D. Tsang, *Rapid Commun. Mass Spectrom.*, **2005**, 19, 825-832
126. O. Van den Hauwe, J. Perez, J. Claereboudt, C. Van Peteghem, *Rapid Commun. Mass Spectrom.*, **2001**, 15, 857-861
127. O. Van den Hauwe, F. Dumoulin, J. Antignac, M. Bouche, C. Elliott, C. Van Peteghem, *Anal. Chim. Acta*, **2002**, 473, 127-134
128. O. Van den Hauwe, F. Dumoulin, C. Elliott, C. Van Peteghem, *J. Chromatogr. B*, **2002**, 817, 215-223
129. C. Baiocchi, M. Brussino, M. Pazzi, C. Medana, C. Marini, E. Genta, *Chromatographia*, **2003**, 58, 11-14
130. K. Barnes, R. Fussell, J. Startin, H. Mobbs, R. James, S. Reynolds, *Rapid Commun. Mass Spectrom.*, **1997**, 11, 159-164
131. R. Batlle, H. Carlsson, E. Holmgren, A. Colmsjö, C. Crescenzi, *J. Chromatogr. A*, **2002**, 963, 73-82
132. C. Sánchez, H. Carlsson, A. Colmsjö, C. Crescenzi, R. Batlle, *Anal. Chem.*, **2003**, 75, 4639-4645
133. R. Batlle, C. Nerin, C. Crescenzi, H. Carlsson, *Anal. Chem.*, **2005**, 77, 44241-4247
134. E. Holmgren, H. Carlsson, P. Goede, C. Crescenzi, *J. Chromatogr. A*, **2005**, 1099, 127-135
135. C. Crescenzi, J. Albiñana, H. Carlsson, E. Holmgren and R. Batlle, *J. Chromatogr. A*, **2007**, 1153, 186-193
136. R. Tachon, V. Pichon, M. Le Borgne, J.-J. Minet, *J. Chromatogr. A*, **2007**, 1154, 174-181

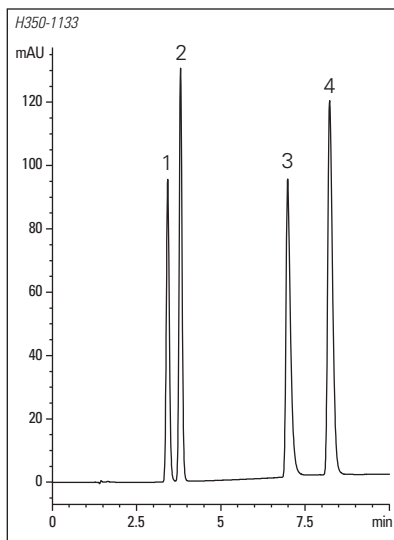
Application Chromatograms

Allantoin



Column: Hypercarb, 3 μ m, 50 x 2.1 mm
 Part Number: 35003-052130
 Mobile Phase: A – H₂O + 0.1 % Formic acid;
 B – MeCN + 0.1 % Formic acid.
 Isocratic: 95% A + 5% B, run for 5 min.
 Flow Rate: 0.3 mL/min.
 Detection: UV @ 205 nm; MS: ESI –ve,
 Temperature: 30 °C.
 Injection Volume: 5 μ L

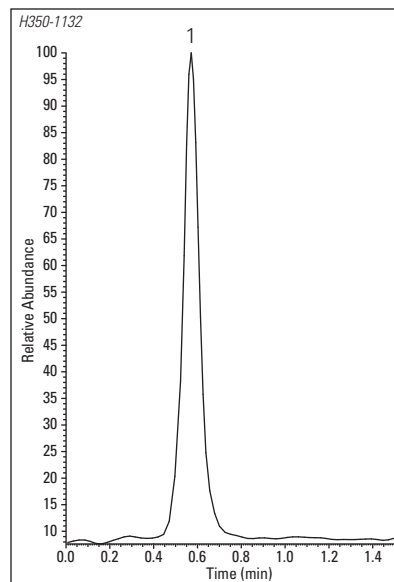
Cyclic Monophosphates



Column: Hypercarb, 5 μ m, 100 x 4.6 mm
 Part Number: 35005-104630
 Mobile Phase: A = 20 mM Ammonium Acetate
 (no pH modification)
 B = MeCN
 Gradient: 20 – 45% B in 10 minutes
 Flow Rate: 1.0 mL/min
 Detection: UV @ 254 nm
 Temperature: 25 °C
 Injection Volume: 5 μ L

1. Cytidine 3', 5' – cyclic monophosphate
2. Uridine 3', 5' – cyclic monophosphate
3. Guanosine 3', 5' – cyclic monophosphate
4. Adenosine 3', 5' – cyclic monophosphate

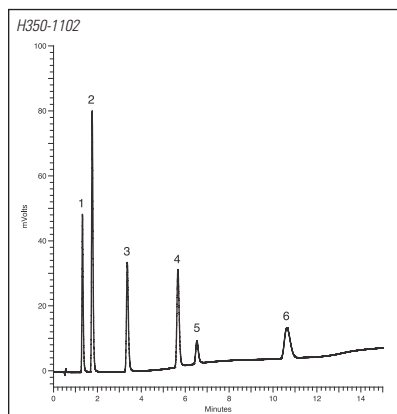
L-Carnitine



Column: Hypercarb DASH HTS,
 5 μ m, 20 x 2.1 mm
 Part Number: 35005-022150
 Mobile Phase: H₂O + 0.1% TFA
 Flow Rate: 0.5 mL/min
 Detection: MS, +ve ESI
 Temperature: 30 °C
 Injection Volume: 0.5 μ L

1. L-Carnitine

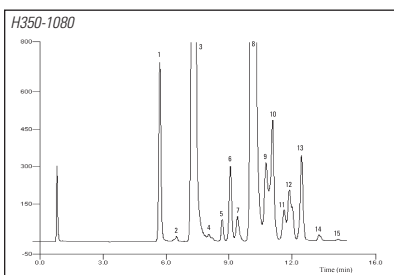
Purines and Pyrimidines (UHT-LC)



Column: Hypercarb, 5 μ m, 100 x 4.6 mm
 Part Number: 35005-104646
 Mobile Phase: H₂O
 Flow Rate: 2 mL/min
 Detection: UV at 254 nm
 Temperature: 150 to 200 °C at 15 °C/min;
 hold at 200 °C

- | | | |
|-------------|-----------------|-------------|
| 1. Cytosine | 3. Thymine | 5. Guanine |
| 2. Uracil | 4. Hypoxanthine | 6. Xanthine |

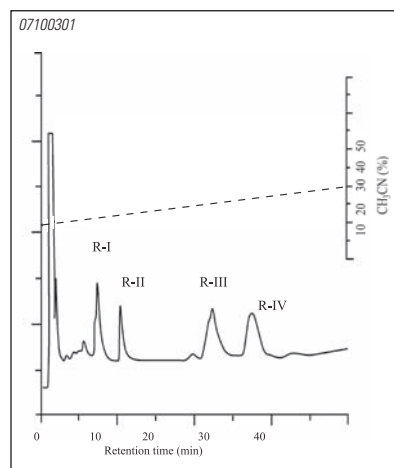
Ceramides



Column: Hypercarb, 5 μ m, 100 x 2.1 mm
 Part Number: 35005-102130
 Mobile Phase: A: MeOH
 B: CHCl₃
 Gradient: 45 to 80% B in 15 min
 Flow Rate: 0.4 mL/min
 Detection: ELSD
 Temperature: 50 °C
 Source: K. Gaudin, Laboratoire de Chimie Analytique, Université Paris Sud, France

- Ceramides:
- | | | |
|---------------|----------------|----------------|
| 1. d18:1c16:0 | 6. d18:1c20:0 | 11. d18:1c23:0 |
| 2. d18:0c16:0 | 7. d18:1c23:1 | 12. d18:1c26:1 |
| 3. d18:1c18:0 | 8. d18:1c24:1 | 13. d18:1c24:0 |
| 4. d18:0c18:0 | 9. d18:1c22:0 | 14. d18:1c25:0 |
| 5. d18:1c22:1 | 10. d18:1c25:1 | 15. d18:1c26:0 |

RNB-Glycopeptides

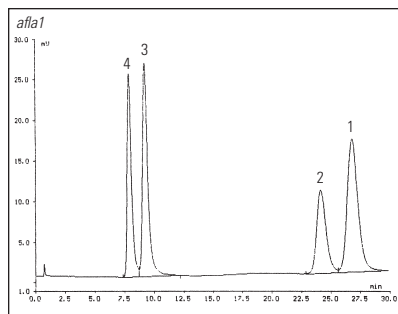


Column: Hypercarb, 5 μ m, 100 x 4.6 mm
 Part Number: 35005-104630
 Mobile Phase: A: H₂O
 B: ACN
 Gradient: 10 to 50% B in 50 min
 Flow Rate: 1 mL/min
 Detection: UV at 210 nm
 Temperature: 40 °C

Source: J. Fan and A. Kondo, Anal. Biochem. 219, 224 (1994).
 Reprinted with permission

- | | |
|--|--|
| 1. R-I (Man ₅ GlcNAc ₂ Asn) | 3. R-III (Man ₅ GlcNAc ₂ AsnLeu) |
| 2. R-II (Man ₅ GlcNAc ₂ Asn) | 4. R-IV (Man ₅ GlcNAc ₂ AsnLeu) |

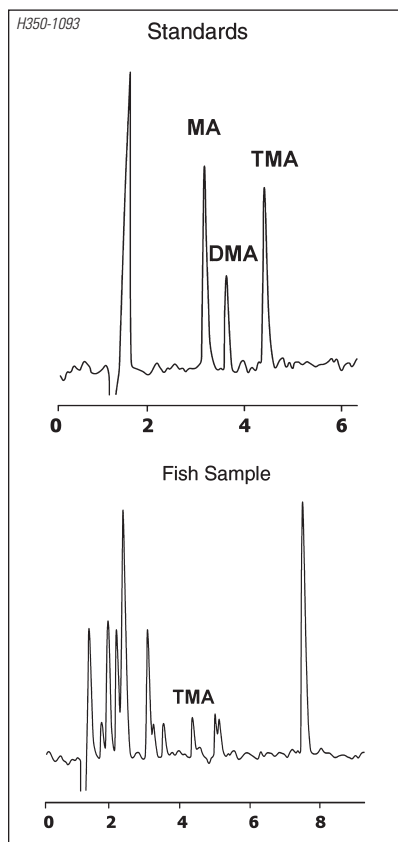
Aflatoxins



Column: Hypercarb, 5 μ m, 100 x 3.0 mm
 Part Number: 35005-103030
 Mobile Phase: A: Dioxane
 B: CHCl₃
 Isocratic: 10:90
 Flow Rate: 0.8 mL/min
 Detection: Fluorescence
 (exc 365 nm, em 418 nm)
 Source: Rhemrev-Boom,
 M.M, Amro Emmen

1. Aflatoxin B₁ 3. Aflatoxin G₁
 2. Aflatoxin B₂ 4. Aflatoxin G₂

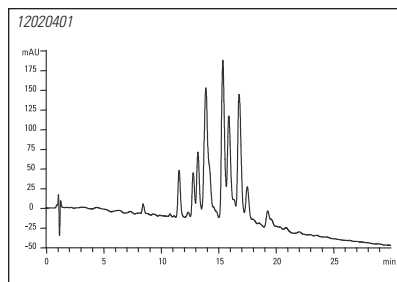
Methylamines in Fish



Column: Hypercarb, 7 μ m, 100 x 4.6 mm
 Part Number: 35007-104630
 Mobile Phase: 5 mM Heptanesulfonic acid +
 5 mM KH₂PO₄ at pH 9
 Flow Rate: 1 mL/min
 Source: Lofti I. Monser, Analytica Chimica
 Acta, 322 (1996) 63-68.

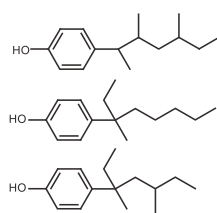
1. Trimethylamine (TMA) 3. Methylamine (MA)
 2. Dimethylamine (DMA)

Nonylphenol Isomers

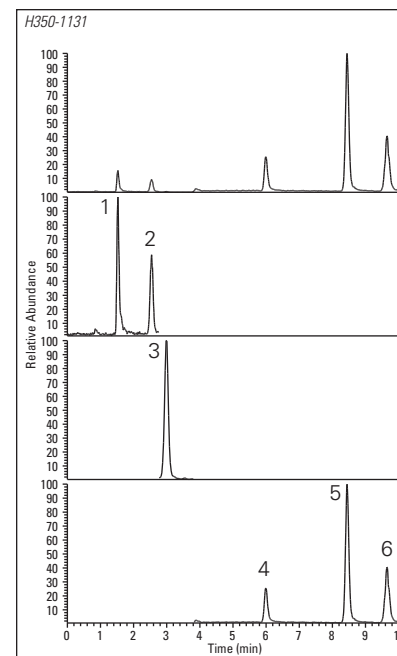


Column: Hypercarb, 3 μ m, 100 x 0.32 mm
 Part Number: 35003-100365
 Mobile Phase: A: 0.1% Formic acid
 B: ACN + 0.1% Formic acid
 Gradient: 50 to 70% B in 30 min
 Flow Rate: 6 μ L/min
 Detection: UV at 204 nm

Sample: p-Nonylphenol (some of the possible isomer structures represented below)



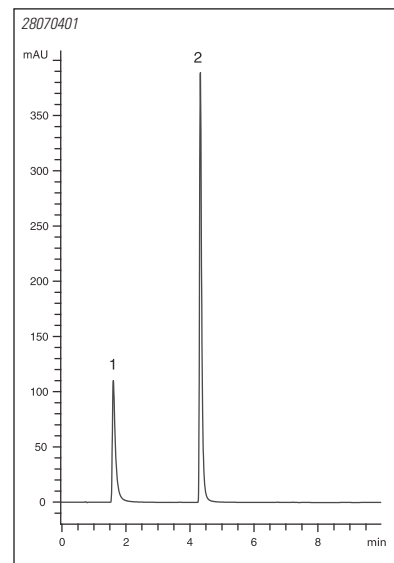
Water Pollutants



Column: Hypercarb, 5 μ m, 100 x 2.1 mm
 Part Number: 35005-102130
 Mobile Phase: A – H₂O + 0.1% Formic acid
 B – ACN + 0.1% Formic acid
 Gradient: 10 to 100% B in 10 mins
 Flow Rate: 0.2 mL/min
 Detection: MS, +/- ESI
 Temperature: 68 °C
 Injection Volume: 10 μ L

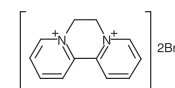
1. Ammeline 4. Atrazin desethyl desisopropyl
 2. Ammelide 5. Atrazin desethyl
 3. Cyanuric Acid 6. Atrazin desisopropyl

Quaternary Ammonium Salts

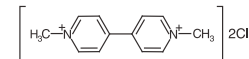


Column: Hypercarb, 5 μ m, 50 x 4.0 mm
 Part Number: 35005-054030
 Mobile Phase: A: H₂O + 0.05% TFA
 B: ACN + 0.05% TFA
 Gradient: 5 to 35% B in 10 min
 Flow Rate: 0.8 mL/min
 Detection: UV at 295 nm to 3 min, 245 nm
 from 3 to 10 min
 Temperature: 25 °C

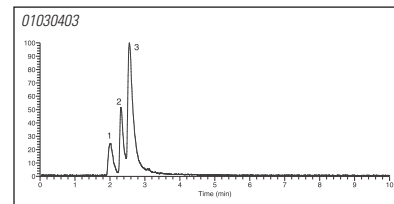
1. Diquat



2. Paraquat



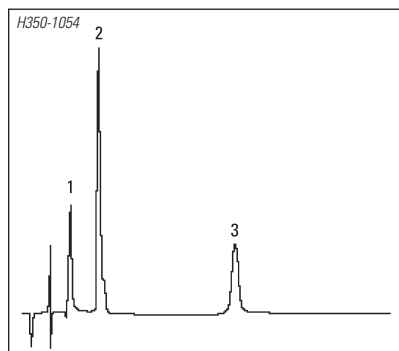
Arginine and Methylated Arginines



Column: Hypercarb, 3 μ m, 100 x 2.1 mm
 Part Number: 35003-102130
 Mobile Phase: A: 10 mM NH₄COOH at pH 3.5
 B: ACN
 Gradient: 10 to 50% B in 10 min
 Flow Rate: 150 μ L/min
 Detection: + ESI
 Temperature: 40 °C

1. L-arginine
 2. Methyl-L-arginine
 3. Asymmetrical dimethyl arginine

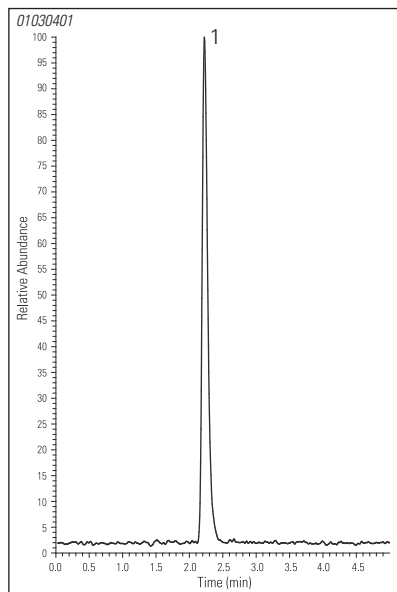
Creatine in Serum



Column: Hypercarb, 5 μ m, 100 x 4.6 mm
 Part Number: 35005-104630
 Mobile Phase: A: ACN
 B: TFA
 C: H₂O
 Isocratic: 3:0.1:96.9
 Flow Rate: 1 mL/min
 Detection: UV at 210 nm
 Source: C. Lim, IRC, Centre for Mechanism of Human Toxicity, Leicester, UK

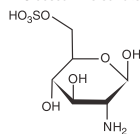
1. Oxalic acid
2. Creatine
3. Creatinine

Glucosamine Sulfate

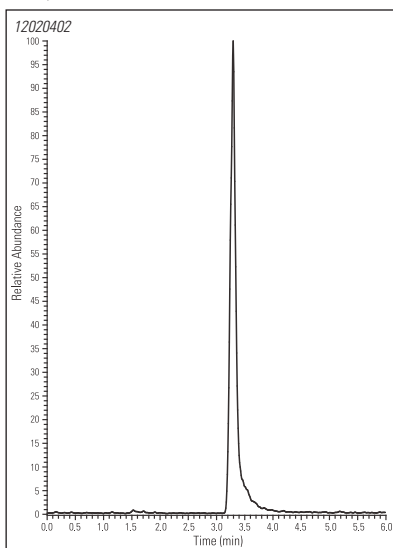


Column: Hypercarb, 3 μ m, 100 x 2.1 mm
 Part Number: 35003-102130
 Mobile Phase: A: 0.1% NH₃ (aq)
 B: ACN
 Isocratic: 50:50
 Flow Rate: 0.2 mL/min
 Detection: - ESI
 Temperature: 60 °C

1. Glucosamine sulfate



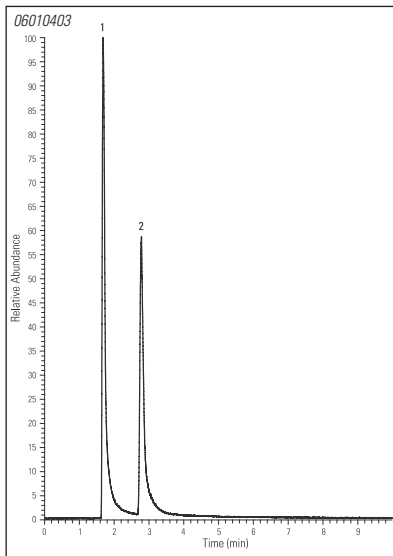
Acyclovir



Column: Hypercarb, 3 μ m, 100 x 2.1 mm
 Part Number: 35003-102130
 Mobile Phase: A: H₂O + 0.1% Formic acid
 B: ACN + 0.1% Formic acid
 Gradient: 30 to 100% B in 10 min
 Flow Rate: 0.2 mL/min
 Detection: + ESI
 Temperature: 40 °C

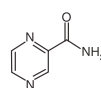
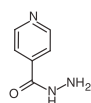
Acyclovir

Tuberculostatics

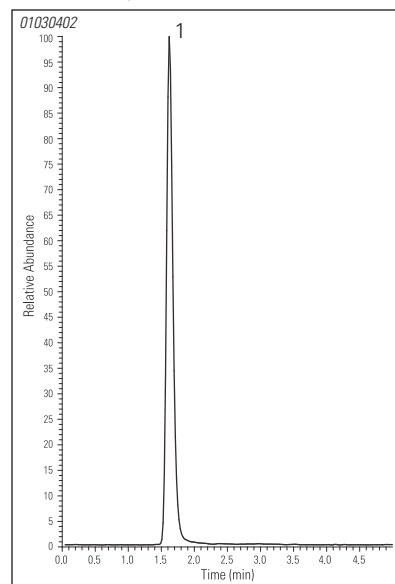


Column: Hypercarb, 3 μ m, 100 x 2.1 mm
 Part Number: 35003-102130
 Mobile Phase: A: 0.05% TFA
 B: ACN + 0.05% TFA
 Isocratic: 70:30
 Flow Rate: 0.2 mL/min
 Detection: + ESI
 Temperature: 40 °C

1. Isoniazid
2. Pyrazinamide

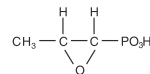


Fosfomycin

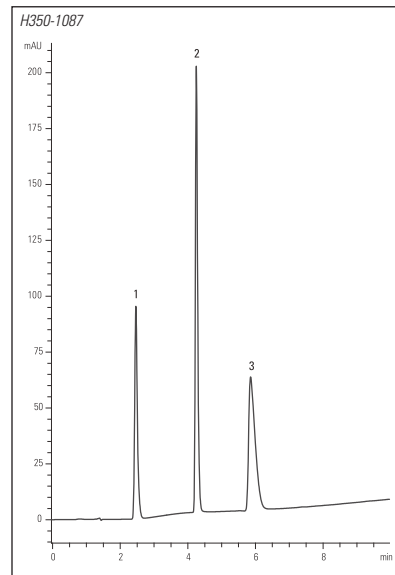


Column: Hypercarb, 3 μ m, 100 x 2.1 mm
 Part Number: 35003-102130
 Mobile Phase: A: 0.1% NH₃ (aq)
 B: ACN
 Isocratic: 90:10
 Flow Rate: 0.15 mL/min
 Detection: - ESI
 Temperature: 30 °C

1. Fosfomycin (phosphomycin)



Uracil and Metabolite



Column: Hypercarb, 5 μ m, 100 x 4.6 mm
 Part Number: 35005-104630
 Mobile Phase: A: H₂O
 B: ACN
 Gradient: 5 to 50% B in 10 min
 Flow Rate: 1 mL/min
 Detection: UV at 210 nm
 Temperature: 40 °C

1. 5,6-Dihydrouracil
2. Uracil
3. 5-Fluorouracil

Ordering Information

Hypercarb Columns




Particle Size	Length (mm)	4.6 mm ID	3.0 mm ID	2.1 mm ID	1.0 mm ID
3 µm	30	35003-034630	35003-033030	35003-032130	35003-031030
	50	35003-054630	35003-053030	35003-052130	35003-051030
	100	35003-104630	35003-103030	35003-102130	35003-101030
	150	35003-154630	35003-153030	35003-152130	–
5 µm	30	35005-034630	35005-033030	35005-032130	35005-031030
	50	35005-054630	35005-053030	35005-052130	35005-051030
	100	35005-104630	35005-103030	35005-102130	35005-101030
	150	35005-154630	35005-153030	35005-152130	35005-151030
7 µm	50	35007-054630	35007-053030	inquire	–
	100	35007-104630	35007-103030	inquire	–

Other column dimensions are also available. Please call Customer Service for more information. For high temperature applications please refer to columns listed below.

Hypercarb Drop-in Guard Cartridges (pk/2)



Particle Size	Length (mm)	4.6 mm ID	3.0 mm ID	2.1 mm ID	1.0 mm ID
3 µm	10	35003-014001	35003-013001	35003-012101	35003-011001
5 µm	10	35005-014001	35005-013001	35005-012101	35005-011001
7 µm	10	35007-014001	35007-013001	35007-012101	35007-011001
UNIGUARD™ Direct-Connect Drop-in Guard Cartridge Holder		 850-00	852-00	852-00	851-00

Hypercarb KAPPA Capillary Columns

Particle Size	Length (mm)	500 µm ID	320 µm ID	180 µm ID	100 µm ID	75 µm ID
5 µm	50	35005-050565	35005-050365	35005-050265	35005-050165	35005-050065
	100	35005-100565	35005-100365	35005-100265	35005-100165	35005-100065

Hypercarb Nanobore Columns

Particle Size	Length (mm)	IntegraFrit	IntegraFrit Multipack	IntegraFrit	IntegraFrit Multipack
		75 µm ID	75 µm ID	150 µm ID	150 µm ID
5 µm	10	35005-017563	35005-017564 (4/pk)	35005-011563	35005-011564 (4/pk)
	50	35005-057563	35005-057564 (3/pk)	35005-051563	35005-051564 (3/pk)
5 µm	10	PicoFrit 75 µm ID x 15 µm Tip	PicoFrit Multipack 75 µm ID x 15 µm Tip		
	50	35005-017581	35005-017583 (4/pk)		
		35005-057581	35005-057582 (3/pk)		

Hypercarb Specialized Column Hardware for High Throughput



Particle Size	Quantity	DASH™ HTS 20 x 2.1 mm	Javelin™ HTS 20 x 4.0 mm	Javelin HTS 20 x 2.1 mm	Javelin HTS 20 x 1.0 mm
5 µm	3	35005-022151	35005-024035	35005-022135	35005-021035

Hypercarb Preparative Columns

Particle Size	Length (mm)	10 mm ID	21.2 mm ID	30 mm ID	50 mm ID
5 µm	50	35005-059070	35005-059270	35005-059370	35005-059570
	100	35005-109070	35005-109270	35005-109370	35005-109570
	150	35005-159070	35005-159270	inquire	inquire
7 µm	50	35007-059070	35007-059270	35007-059370	35007-059570
	100	35007-109070	35007-109270	35007-109370	35007-109570
	150	35007-159070	35007-159270	35007-159370	35007-159570

Hypercarb High Temperature Columns

Particle Size	Length (mm)	4.6 mm ID	3.0 mm ID	2.1 mm ID	1.0 mm ID
3 µm	30	35003-034646	35003-033046	35003-032146	35003-031046
	50	35003-054646	35003-053046	35003-052146	35003-051046
	100	35003-104646	35003-103046	35003-102146	35003-101046
5 µm	30	35005-034646	35005-033046	35005-032146	35005-031046
	50	35005-054646	35005-053046	35005-052146	35005-051046
	100	35005-104646	35005-103046	35005-102146	35005-101046

Please note that these columns are for use with elevated temperatures. For other dimensions, please inquire.

Chromatography Resources

Every piece of the solution at your fingertips, precisely when you need it.

Download a copy of our Method Development Guide for Hypercarb Columns.

www.thermo.com/hypercarb

Our bi-monthly Separated by Experience newsletter keeps you up-to-date on the latest technical and product information of interest to chromatographers. Subscribe today!

www.thermo.com/columns

Our Chromatography Columns and Consumables catalogs helps you find all your chromatography needs in a single resource. Order your copy now!

www.thermo.com/columns

Our Chromatography Resource Centre provides an extensive, fully searchable library of chromatography applications which currently includes over 6000 applications and references encompassing liquid chromatography, gas chromatography and solid-phase extraction.

www.thermo.com/columns



In addition to these offices, Thermo Fisher Scientific maintains a network of representative organizations throughout the world.

USA and Canada

+1 800 532 4752
+1 561 688 8731 fax
analyze.us@thermo.com

United Kingdom

+44 (0) 845 702 3964
+44 (0) 1707 391 311 fax
lccg.consumables@thermofisher.com

France

+33 (0) 1 60 92 48 00
+33 (0) 1 60 92 49 00 fax
analyze.fr@thermo.com

Germany

+49 (0) 6103 408 1140
+49 (0) 6103 408 1111 fax
analyze.de@thermo.com

India

+1 800 22 8374 toll free
+91 22 67162200
+91 22 67162244 fax
contact.LPG.in@thermofisher.com

Japan

+81 45 453 9120
+81 45 453 9122 fax
analyze.jp@thermo.com

Switzerland

+41 56 618 41 11
+41 56 618 41 41 fax
info.ch@thermofisher.com

All Other Enquiries

+44 (0) 1928 581 000
+44 (0) 1928 581 078 fax
salesorders.columns.uk@thermofisher.com

www.thermo.com/columns

ANGSCHYPERCARB0609

Thermo
SCIENTIFIC